Into the Void: Mass Function of Supermassive Black Holes in the local universe

A Thesis
Presented to
The Division of Mathematics and Natural Sciences
Reed College

In Partial Fulfillment
of the Requirements for the Degree
Bachelor of Arts

Farhanul Hasan

May 2018

Approved for the Division
(Physics)

Alison Crocker

Acknowledgements

Writing a thesis is a long and arduous process. There were times when it seemed further from my reach than the galaxies I studied. It's with great relief and pride that I realize I made it this far and didn't let it overpower me at the end. I have so many people to thank in very little space, and so much to be grateful for.

Alison, you were more than a phenomenal thesis adviser, you inspired me to believe that Astro is cool. Your calm helped me stop freaking out at the end of February, when I had virtually no work to show for, and a back that ached with every step I took. Thank you for pushing me forward. Working with you in two different research projects were very enriching experiences, and I appreciate you not giving up on me, even after all the times I blanked on how to proceed forward. Thank you Johnny, for being so appreciative of my work, despite me bringing in a thesis that I myself barely understood when I brought it to your table. I was overjoyed when I heard you wanted to be on my thesis board!

Thanks to Reed, for being the quirky, intellectual community that it prides itself on being. The four years here were the most meaningful of my life and helped me grow in ways I would not have imagined possible before I came here. It's been difficult – Reed is one of the hardest schools to go to college to – yet it's been the greatest adventure of my life so far and I'm grateful that I (almost) made it! My professors were some of the most intellectually passionate and inspiring people I ever had the pleasure of meeting. A special thanks first, to Joel, for his mathematical insight into solving a critical integral in my thesis. To both Alison and John, thank you for writing me recommendation letters that got me into grad school! I've been fortunate to discover an entire passion for music while I've been here, and that is in no small part due to classes I took in the music department, especially with Mark, whose understanding of music and how it works in historical contexts was transformative in how I see the world. Lucia, thanks for being the most stylish and badass Hum conference leader; Kelly, thanks for being a beacon of hope for every minority student in this school and everyone who thinks their path through academia is unconventional. Thanks to incredible staff members I've had the pleasure of working with over the years, including Dana, Rachel, Meredith, Tara, Mark and Logan.

I've met some of the most incredible human beings of my life at this place. Skye, Revant, Mauricio, Simue, Sarah, Jethary, Mitchell, Cecile, Ophelia, Shira, Roselyn, Ribby, Ali, Iris, Nat, Emily, Hwan, Akrish, Duncan, Beadle, Rikky, Nick, Austen, Saga, Arek, Langston, Drew, Makana, Andie, Celia, Carmen, Leo, Aiman, Avehi, Pallavi, Hanna, Shabab, Kaustuv, and Jack: I LOVE YOU. Yeah, I learned who I was, explored my intellectual interests in this place, yada yada, but none of it would be worth it if it wasn't for meeting these amazing people (and many others I forgot to mention in the rush of writing this) throughout the years.

Thanks to my family; my parents, my sister, and my cousins who've never given up on me and trusted me to always do the right thing. Thank you for the faith and the love. Thanks to my host family, Duncan, Jenny, Gus and Truman, for welcoming me with such warmth and open arms to this very strange corner of the world. A special thanks to HCC nurse practitioner Anne for giving me strength when I thought I was going to have to take a semester off because of my back, and to Dr. Dan Beeson, for his valuable chiropractic and (in equally important portions) mental support through some of the hardest days of my life this past semester. Thanks to my thesis office mates Ribby, Ali and Dan, and to others like Matyas, Anthony, Helen, Amanda, Sarah, Aja, Andrew and Noah, whose indomitable spirits kept the subbasement alive and myself sane.

Table of Contents

Abstract

Statistical approaches are used to assess the demography of supermassive black holes (SMBHs) in terms of their mass. A statistically complete sample of galaxies from the Sloan Digital Sky Survey (SDSS) with redshifts $0.03 \leqslant z \leqslant 0.1$ is used in the formulation of the Black Hole Mass Function (BHMF). The strong correlation between black hole mass, M_{BH}, and galaxy velocity dispersions, σ, in the nearby universe, as well as the existence of a fundamental plane, suggests some mechanism regulating the coevolution of SMBHs and their host galaxies. The distributions in both σ and M_{BH} can be approximated by a 4-parameter Schechter-like function, with a power law and an exponential fall-off. The derived BHMF indicates there are far more SMBHs with masses between 10^6 M$_\odot$ and 10^8 M$_\odot$ than there are larger ones. Assuming an average radiative efficiency, the mass density accreted by local SMBHs matches that observed from high-redshift Active Galactic Nuclei (AGN), implying that the same phenomenon powers both types of objects and that mass accretion is the primary mode of growing SMBHs. Uncertainties in the methodology and limitations to observational data are discussed.

Introduction

The evolution of the universe can be likened to a display of fireworks that has just ended: some few red wisps, ashes, and smoke. Standing on a well-chilled cinder, we see the fading of the suns and try to recall the vanished brilliance of the origin of the worlds.

- George Lemaitre

Research is to see what everybody else has seen and to think what nobody else has done.

- Albert Szent-Gyorgyi

Science often has a way of appearing mere steps removed from fantasy. Often the deepest questions we ponder about the world which we inhabit lead us to the strangest and wildest answers. Black holes were once a mathematical curiosity, an abstract fascination of theoretical physicists reveling in the possibilities of the modern era of atoms, photons and a curious idea called general relativity. A century later, the study of these objects inside of which supposedly all laws of Physics break down, is of paramount importance to astronomy. A slew of breakthroughs in recent years have enabled us to observe two stellar-mass black holes[1] merging to form bigger ones many, many years ago, in the farther reaches of the observable universe (Fig. 1).

But presently we have enough evidence to comfortably believe that black holes exist in extreme proportions too: **SuperMassive Black Holes (SMBH)** as massive as millions to billions of suns, lie at the hearts of galaxies that populate our universe. While two decades ago we were trying to prove SMBHs exist, today we've moved past this 'proof-of-concept' phase to study their demographics, how they form, and even how influential they are to the origin tales and evolution of galaxies in which they rest. Most astronomers now believe the seemingly incredible hypothesis that SMBHs reside at the centers of most, if not all, galaxies in the universe (including our own – more of that later in this chapter).

Despite our misfortune of not being able to see black holes, there is one very important characteristic of theirs that we can measure – mass. In this thesis, I will construct a complete census of the mass of SMBHs, M_{BH}, in our nearby (local) universe and their evolution by means of a SMBH mass function. I will use observations which produced reliable estimates of M_{BH} in galaxies nearby. These, I will couple

[1] A black hole that is about 5 to a few tens of times as massive as the sun

to empirical relationships observed between M_{BH} and properties of the host galaxies to estimate M_{BH} of galaxies that are simply too far away to *measure* the mass of their central black holes. This information will be exploited to create a SMBH Mass Function, or the **Black Hole Mass Function (BHMF)**. The mass function allows us to determine how densely packed our present-day (local) universe is with SMBHs of a given mass and is one of the key empirical tools in our arsenal for investigating SMBHs, and for constraining theoretical models for how the SMBH population grows. It's important to note that Intermediate Mass Black Holes (IMBHs) as light as a few tens of solar masses to just less than a million, are also believed to exist, but their existence is still a matter of debate and are not considered in this thesis. In the rest of this introduction, I will provide a brief historical overview of the fascinating developments arising from SMBH research and motivate the reasons for my study.

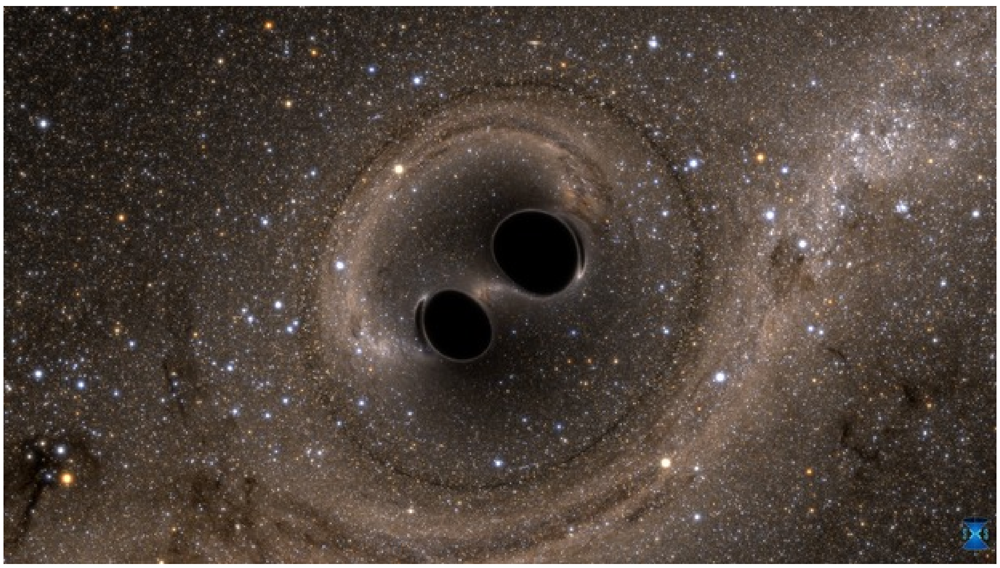

Figure 1: A simulated image of two black holes merging into one. Image Credit: SXS, the Simulating eXtreme Spacetimes (SXS) project (http://www.black-holes.org).

The greatest ideas in astronomy have always faced the mightiest of skeptics. One need merely look at the nearest reference point civilization in the Western canon – ancient Greece. Despite spectacular advances like using Babylonian records of the heavens to predict solar eclipses (Thales of Miletus), figuring out that the Earth was orange-shaped instead of a plane, and even postulating the Earth *wasn't* at the heart of the solar system (Aristarchus of Samos), Aristotle's fantastic and unfortunately inaccurate model of the Earth being centered around many (*55*, in fact) concentric spheres endured for thousands of years. Aristotelean Cosmology gave birth to the notion of objects *naturally* moving in circles, and also the idea that our humble blue planet is the unequivocal focus of the universe. The Catholic Church endorsed this zealously and most people until medieval times didn't bother questioning it. Why would you risk contradicting the most important natural philosopher west of the Himalayas?

For all of Aristotle's faults, I will concede that the *science* of cosmology began with the model he presented in *On the heavens* and *Meteorologica* – arguably the first known scientific theory in cosmology. He observed the positions of objects in the sky change and formulated the hypothesis that heavenly bodies all move in circles around the Earth. He used this hypothesis to make predictions, such as where these bodies might be seen a year from now, which were verified by recorded observations. With the backing of the church, four hundred years after Aristotle's model, Ptolemy proposed an updated version, with 8 spheres culminating in heaven (Fig. 2). Despite opposition by many, including medieval Islamic scholars who rejected some of the basic Ptolemaic postulates such as an infinite universe, a stationary Earth and so on, a geocentric universe remained accepted knowledge until the Renaissance. [For a modern history of cosmology traced from antiquity to the present day and across different cultures, see Refs.[1] and [2]]

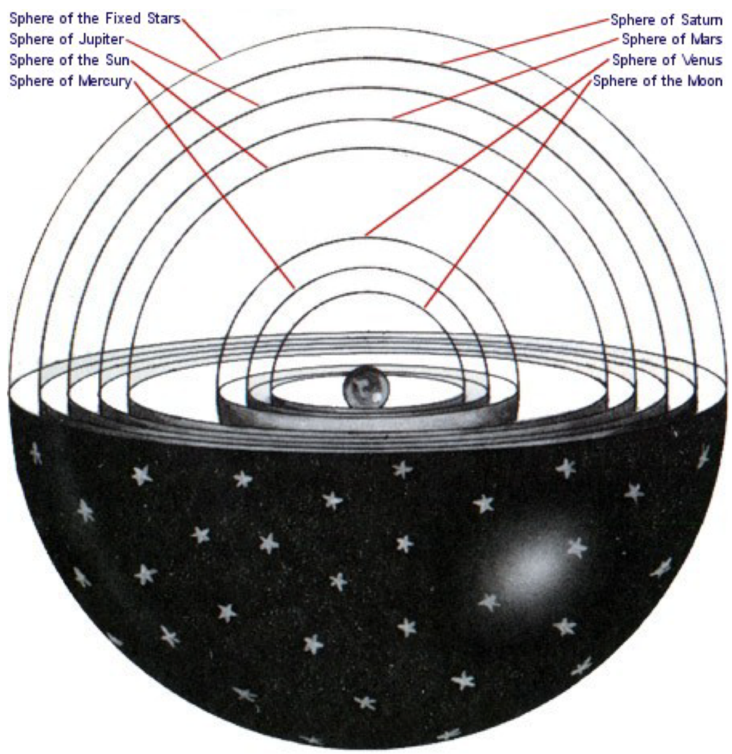

Figure 2: Ptolemy's geocentric model of the universe. Figure from Steven Hawking's *A brief history of time* [3].

It can be argued that the first truly satisfying breakthrough in western science came from a Polish astronomer and polymath in 1543, some 1800 years after Aristotle. The publication of Nicolaus Copernicus's *De revolutionibus orbium coelestium* (On the Revolutions of the Heavenly Spheres) kickstarted the scientific revolution. In it, Copernicus de-seats Earth from its "rightful" place at the center of the universe and instead proposes that it goes around the sun, along with the other known planets. Johannes Kepler, a German astronomer, modified Copernicus's theory by suggesting planets move in ellipses, birthing the heliocentric model of the universe we still use today. The discovery of the four largest moons of Jupiter orbiting the gas giant, of Italian astronomer and scourge of the Catholic church, Galileo Galilei, lent incontrovertible evidence to this model. Humanity was progressing from natural philosophy to the modern scientific method.

As our technology improved and our available resources maximized, we've been able to peer deeper and probe farther into the darkness of space than our ancestors might have imagined. With the advent and expansion of modern astronomy, we've travelled past moons of Jupiter and Saturn, past comets and asteroids, and outside the edge of our own galaxy – the Milky Way. Going back to the Greeks, Democritus in the fifth century B.C.E. believed that the patchy bright band in the night sky was actually made up of light from distant stars. Two millennia later, Galileo verified just this by peering through his telescopes[2]. For decades, the foremost intellectual debates in astronomy centered around what we now accept as fact – that there are more galaxies like our own, composed of billions of stars like our sun (and many unlike our sun). The belief that distant nebulae were actually galaxies very far away was countered by the discomfort of leaving a finite, single-galaxy universe to a seemingly infinite ocean of these "island universes[3]."

This went so far that written in the annals of modern astronomy is the story of "the Great Debate" of 1920 – a public debate about the scale of the observable universe between two of the foremost astronomers of the day. Harlow Shapley of the Harvard College Observatory passionately advocated for spiral nebulae such as Andromeda (M31) being inhabitants of the Milky Way, while Heber Curtis of the UCO Lick Observatory steadfastly contended that these nebulae were galaxies of their own (the published version of the debates can be found in Refs. [5, 6]).

Edwin Hubble settled the debate four years later, and proved Curtis right. Hubble published an article in the *New York Times* in November 1924, and a couple months later, in the 1925 meeting of the American Astronomical Society (AAS), presented a paper unassumingly titled, "Cepheids in Spiral Nebulae" that proved the Andromeda nebula must be a galaxy of its own. He used the 2.5 meter Hooker Telescope at Mount Wilson Observatory (largest in the world at the time) to resolve stars in Andromeda. The telescope allowed him to resolve individual stars and by one of the happiest accidents in 20th century physics, locate a class of stars called Cepheid Variables in the nebula. Cepheid variables are radially pulsating stars whose existence had been known to us for centuries.

Earlier in the twentieth century, one of the many criminally under-appreciated women in modern astronomy (more of whom are to appear in this chapter), Henrietta Swan Leavitt, established a relationship between the apparent brightness and pulsation period of classical Cepheid stars. Leavitt made use of the fact that by measuring apparent brightness of a star (incoming flux), we can deduce how far it is, given we know its intrinsic brightness (luminosity). The brighter a Cepheid ap-

[2]Scottish poet Thomas Seget once said, "Columbus gave man lands to conquer by bloodshed, Galileo new worlds harmful to none. Which is better?"

[3]The term was first coined in the 18th century by German philosopher Immanuel Kant, who was one of the first proponents of an extragalactic cosmos [4].

peared, the higher was its pulsation period, Leavitt found, and consistency of this period-luminosity relation could be harnessed in using Cepheids as benchmarks, or “standard candles” with well-defined intrinsic luminosities; all we have to do is measure their period of pulsation and we end up with a very reliable estimate of how far they are from us. This is precisely what Hubble did in 1924, and by measuring the period of Cepheids in the Andromeda nebula, he found that it was 900,000 light years away from us. In an ironic twist of fate, a couple years prior to this, Harlow Shapley himself found globular clusters – dense collections of stars signifying the edge of the Milky Way – to be at most 100,000 light years away. Andromeda was thus about 9 times as far as from where we thought the observable universe ended. The field of extragalactic astronomy was born.

We now find ourselves a lonely island universe among two *trillion* (2×10^{12}) others [7], and we’re actually all moving *away from each other.* In our current model of the expanding, accelerating universe, galaxies are the basic building blocks on a cosmological scale, yet we’ve had tough luck cracking the mystery of their origins. About 17 years ago, astrophysicists started entertaining an extraordinary possibility: black holes – very big ones – might have evolved alongside galaxies and could hold the key to understanding how they grew to be where they are today. One of the most extreme objects in our observable universe could help explain the evolution of its most ubiquitous residents, and in turn, tell us where we came from.

The story of supermassive black holes begins with an apple falling (or not) and a very powerful idea emerging from that (possibly fictitious) encounter. Isaac Newton developed the methods of calculus and proposed a mysterious force that accounts for the motion of heavenly bodies around the sun as well as things like why we fall back to the Earth after we jump. In 1687, upon the publication of *Philosophiæ Naturalis Principia Mathematica* (Mathematical Principles of Natural Philosophy), we were awakened to the three basic laws of motion (of everything, it was thought at the time), and the attractive force that each body with mass exerts on other bodies with mass – gravity. With this force, Newton derived Kepler’s laws of planetary motion and explained Galileo’s discovery of Jupiter’s moons revolving around it.

Newton’s law of universal gravitation states that an object with mass m_1 should attract another object with mass m_2 with a force, F, that varies inversely with the distance, d, between them given by:

$$F = -G\frac{m_1 m_2}{d^2}, \tag{1}$$

where G is the universal gravitational constant. So if you replace the sun with a star twice as heavy, it would exert twice as big a gravitational force on us. Or if you moved the earth twice as far from the sun, we would feel a quarter of the gravitational force we feel now.

Principia might have set the world of physics in motion (no pun intended), but it didn’t shake the entire world immediately. Intellectual leaders of the enlightenment, the likes of Gottfried Wilhelm Leibniz (whose feud with Newton over the invention of calculus is among the storied lores of science and mathematics – boy, physicists love to argue), Réne Descartés, and Christiaan Huygens, had their own formulations of what causes motion and only partially accepted Newton's model, if at all. Walter Bryant believed that it wasn't until 1738, when French philosopher Voltaire published a popular treatise in support of Newton's laws, that they were beginning to accumulate universal acceptance [8]. Ten years after that, the French Academy of Sciences offered an award to anyone who could solve the perturbations in the orbits of Jupiter and Saturn around the sun predicted by Newtonian gravity. These were solved by two of the giants of 18th century mathematics – Leonhard Euler and Joseph-Louis Lagrange.

The other major player in this story is another of nature's mystical phenomena – light. Newton believed that light was made up of particles, while others such as Dutch physicist Christian Huygens believed light was a wave. We now know they're both correct – the wave-particle duality of light implies it can behave as both particle and wave (as a matter of fact, so can *all* matter). Until much of the 17th century, there was not much reason to doubt that light traveled infinitely fast. In 1676, Danish astronomer Ole Christensen Rømer, observed that the moons of Jupiter appeared to orbit it faster when the earth was approaching Jupiter than when it was moving away from it. This, he reasoned was due to light from the moons taking different times to reach us depending on our velocity relative to them. So if light travels a finite distance in a finite amount of time, it must be a finite quantity. He calculated that light traveled a staggering 220,000 kilometers a second in vacuum, which is about 26% lower than the currently accepted value of $\sim$299,800 kms^{-1}. The decade prior to *Principia*, Newton defined his corpuscular theory of light, which basically treats light as many tiny particles. He was sure that not even these corpuscles of light could escape the pull of gravity.

As early as the 18th century, scientists began speculating about the extremes of the interaction of light with gravity. In 1783, the English reverend and polymath John Michell sent a paper to Lord Henry Cavendish of the Royal Society, predicting the existence of "dark stars." Michell predicted that a star about as dense as the sun but about 500 times as wide in diameter would have an escape velocity – the minimum speed needed to overcome the gravitational pull of the star – bigger than the speed of light. In other words, he believed that not even light can escape the gravitational attraction of a star that is sufficiently large and dense. The problem with these stars, of course, is that we wouldn't be able to see them. However, Michell offered a brilliant solution for that too [9]:

> "...yet, if any other luminous bodies should happen to revolve about them we might still perhaps from the motions of these revolving bodies infer the existence of the central ones with some degree of probability, as this might afford a clue to some of the apparent irregularities of the revolving bodies, which would not be easily explicable on any other hypothesis."

Aha, use of the law of gravity in action! It's quite remarkable that in 1783, we'd already predicted that we were going use the super-sped up motion of stars around a central body to infer the existence of supermassive black holes! But more on that in a bit. In the meantime, the president of the Institute de France, Pierre-Simon Laplace[4] developed this idea of dark stars independently and prophesied what astronomers now know to be true:

> "The largest luminous bodies in the universe may thus be invisible by reason of their magnitude"

This he included in his famous treatise on the solar system *Exposition du systéme du monde* in 1796 [10]. He even followed it up with a mathematical proof three years later, where he demonstrated that a body as dense as the earth wouldn't let any light escape it if its diameter was 250 times as much. It is interesting that even though both of these scientists were spot on about the existence of the object in question, they were pretty far off (in fact, barking up the wrong tree) in predicting its *form*. In any case, Huygens' wave theory of light was gaining rapid popularity around the beginning of the 19th century, especially after the success of Young's double slit experiment (1803) and Fresnel's work on the diffraction of light (1818). It wasn't clear how this wave description of light would interact with Newtonian gravity, so the effect of a star's gravity on the light it emits became a much more difficult problem to solve. And probably accordingly, Laplace omitted the idea of dark stars from the 3rd edition of *Exposition* [11].

The 18th and 19th centuries saw the development of various subfields of physics, from classical mechanics to thermodynamics to optics to electrodynamics. By the early 19th century, we were beginning to understand the electricity that lightning carries. Ørsted's (1819) and Ampéré's (1820) curious discoveries of compass needles and other magnets being affected by wires carrying electrical current culminated in Michael Faraday (1831) showing how a changing magnetic field sets up an electric field. Electrical generators and motors were invented, heralding the electrical revolution. In 1865, Scottish mathematical physicist James Clerk-Maxwell showed that electromagnetic fields travel through space as waves with the same speed...the speed of light! More impressive still, he developed the earliest forms of the four equations that govern all electromagnetic phenomena in classical physics, allowing us to describe light precisely in mathematical form for the first time. As the century was wrapping up, Serbian engineer Nikola Tesla founded the principles upon which we built the alternating current (AC) supply system we use today.

But as Tesla was making wondrous generators that flashed lightning, we had not progressed much further on the first fundamental force, the one that started it all. Newtonian gravity was useful for predicting most terrestrial motion, but physicists had realized that perturbations in Mercury's orbit could not be explained by it. An even bigger issue was with the fundamental nature of gravity. According to Newton, it was an instantaneous force that acts at a distance and it relied on the notion that time is absolute. A more satisfactory answer to the nature of reality was finally provided in the early years of the last century.

In 1905, a 26 year old German patent clerk found a new way of looking at the physical world. Albert Einstein presented his theory of special relativity, which in a

[4] Also father of Bayesian probability and general math wiz.

dramatic sweep of events de-seated Newton's classical mechanics. Einstein suggested that there was no such thing as absolute time, and as a matter of fact, no privileged reference frames with which to view the world. Einstein's two major ideas were that the laws of physics will appear the same to any observer who is at rest or at least not accelerating, and that all observers measure the same value for speed of light in vacuum (giving us a constant we delight in calling c), which is the maximum speed anything can be achieve in our physical world. In 1916, Einstein completed his radical idea to unveil the nature of gravity. In the theory of general relativity, the triumphant breakthrough was to look at space and time *geometrically*; if you imagine space-time as a sort of fabric, then gravity is simply the result of smaller bodies being pulled by the dent in the fabric caused by massive bodies (Fig. 3a). With his famous field equations, he described the geometry of space-time via their interaction with matter and radiation.

The story goes that Einstein became famous overnight after the total solar eclipse of May 1919 proved him right. A team led by Sir Arthur Eddington confirmed that light from stars passing close to the sun was deflected as predicted by general relativity (Fig. 3b), granting global superstardom to Einstein. Gravity does influence light under this strange new theory, but its strangest result would take us back, as luck would have it, to John Michell and Pierre Laplace in the late 18th century...

In 1916, a few months after publication of Einstein's field equations, Karl Schwarzschild worked out their first exact solutions in the World War I battlefield. The Schwarzschild metric, as it's now called, offered a remarkable finding of general relativity: for a star of a given mass, there exists a critical radius of the star at which we get a *singularity*. Mathematically, this meant that some of the terms of the equation become infinite or undefined: physically speaking, the laws of physics break down! This implied that time would be infinitely dilated if the star in question reached that critical radius, termed the Schwarzschild radius, r_s, i.e. if:

$$r_s \leqslant \frac{2GM}{c^2}, \tag{2}$$

where G is the same constant from (1), M is the mass of the star, and c the speed of light. Light simply cannot escape from the surface of such a star. In other words, our new model of the universe incorporates the idea of an object so dark that it cannot be seen any distance from it. *Dark stars can exist.*

Of course, this idea was received with much skepticism and at best, as an interesting theoretical conjecture to be contemplated upon. Einstein himself didn't think such light-sucking monsters could exist out in space and Eddington mathematically disproved the existence of such a singularity by making a change of coordinates in the Einstein field equations.

But what about *real* stars? You know, things we can actually observe? In 1930, a 20 year-old graduate of the Presidency College in Madras, India, named Subrahmanyan Chandrasekhar, began his journey to Cambridge University for his doctoral degree. On his voyage, he worked out a correction to the work of his soon-to-be-adviser and collaborator, Ralph Fowler, on the statistical mechanics of white dwarf stars. White dwarfs were believed to be the final stage of a low-mass (mass 8 times

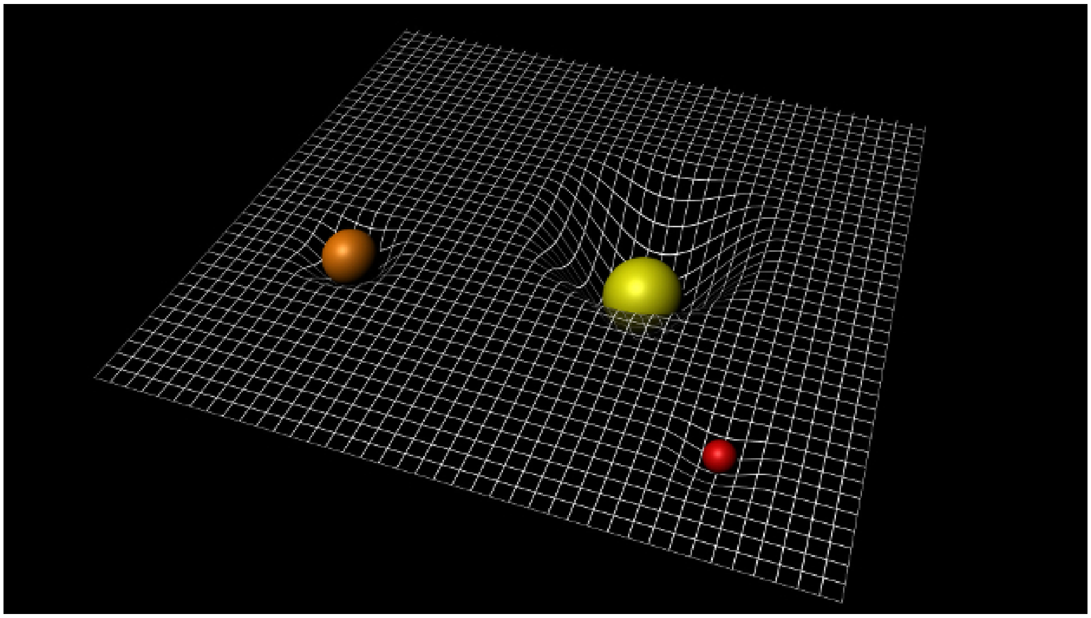

(a) The curvature of space-time, predicted by general relativity. More massive objects create a larger dent in the fabric of space-time than less massive ones. Image credits: *ESA*.

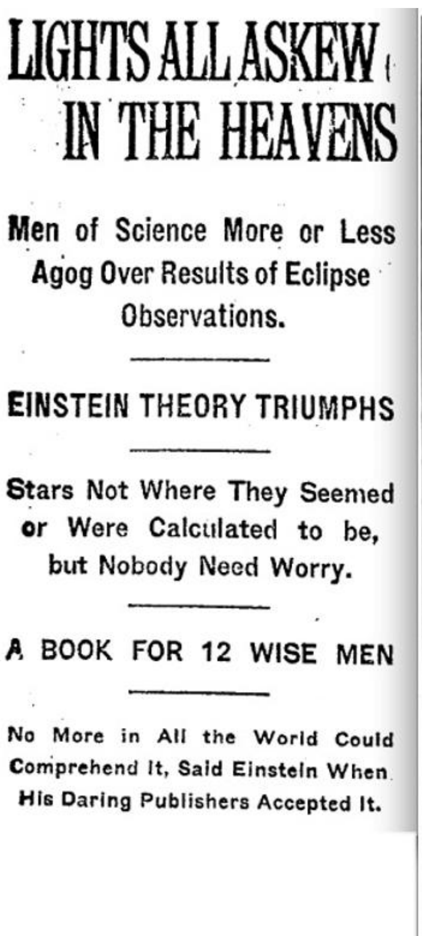

LIGHTS ALL ASKEW IN THE HEAVENS

Men of Science More or Less Agog Over Results of Eclipse Observations.

EINSTEIN THEORY TRIUMPHS

Stars Not Where They Seemed or Were Calculated to be, but Nobody Need Worry.

A BOOK FOR 12 WISE MEN

No More in All the World Could Comprehend It, Said Einstein When His Daring Publishers Accepted It.

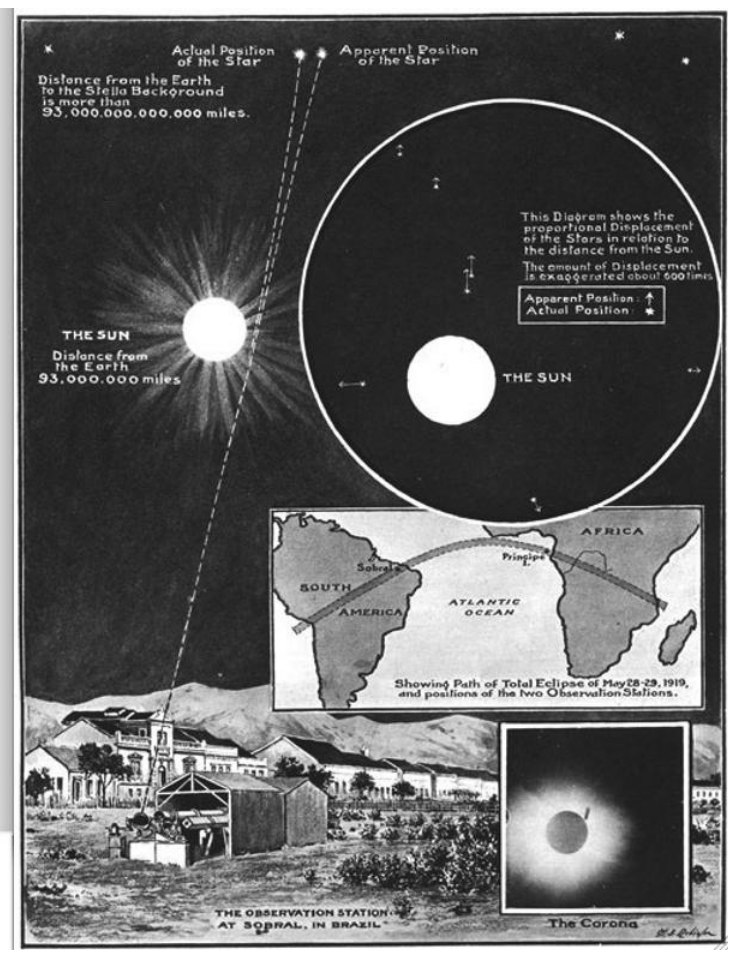

(b) Newspaper reports of the solar eclipse of May 1919 verifying Einstein's theory of general relativity from *The New York Times* (L) and *The Illustrated London News* (R). Image credits: *Forbes*.

Figure 3: Model of (a) general relativity and (b) verification in 1919.

or less than the Sun's) star's lifespan, formed when stars burn through most of their fuel and shed off their outer layers to leave behind a very hot, dense core. A cubic centimeter of a white dwarf would weigh about a ton [12]! What Chandrasekhar found was that there was limit to how heavy these objects can get.

The truth about stars is that they need something to fight the ever-present attraction of gravity, which in their normal lifetimes is the heat generated by their nuclear fuel. When a star burns out of its nuclear fuel and shrinks to a white dwarf, the particles it is composed of, including electrons, get much closer to each other, reducing it to a bunch of positively-charged ions surrounded by a sea of electrons (instead of a collection of individual atoms). By virtue of what is called the "Pauli exclusion principle" (named after Austrian physicist Wolfgang Pauli), no two electrons can occupy the same *quantum state*. What this means is that the electrons in a gas must be in different discrete energy levels and so must have different speeds with which they travel. Consequently, the electrons in a white dwarf must move away from each other and prevent the star from compressing further, allowing the white dwarf to live out the rest of its days in peace.

But recall that nothing moves faster than light in vacuum. Accounting for this maximum limit, Chandrasekhar reasoned that when a white dwarf's mass gets close enough to the Sun's, even the repulsion guaranteed by the exclusion principle could no longer defeat gravity's pull in this stellar tug-of-war. The white dwarf can no longer support itself against its own gravity and simply...collapse [13]! Later, the value of 1.4 $M_\odot$ (1.4 $\times$ the mass of the Sun) was adopted as this maximum mass, which is famously known as the "Chandrasekhar limit." Chandrasekhar's work pioneered the physics of degenerate matter, and in 1983, he and Fowler became the first astrophysicists to win the Nobel Prize in Physics.

Chandrasekhar's theory accounts for about 97% of the stars in the Milky Way, but what happens when a white dwarf's mass exceeds 1.4 $M_\odot$? Russian physicist Lev Landau found another possible final state of stellar evolution – the ultra-dense neutron star. When you have a star that starts with at least 8 $M_\odot$, it can collapse into a state where the attraction of gravity may be balanced with the repulsion between neutrons and protons, instead of electrons, and where the star is composed primarily of neutrons (hence the name neutron star). These aged relics of once shining spectacles in the emptiness of space are much, much denser than white dwarves – in fact, a Rubik's cube's worth of neutron star material would weigh several *billion* tons [14]! It would appear at this point that stars simply got denser as you put more mass into them in these final stages. This begs the obvious question: do they eventually collapse to infinite density?

In 1935, to a doubtful audience at the Royal Astronomical Society, Chandrasekhar posited that nothing could stop the collapse of a white dwarf past the Chandrasekhar limit. Eddington, with whom Chandrasekhar actually voyaged to England for the first time, vigorously opposed this. Robert Oppenheimer, father of the Manhattan projects, presented a similar argument for neutron stars (1938). The physics community was once again divided by another major controversy, over the existence of gravitational singularities. The debates, at least from a theoretical standpoint, ended when Oppenheimer and one of his students, Hartland Snyder, published a paper in

1939 titled, “On continued gravitational contraction” [15].

In their pioneering work, Oppenheimer and Snyder asserted two fundamental tenets of gravitational singularities: i) Through our old friend the Einstein field equations, we find that unless a dying star shrinks to below the Chandrasekhar mass, it will continue to collapse indefinitely under the force of gravity and ii) Though an observer from the outside would see this collapse play out over a finite period of time (in the order of a day), after the star has collapsed to a certain radius (remember equation (2)?), light would take an infinite amount of time to escape it – rendering the star invisible to anyone who wishes to observe it. Neutron stars, as it turns out, also have a maximum mass – of about 3 $M_\odot$.

But enough about the theory of gravitational singularities, what observations could back up such extreme conjectures? It took until 1943, when an American astronomer at Mt. Wilson, Carl Seyfert, published his discovery of galaxies so bright at their centers that the core brightness matches the brightness of all the stars in the entire galaxy combined (Fig. 4) [16]. Seyfert also noted that these twelve galaxies had unusually broad lines in their emission line spectra; this had the remarkable implication that the gas and other matter surrounding the center was moving at several thousands of kilometers a second. This beats even the speed of matter expelled when stars explode in supernovae in our galaxy!

Light ranges over the electromagnetic spectrum: our eyes can only see a tiny sliver of it (400-700 nanometers in wavelength). Waves from the radio part of the spectrum are about a million times as large as those we can see. Radio waves were first detected in outer space in 1932 at the center of our galaxy by Bell Labs' Karl Jansky. In the 1950s though, as the search for radio sources gained traction, we discovered them outside of our galaxy: Baade & Minkowski (1954) realized the radio source Cygnus A was actually born out of plasma in the center of the galaxy M87. More spectacular still, the radio waves shot out of the galaxy's nucleus in *jets* traveling in opposite directions. And like Seyfert, they found ionized gas with unusually broad emission lines in their emission spectra, implying the matter from the radio-bright center was moving very fast. Something weird was happening in the center of M87 that no one could explain. Then, we saw stranger radio sources much further away in the observable universe.

Much like the political, social and cultural arenas, the ‘60s were an eventful decade for extragalactic astronomy. While the Beatles were taking Earth by storm, astronomers started finding the brightest bodies in the heavens. Caltech astronomer Maarten Schmidt found optical emission lines of radio source 3C-273 at unexpected wavelengths and suggested these were the same lines as Hydrogen's[5], simply shifted by 16% to the higher frequency, or red end of the spectrum. He realized this object was at a considerable *redshift*. Since the universe is expanding, the further a galaxy is from us, the faster it is moving away from us: this corresponds to a shift in wavelength and frequency of light from the galaxy, which makes us see the light as redder than it actually is. We observe this on a pedestrian scale when we hear the siren from an ambulance whizzing past us – as it's moving toward us, the siren seems to increase

[5] $H\alpha$, $H\beta$, $H\gamma$, $H\delta$, $H\epsilon$

(a) NGC 7742. Credits: *Hubblesite.*

(b) NGC 4258 (M106). Credits: *Hubblesite.*

(c) NGC 1642. Credits: *Hubblesite.*

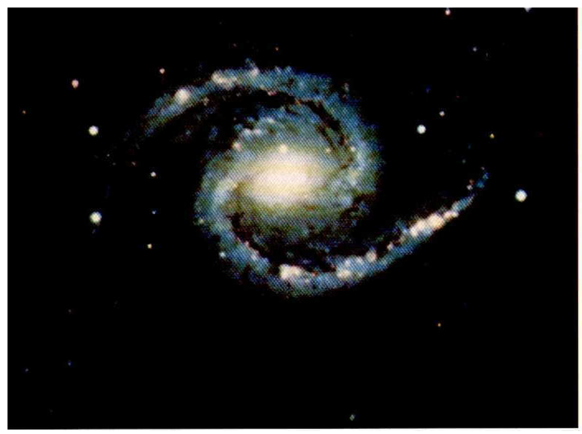

(d) NGC1542. Credits: *High Energy Astrophysics group*, Max Planck Institute of Extraterrestrial Physics.

Figure 4: Some examples of Seyfert galaxies, whose centers are as bright as the rest of the galaxy combined.

in pitch; as it moves away from us, the siren becomes less shrill. By measuring this observed frequency shift, we get redshift – this tells us how far the light source is from us. In fact Schmidt shocked the world of astronomy (and appeared on the March 1966 cover of *Time* magazine), when he found that despite appearing a 100 times brighter than the Milky Way, 3C-273 was over 2 billion light years away from us! It was the first ever quasar, or quasi-stellar object (QSO), we detected.

The biggest shock these quasars would provide is that their light originates from regions mere light hours and light weeks to at most a few light years across – smaller than the size of a solar system! 3C-273 was far from being an entire galaxy; it's simply a small region at the center, much like the strong nuclear emission from Seyfert's galaxies. The key to realizing this fact was to look at the *variability* of quasar luminosities. It was found that quasars vary in brightness by significant amounts in the span of months, weeks, days, and even hours. A rise and fall in brightness of a quasar over a period of a week means that light would take a week to travel the length of the quasar. And on account of nothing traveling faster than light in free space, the size of the quasar can not exceed a light week. Most of the distant quasars we see emit radiation in the order of trillions ($\times 10^{12}$) or more times that of the sun.

This created an absolutely unavoidable energy crisis. How could so much energy be produced in a tiny region smaller than a solar system of a single sun? How could you possibly pack the weight of billions of suns into this space (which is less than a millionth the size of a galaxy)? Astrophysicists were stumped as to what process could generate energy so incredibly efficiently. The usual suspect in astrophysical energy conversion processes is thermonuclear reactions such as nuclear fusion in the core of the sun. These are at most 0.7% efficient, failing miserably to explain what powered quasar engines. Some considered high energy gamma rays and supernovae explosions, but these are very transient phenomena, lasting at most a few weeks. The answer, as you may have anticipated by now, came from the oldest trick in the physicist's playbook – gravity.

In the early '60s, Einstein's theory of general relativity once again crossed paths with astrophysics. In an attempt to explain radio sources in the sky, William Fowler and Fred Hoyle proposed a very massive (millions to hundreds of millions of times the sun's mass; $10^6 - 10^8$ $M_\odot$) star-like object collapsing under its own gravity to form a disc of matter around the central collapse [17]. In 1963, the Texas Symposium on Relativistic Astrophysics was founded, and some of the world's most illustrious astronomers argued the case for a gravitational energy source at the heart of quasars. Authors such as Hong-Yee Chiu (who coined the term "quasar" in 1964), Ivor Robinson, Alfred Schild and Lloyd Berkner believed that the principles of relativity lead to the unavoidable conclusion that very dense objects at the centers of quasars convert matter falling into them, releasing the intense radiation we observe from them [18].

In 1964, both British astronomer Edwin Salpeter, and Soviet physicist Yakov Zel'dovich, suggested that objects heavier than a million (10^6) $M_\odot$ could passionately consume matter onto themselves by force of their deep gravitational potential well. The matter, they suggested, would be converted to radiation by virtue of the most famous equation in all of physics:

$$E = mc^2. \tag{3}$$

The stunning implication was that these very dense, massive objects at the centers of galaxies *grow* by feeding on matter around them and releasing energy through this accretion process. John Wheeler, in the same year, suggested that the source of this energy was a gravitational singularity, bringing back echoes of the ideas of Schwarzschild, Chandrasekhar, Oppenheimer, Snyder, and others. He also proposed we call such singularities **black holes**. By the end of the decade, English astrophysicist Donald Lynden-Bell had suggested that the engines powering quasars were large collapsed masses in galactic nuclei. He went one step further to claim that quasars exist not only in distant galaxies as we observe them, but also in the nearby ones, as "dead" quasars in their centers (How do quasars die? More on that in a bit).

Of course, theory can only provide so much satisfaction in explaining the nature of reality. It was an observational triumph in 1967 that propelled the idea of black holes from an intellectual quest to a matter of meticulous experimental investigation. Jocelyn Bell Burnell was a graduate student at Cambridge University in 1967 when she noticed extremely fast and consistent radio signals coming from a source in the sky. Having observed a signal every 4/3 of a second, she realized no known object in the sky ticked so consistently like a clock. The source was initially dubbed "LGM-1" (LGM = Little Green Men) because the possibility of an alien civilization emitting these signals wasn't entirely off the table! By the next year, Bell Burnell's findings had been published [19] and other radio telescopes around the world confirmed the frequency and consistency of the signals. LGM-1 was understood to be a rapidly rotating neutron star (rotating due to interaction between its magnetic field and matter surrounding it) and these objects were dubbed "pulsars" (short for pulsating star). Unfortunately, the 1974 Nobel Prize in Physics for the first ever discovery of a neutron star didn't go to Bell Burnell – instead it went to her Ph.D advisor Anthony Hewish and collaborator Martin Ryle. So much for progress in the astronomical sciences...

This exciting discovery of the ultra-dense state of degenerate matter left astrophysicists with the million dollar question: if neutron stars can exist, why can't black holes? In 1971, the newly launched Uhuru X-ray satellite picked up strong X-ray signals from a source called Cygnus X-1 and found that its magnitude varied on mere milliseconds (indicating, of course, that this radiation was produced in a very small region – about a 100 miles) [20]. What baffled astronomers was that the X-rays were emanating from a blue supergiant star, which is most certainly not capable of producing such high energy radiation by itself. The only way to account for these X-rays was that another star in close orbit was pulling in gas from this one and rotating the gas in high speed, thereby heating it up to billions of degrees at which point it can emit X-rays (Fig. 5). The blue supergiant is part of what we call a binary star system; the star sucking its gas to produce variable X-rays is at least 10 times as heavy as the sun. This is well beyond 3 $M_\odot$, so it couldn't be a neutron star [21]. After 200 years of mathematical conjectures, theoretical predictions, and observational breakthroughs, we finally found in Cygnus X-1 a black hole in real life.

The secure detection of a black hole candidate set the stage for finding something even more fantastic. We now had confidence that the existence of massive dark objects in the sky could be inferred from high quality observations. By the '80s, the consensus in the astrophysics community was that the power source of distant quasars were gravitational in nature, and the search for such powerhouses were being conducted in nearby galaxies. Thankfully for us, matter on galactic scales moves around large masses by the same laws of orbital motion discovered by Johannes Kepler in the 1600s that explained the motion of planets in the solar system, enabling us to greatly simplify our calculations of the motion of matter in our galaxy and others.

In 1978, Sargent et. al. found that the velocity dispersion and rotational velocity of the galaxy M87 keeps increasing toward its center – something was causing stars to

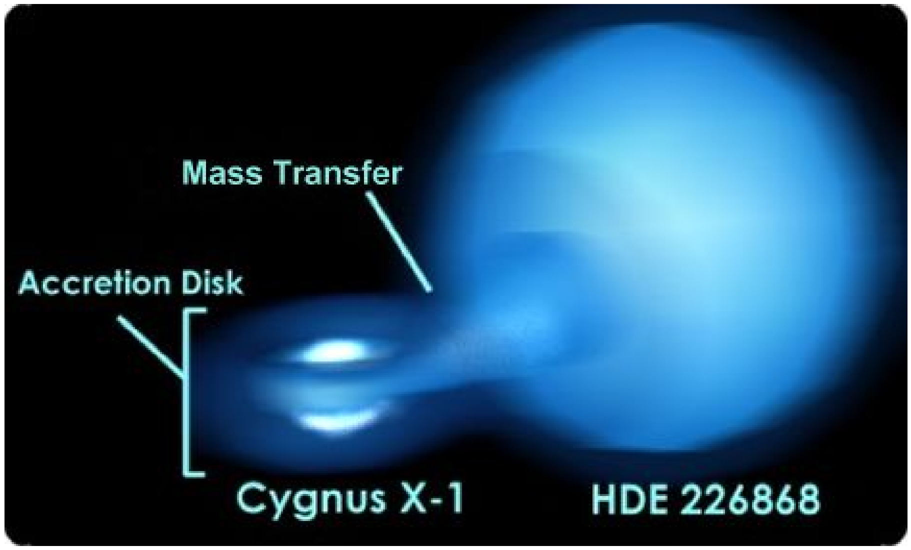

Figure 5: Illustration of Binary star system containing Cygnus X-1(left) and blue supergiant companion HDE 226868 (right). Mass from the supergiant is pulled in by gravitational attraction of the black hole and heated up in an accretion disk around it. Image credits: Brian Ventrudo, *The One Minute Astronomer*.

orbit extremely fast near the very center.[6] Their calculations revealed that the only explanation for such motions was the gravitational pull of a central mass of 5 $\times 10^9$ (5 billion) $M_\odot$ lurking in M87's nucleus [23]. Similarly, galaxy dynamics were used to argue for the existence of central mass concentrations of 3 $\times 10^7$ $M_\odot$ in Andromeda (M31) [24] and 2 $\times 10^6$ $M_\odot$ in M32 [25] a few years later. There was now a growing body of evidence for very, very large black holes at the centers of galaxies.

Quasars are only one of the members of a class of interstellar objects we call **Active galactic nuclei (AGN)**. Another example is the aforementioned Seyfert galaxies. A critical shortcoming of AGN research as we moved into the '80s was the relative lack of such powerful objects seen in the nearby universe. Why do we see so many more AGNs in galaxies many billions of years in the past (at redshifts of 2 and above) and only one AGN in 500 in nearby galaxies? If SMBHs exist in M31, M32, and M87, why don't their cores shine as brightly as those of high redshift galaxies? The answer to this paradigm was already alluded to by Donald Lynden-Bell in 1969, which Polish astronomer Andrzej Soltan used as the building block to a compelling theory he proposed in 1982, famously dubbed "Soltan's Argument."

Building on the assumption that quasars are powered by mass accretion on to SMBHs, Soltan used available observational data on quasars to estimate the energy density, and subsequently, the mass density of matter accumulated by SMBHs in quasars. He found that it is statistically likely that a SMBH would be found a few megaparsecs[7] from us. In other words, the engines powering AGNs didn't just

[6]The key ingredient was the *rotation curve* of the galaxy – essentially a plot of the orbital speeds of visible matter versus their radial distance from that galaxy's centre. Rotation curves were also the key to figuring out the existence of dark matter. See Ref. [22].

[7]1 Megaparsec (Mpc) $\approx$ 326 million light years. For context, the nearest massive galaxy, An-

disappear (try explaining your way out of *that* one!), but rather they became *dormant*, like volcanoes do. Soltan, and many others after him, hypothesized that SMBHs which were actively feeding on matter around them and expelling ungodly amounts of energy in the distant universe, were simply not feeding as voraciously in more recent times. This explained why we only see a handful of active nuclei in nearby galaxies, but perhaps even more excitingly, it agreed with the notion that SMBHs could exist in galaxies as close as M31, M32, and M87.

In 1990, the Hubble Space Telescope *(HST)* was launched into orbit, ushering in a new era of astronomical discoveries. This was the big break the field of massive black hole research needed – *HST's* expansive, extended vision from outer space allowed us to peer deep into the hearts of galaxies nearby. What followed was the study of *gas dynamics* in galactic centers: spectrographs on board the *HST* showed us disks of ionized gas rapidly orbiting about the centers of galaxies. Gas on either side of these disks appeared to move very fast in opposite directions, indicating rapid rotation about the center. Gas in a disk about 5 parsecs to the center of M87 was found to rotate at a whopping 550 kilometers per second on either side of the disk, confirming that over 3 billion suns' worth of mass was somehow packed in its central 11 pc [26]. The rapid motion of ionized gas was used to infer that M87's neighbor, M84, must also be harboring a SMBH of over 10^9 $M_\odot$ at its center. With the advancements in telescope technology in the '90s, we were beginning to find strong dynamical evidence that SMBHs exist outside our tiny Local group.

The most powerful evidence to date however, lies in our own backyard, so to speak. In 1974, four decades after Jansky's discovery of radio waves from the center of the Milky Way, the baseline interferometer at the National Radio Astronomy Observatory (NRAO) detected synchrotron radiation from a very small region (less than 3 light years across) at the center. Synchrotron emission is what you get when electrons moving near the speed of light accelerate – as a matter of fact, spiral – through magnetic fields. Moreover, there were no counterparts to this source in the optical, infrared or X-ray. The mythos of this source, named Sagittarius A* (or Sgr A*), and the galactic center, began intensifying as we observed rapid motion of gas clouds near the center in infrared. Pretty soon, spectroscopy of ionized gas disks led to the conclusion that Sgr A* is the location of a SMBH weighing about 2.5 $\times 10^6$ $M_\odot$ [27].

However, we did one better. A great advantage of studying the center of the Milky way is that because of its proximity to us, we can observe, with exceedingly great detail, the motion of *individual stars* near the center and not just that of accumulated gas (which can be easily knocked around, being light). For years, astronomers focused on a cluster of about 20 bright stars located within 0.05 pc of Sgr A*, mapping out their elliptical orbits about the center (Fig. 6). Monitoring of these stars began at the European Space Observatory (*ESO*) in 1992, and in 2003, the orbit of the brightest star in this cluster, S0-2[8], was published as the star was already about 2/3 into a complete orbit [28]. Such staggeringly fine detail presented us the most reliable

dromeda, is about 2.5 Mpc from Earth

[8]At least that's what UCLA's Galactic Center group named it. Germany's Max Planck Institute for Extraterrestrial Physics (MPE) calls it S2.

evidence ever of a SMBH: it is now widely accepted that Sgr A* harbors a black hole the mass of $\approx 4 \times 10^6$ $M_\odot$ at the very center of the Milky Way. As a bonus, we also know we are located about 27000 light years (∼8 kpc) from it.

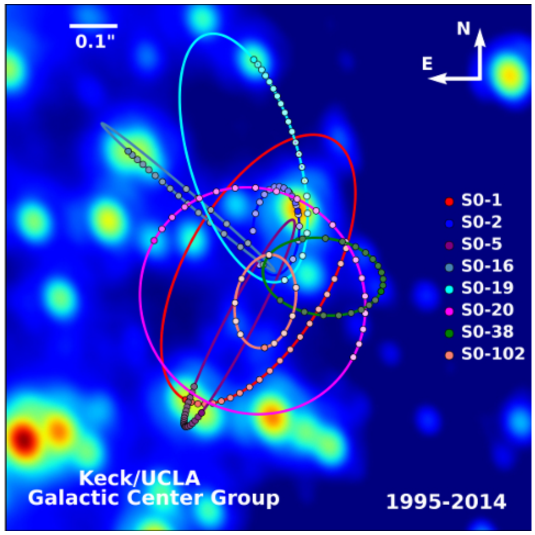

Figure 6: Orbit of stars within 0.02 pc of the Sgr A* at the center of our galaxy. The orbits around the unseen central mass and their associated orbital velocities make a strong case for a supermassive black hole of 4 million solar masses. Image credits: Andrea Ghez and *UCLA Galactic Center Group*.

But how integral is a SMBH to a galaxy? In the year 2000, an astonishing connection was made between SMBHs and the origin and evolution of galaxies. By this time, the astronomy community already began noticing that the larger the mass of the central spheroid of stars[9], the greater the central black hole's mass would be; the SMBH would weigh about 0.5-1% as much as the galaxy. Since mass can be scaled to light, this implied that M_{BH} and L_{sph}, the luminosity of the stellar spheroid, were proportional quantities.

However, an even more compelling correlation was reported by two groups of researchers. They found that for over two dozen nearby galaxies, M_{BH} seemed to be strongly correlated with the central velocity dispersion, σ, of a galaxy's bulge [29, 30]. Functionally, this meant that the speeds of stars throughout the galaxies are directly related to the mass of the SMBH at their centers! With small enough scatter, it was found that M_{BH} is directly proportional to the fifth power of σ:[10]

$$M_{BH} \propto \sigma^5 \tag{4}$$

The exciting aspect of this finding was that it was a "tight correlation." The observed scatter around the M_{BH}-σ relation was found to be about 0.3 dex[11] over a large range of masses, most of which was attributed to observational errors. So

[9]see section 1.1.

[10]There is considerable controversy over whether or not this power is 4 or 5. See section 1.3.

[11]A dex is simply an order of magnitude. 0.3 dex translates to a factor of $10^{0.3} \approx 2$.

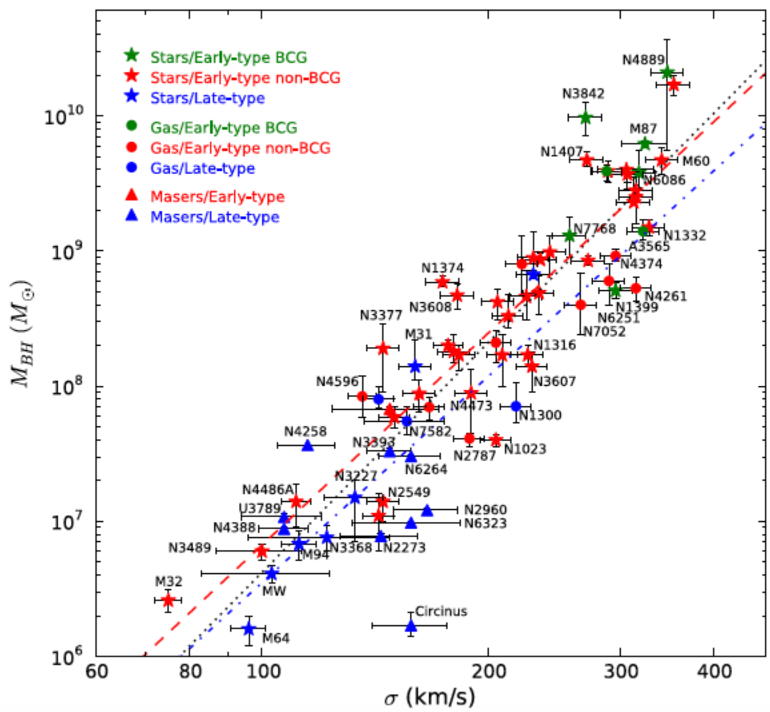

Figure 7: M_{BH}-σ relationship for a sample of 72 galaxies found by McConnell & Ma 2013 [31]. The plot notes the galaxy type and method by which M_{BH} was measured.

these data were so good, that after accounting for the measurement errors, all the scatter was accounted for; suggesting that we could claim a new law of physics in this **M-sigma relation**. Excitement spread from the fact that, based on this new "law," a difficult quantity to measure, M_{BH}, could be estimated from a much simpler observation to make, σ.

Was a fundamental relationship between SMBHs and their host galaxies found? While we still don't know the answer to this question, the more M_{BH} measurements we made, the stronger the case became for a tight correlation between black hole mass and velocity dispersion. Having taken caution in removing poorly resolved measurements, the scatter in the M_{BH}-L_{sph} relation is also reduced significantly, allowing us to make a stronger case for relating the growth of a SMBH to the formation of the galactic spheroid wherein it rests. Black hole mass measurements in nearby galaxies increased from a few in 1998, to three dozens in 2004, to nearly three hundred by 2016 [32]. SMBHs have been discovered in most galaxies more massive than 10 billion $M_\odot$, and even in much smaller ones, the so-called "dwarf galaxies."

We've come a long way since debating the existence of other galaxies. Heck, we've come a long way since first wondering how quasars could shine ultra bright despite being billions of light years away from us. Yet, the study of SMBHs has barely scratched the surface of the treasure chest of information that awaits opening. For starters, we don't yet know how SMBHs form. Among the hypothesized origins of a SMBH are the collapse of primordial gas clouds in the early universe and the merging of several smaller black holes bound together in a cluster, although studying the exact physical mechanisms that create a SMBH is beyond the scope of this thesis. If SMBHs and their host galaxies do co-evolve, what are the ways in which a SMBH regulates the growth of its host?

While theoretical simulations are providing a wealth of insights, the fact remains today, that our theoretical understanding of the topic can only advance with the leaps made by our observational exploits. The BHMF is the primary empirical tool available to us for investigating how SMBHs evolve. Regardless of the formation scenario(s) we prefer, it sets interesting constraints on how SMBHs have grown up to the present day. It's also our gateway to characterizing the SMBH population in terms of its one quantity we can measure, mass.

The scaling relationships between M_{BH} and a galaxy's properties allow us to estimate the M_{BH} for a much larger sample of galaxies than the few for which we have M_{BH} measured. This gives us a distribution function, or simply a number density of galaxies for a given property, such as the aforementioned σ. By some neat statistical machinery, we can convert this into a number density of SMBHs of a given mass. This can lead to an estimate of the density of mass accumulated by SMBHs to the present day, helping us better understand how they grow and *how much* they grew. The number density, mass density, and the shape of the BHMF are all important guiding stones in constructing a complete picture of the origins, evolution, feeding habits, and eventual fate of SMBHs. While the primary goal of this thesis is to gain insight into SMBHs by means of the BHMF, I will also engage with how such an analytical tool can help us in uncovering useful science.

Chapter 1

Observations: Black hole masses and velocity dispersions

This chapter starts with a brief overview of galaxies, their SMBHs, and aspects of cosmology which we will be using later on. Then I move on to describe some of the observations which will fuel my analysis, as well as describe where most of the data on nearby galaxies I'm using comes from. In what follows, I will use the terms "source" and "object" interchangeably.

1.1 Some background

1.1.1 The structure of galaxies and galactic nuclei

A galaxy is a system of stars, dust, interstellar gas, dark matter, and perhaps one or more supermassive black hole(s), gravitationally bound together. Galaxies can be as heavy as anywhere from 10^7 $M_\odot$ (dwarfs) to 10^{13} $M_\odot$ (giants). The earliest forms of galaxy classification relied on morphological characteristics. Visual morphology was the key to Hubble's (1926) famous classification scheme, often referred to as the "tuning fork diagram" (Fig. 1.1). The so-called **Hubble sequence** divides galaxies into 3 main categories: elliptical, spiral, and lenticular, and 1 secondary category for irregular galaxies – those that don't fit any of those defined shapes. Hubble envisioned the tuning fork diagram to be an evolutionary sequence – so that galaxies evolved from the early-type ellipticals and lenticulars on the left-hand side to the late-type spirals on the right. The picture, in reality, is far more complex than simple visual characteristics however, since we need to take into account crucial features such as star formation activity and history of interaction, or mergers, with other galaxies. Regardless, his nomenclature is still useful for quickly differentiating between the main types of galaxies we observe, so I will refer to elliptical and lenticular galaxies as early type galaxies and spiral galaxies as late type galaxies.

When present, SMBHs are always found in galactic nuclei, whether they be in the spheroid (or ellipsoids) of stars making up an elliptical galaxy, or in the central bulge of stars in a spiral or lenticular galaxy. Ellipticals are almost entirely smooth

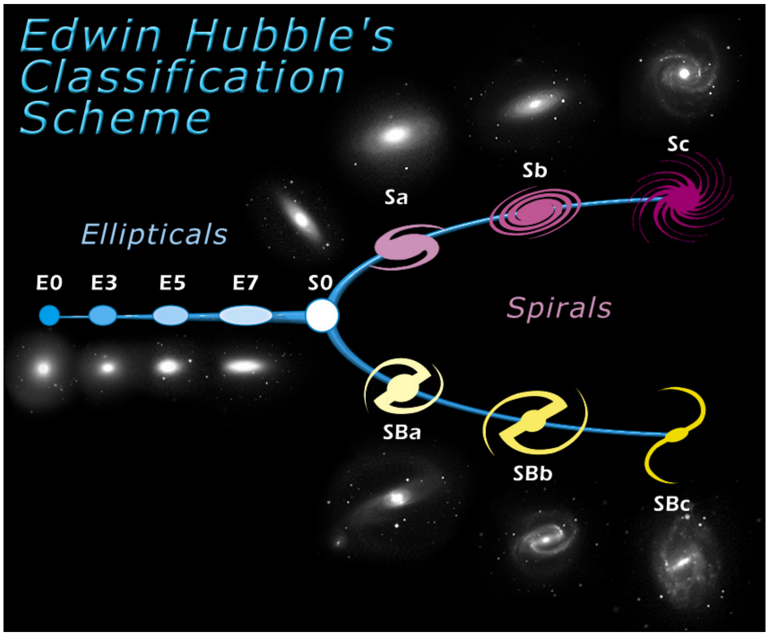

Figure 1.1: The tuning form diagram, illustrating the Hubble sequence. Ellipticals (E0-E7) and lenticulars (S0) are referred to as early-type galaxies, while barred spirals (Sa-Sc) and unbarred spirals (SBa-SBc) are referred to as late-type galaxies. Image credits: *Hubble*.

and featureless: all the stars are contained in their stellar spheroids. Meanwhile, spiral and lenticular galaxies have more parts to them – a bulge of stars and a central disk cutting through it. Spirals, as the name suggests, also have a number of spiral arms. Elliptical spheroids and lenticular bulges are known to rotate slowly, while spiral bulges are fast rotators. The one true similarity between spheroids in early and late type galaxies is the light distribution, or the *surface brightness profile*, $I(r)$, which is well-described by a power law: $I(r) \propto r^{1/n}$ (where r is the projected distance from the center and n an integer known as the Sérsic index[1]). I will hereafter refer to spheroids and bulges as simply spheroids, and in the discussion that follows, the distinction isn't very important.

The leading theory of SMBH growth is the idea that they grow by accretion of matter during active phases. As mentioned in the introduction, the Soltan argument made it clear that accretion needs to occur in phases in order to build up the mass density of SMBHs we observe today. Consequently, we have an accepted paradigm, where the nearby galactic nuclei (including our own) with relatively quiescent SMBHs must have had some active phases, where they shone spectacularly, at earlier times. Evidently then, much like star formation, mass accretion on to SMBHs is a cyclic process.

[1] I refer the reader to de Vaucouleurs [33] and Sérsic [34] who provide some of the first mathematical modeling of light distribution in galaxies.

1.1.2 Observational Cosmology

The model of cosmology most widely used today is generally known as the standard model of cosmology, or **Λ-CDM (Cold Dark Matter) cosmology**. The Λ-CDM model postulates a beginning of time with the Big Bang, the subsequent expansion of the universe, and since about five billion years ago, expansion at an accelerated rate. According to the model, only ~5% of the universe we know and love is made up of ordinary, *baryonic* matter we can observe. ~25% is the elusive dark matter[2] and the remaining ~70% is a mysterious vacuum pressure which causes the acceleration of the universe, termed dark energy. To parametrize these constraints, we use dimensionless density parameters:

$$\Omega_M + \Omega_\Lambda + \Omega_k = \Omega_0, \tag{1.1}$$

where Ω_0 is the critical density of the universe, which through recent observations, is given a value of 1. The critical density is the particular density that ensures both that the Universe will not expand forever, and not collapse back on itself. Ω_M and Ω_Λ are the ratios of the average density of matter and dark energy in the universe, respectively, to the critical density. Ω_k describes the curvature of space-time, which we assume to be geometrically flat, i.e. a curvature of zero. Hence, in Λ-CDM, we use $\Omega_M = 0.3$, $\Omega_\Lambda = 0.7$, and $\Omega_k = 0$.

Distances in Cosmology

Because of this complicated business of sources perpetually moving away, distance measurements in cosmology are much more complicated than taking a measuring device and measuring the "length" between two points. The present rate of expansion of the universe is expressed as the **Hubble constant**, H_0, which describes the recession speed, v, of a galaxy as it moves away from us, in terms of its distance, d, from us:

$$v = H_0 d. \tag{1.2}$$

where the value of the Hubble constant is given by $H_0 = 100h$ km s^{-1} Mpc^{-3}. h is a dimensionless number that "parametrizes our ignorance," according to David Hogg (1999). At the time of writing, the most recent and accurate observational determination of the Hubble constant places it at $H_0 = 73.24 \pm 1.74$ km s^{-1} Mpc^{-3} [35]. In Λ-CDM cosmology, it is conventional to take $h = 0.7$, so I take $H_0 = 70$ km s^{-1} Mpc^{-3} throughout my calculations.

I will use the following distance measures as outlined in Hogg (1999) [36]:

- The Hubble distance, D_H: The distance light travels in the Hubble time, which is the inverse of the Hubble constant:

$$D_H = \frac{c}{H_0} = 3000\ h^{-1}\ \text{Mpc}. \tag{1.3}$$

[2]The dark matter is said to be "cold" because it is non-relativistic, hence moving slowly, during the era of structure formation.

- The **comoving distance**: The distance between two objects which remains constant with time, so it accounts for the expansion of the universe. The comoving distance of an object from us, D_C, is given by:

$$D_C = D_H \int_0^z \frac{dz'}{E(z')}, \tag{1.4}$$

where z is the object's redshift and $E(z)$ is a function defined as:

$$E(z) = \sqrt{\Omega_M(1+z)^3 + \Omega_k(1+z)^2 + \Omega_\Lambda}. \tag{1.5}$$

If one were to take a gigantic ruler and measure the distance between, say a distant galaxy and us, D_C is what they would get. Hence, it's the most important distance measure in cosmology. I will use this distance for computation of both the Velocity Dispersion Function (VDF) and the Black Hole Mass Function (BHMF).

- The **luminosity distance**: Distance of an object shining with bolometric (integrated over all wavelengths) luminosity, L, and bolometric flux, S, defined as:

$$D_L = \sqrt{\frac{L}{4\pi S}} = (1+z)D_C. \tag{1.6}$$

D_L is useful for determining the absolute (true) magnitude of a source.

Please refer to Hogg (1999) for derivations and more details on these distance measures.

1.2 Measuring black hole masses

Mass is the primary property of a SMBH and measuring a M_{BH} is often considered parallel to finding evidence for a SMBH in a galactic center. M_{BH} measurements are – especially for nearby galaxies – dynamical: we observe the motion of stars, gas, or other matter near the center and infer a force responsible for this motion. Newton's law of gravity (eq. (1)) helps us easily calculate the mass that caused this force. Kinematical data, such as Doppler shift measurements or integrated stellar spectra, must be resolved spatially on angular scales where the gravitational force is dominated by the SMBH.

The distance within which a central SMBH affects the motion of gas or stars is called the **gravitational influence radius**, r_h. Within r_h, the gravitational potential of the SMBH dominates the gravitational potential of the host galaxy. There are two definitions of r_h;

1. The radius at which the enclosed mass of stars, $M_\star$, equals twice the SMBH mass, i.e:

$$M_\star(r < r_h) = 2M_{BH}. \tag{1.7}$$

   In a galaxy with mass distributed spherically, at r=r_h, 1/3 of the gravitational force comes from the SMBH and 2/3 is from stars. The difficulty in applying this equation to real galaxies is that the stellar mass density is very rarely well-defined inside r_h.

2. The radius at which the velocity of a circular orbit around the SMBH, v_c, is equal to the stellar velocity dispersion, σ:

$$r_h = \frac{GM_{BH}}{v_c^2} = \frac{GM_{BH}}{\sigma^2}. \tag{1.8}$$

   σ, as will be defined soon, is the dispersion about the mean velocity of stars. If the velocity distribution is isotropic, then $\sigma = v_{rms}/\sqrt{3}$, where v_{rms} is the root mean square (rms) velocity of stars of a galaxy. σ can easily be obtained from the 1-D line-of-sight velocity dispersion from an integrated spectrum of stars, within an aperture centered on the SMBH.

The appropriate definition of r_h to use depends on the physical situation being addressed. Definition 1 compares the force from the SMBH to the local force from the stars and is appropriate for interpreting the motion of gas moving in nearly circular orbits around the SMBH. Definition 2 compares the local gravitational effects of the SMBH with the overall effect of the bulge on the motion of the stars. Proper stellar motion or stellar spectrum techniques are useful for this definition. The sphere of influence of a SMBH must be well-resolved in order for a dynamical measurement of M_{BH}. This is why there are only a handful of such measurements in nearby galaxies.

Below, I briefly describe some of the most common methods of measuring SMBH masses dynamically and offer an alternative method of estimating M_{BH} via empirical scaling relations between M_{BH} and properties of the host galaxy, especially stellar velocity dispersion, σ.

Stellar dynamics

Integrated stellar dynamics has been a popular method of measuring SMBH masses since the early days of SMBH research and remains the most widely used method. Stars are reliable in that they're always present near galactic centers and their motion is always gravitational. At the scale of r_h, Newtonian gravity works quite well in predicting the motion of objects around the SMBH. Assuming spherical symmetry of the galaxy, we can get the mean acceleration ($\overline{a}$) of a star as the gradient of its gravitational potential, ϕ[3]:

[3] Not to be confused with the upper-case Φ I'll be using to denote distribution functions later on.

$$\bigtriangledown\phi = \frac{\partial\phi}{\partial r} = \overline{a}, \tag{1.9}$$

where r is the projected distance from the center. This enables us to approximate the mass of the black hole, M_{BH}:

$$G\left[M_\star(r) + M_{BH}\right] \approx r v_{rms}^2. \tag{1.10}$$

Here, $M_\star(r)$ the mass of stars as a function of r, and v_{rms} is the rms velocity of stars, as above. v_{rms} can be measured from how much the absorption lines in an integrated spectrum of stars are broadened. Space-based spectrographs such as the *HST's* Space Telescope Imaging Spectrograph (STIS) have taken such spectra for dozens of galactic centers. The $r^{-1/2}$ dependence of the rms velocity on the radius is a classic sign of a SMBH, and by virtue of Newtonian mechanics, this happens to be the same dependence shown by orbital velocities on the solar system planets. In other words, we have a "Keplerian" dependence. Of course, there's a lot more detailed modeling and practical considerations one needs to take into account when attempting to use stellar spectra to measure a black hole mass. These are discussed in detail in Merritt (2013) [37] and Ferrarese & Ford (2005) [38].

A major problem with this method is that spatially resolved data needs to extend to about 10% of the gravitational influence radius, r_h, which makes it hard to use this technique for galaxies much further than the Local Group. Additionally, a high spectral signal-to-noise ratio is desirable.

Gas dynamics

For several galaxies, there exist relatively regular disks of ionized gas orbiting around the central SMBH. The rotation curve of these gas disks gives us the rotational velocity of the gas, v_c. By the same Newtonian formulation, we can obtain the black hole mass from v_c:

$$v_c^2(r) = \frac{G(M_\star(r) + M_{BH})}{r}. \tag{1.11}$$

With stellar dynamics, since we're taking *integrated* stellar spectra, stellar velocities measured near the SMBH are impacted by stars that orbit to much greater distances, thereby "contaminating" the measurements. This is not a problem for gas disks. Moreover, gas measurements are averaged along the line of sight, so there's less weakening of the signal, which is always a problem with stellar dynamics. But perhaps the biggest advantage of using gas dynamics is that the motion of stars is inherently complex. For example, the rms velocity of stars may differ by direction, due to the random motion of stars. Meanwhile for regular gas disks, there is very little to no random motion as such and there is velocity is only in the circumferential direction.

If a gas disk is present in a galactic center, all we require for detecting a SMBH is that velocity data exist inside r_h (which guarantees that $M_{BH}> M_\star$ in eq. (1.11)). Many galaxies beyond the local group show a clear rise in gas velocities near the

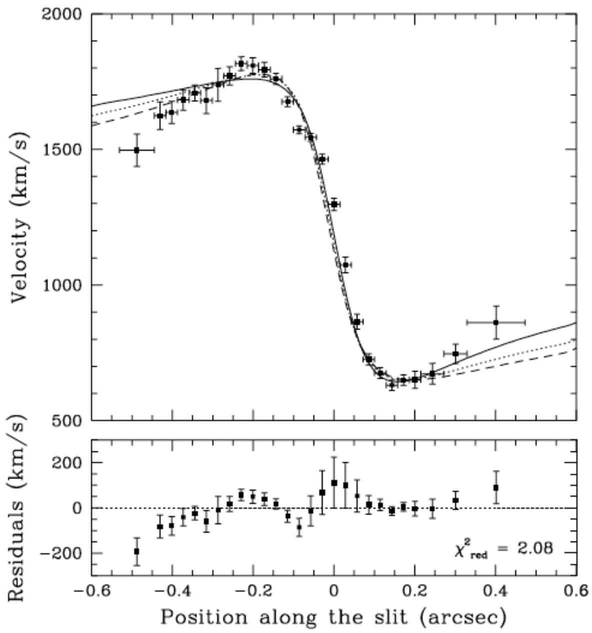

Figure 1.2: Rotation curve of the ionized gas disk in the giant elliptical galaxy M87 (from Macchetto et al. 1997 [26]). The different lines correspond to different model fits to the data, all of which require the presence of a high central mass concentration.

center. The modeling for gas kinematics is a much more straightforward process than for stellar kinematics: either you detect Keplerian motion, in which case a SMBH mass can be measured, or you don't, in which case M_{BH} can't be measured.

But there's one major issue with this method of M_{BH} measurement: gas, unlike stars, is affected by non-gravitational forces. So, things like pressure and radiation can disrupt the regular structure of ionized gas disks and introduce uncertainties in measurements made using them. Because gas disks can be accelerated by non-gravitational forces, the Keplerian rotation may be disturbed. Also, there's the problem of relatively few galaxies containing a nice, regular disk of ionized gas orbiting the center.

Water maser clouds

In a small class of active galaxies, we have the opportunity to measure the rotation of nuclear matter at much higher resolutions than stellar or gas kinematical techniques. These galaxies contain what are known as **water masers**. These are produced when X-rays from the innermost accretion disk around the central SMBH heat up a torus of dense circumnuclear gas and dust [39]. The term maser[4] stands for Microwave Amplification by Stimulated Emission of Radiation. A maser is produced when water molecules absorb energy from their surroundings and re-emit it in the microwave. Similarly, in some galactic nuclei, dense clouds of water molecules surrounding the SMBH accretion disk are stimulated, by accretion disk X-rays, into

[4]think laser

emitting microwave radiation.

The maser emission, which occurs at 22 GHz, can be studied by radio interferometers such as the Very Large Baseline Array (VLBA) at spatial resolutions > 200 times that of optical telescopes such as the *HST*. This leap in resolution corresponds to an ability to detect much less massive SMBHs. Maser clouds exhibit Keplerian motion similar to gas disks and stars around a SMBH. This can be exploited, using a similar Newtonian formalism, to obtain the mass of the black holes around which they orbit.

AGN reverberation mapping

In non-quiescent, active galaxies – even if they're close enough that their SMBH sphere of influence can be reasonably well-resolved – the nuclei are too bright and point-like (as a result of the gaseous, active accretion disk). This diminishes the features in the sphere of influence that are necessary to make dynamical measurements. For these galaxies (AGNs), reverberation mapping can be used to find a measurement of M_{BH}.

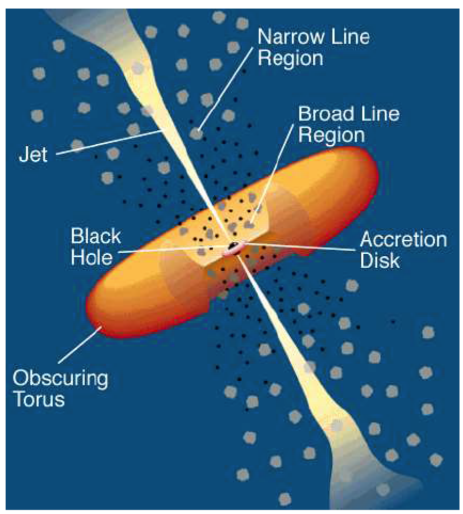

Figure 1.3: AGN structure, showing the Broad Line Region (BLR). Figure from Bentz (2015) [40].

The emission spectra of AGNs show broad emission lines – such as those in the Hydrogen Balmer series – in the optical and ultraviolet. The line widths are presumed to show Doppler broadening and can be mapped on to a velocity broadening function. The quantity of interest from this function is its ΔV, the Full Width at Half Maximum (FWHM). The accretion disk around the central SMBH produces a high-energy continuum that varies with time and photoionizes gas in the central ~ 0.01 pc of the SMBH (a model of AGN structure is shown in Fig. 1.3). The broad emission-line fluxes respond to the changes in the flux from the continuum source, implying that photons from the accretion disk are responsible for the emission lines. However, light travels at a finite speed, so there's a delay between a change in the continuum of the accretion disk and the subsequent response of the emission lines. The region in which this delay takes place is called the broad line region (BLR). Thus, if we can measure the size of the BLR via the delay time, and we're equipped with the observed ΔV, we easily recover M_{BH}:

$$GM_{BH} = fR_{BLR}(\Delta V)^2. \tag{1.12}$$

Here, R_{BLR} is the radius of the BLR, and f is a "form factor" – a constant between 0 and 1 that depends on the geometry and kinematics of the BLR. The form of the BLR is difficult to ascertain and requires high-quality, extensive 3D data, for which f is often determined by modeling the BLR first.

A special case: proper stellar motion in the galactic center

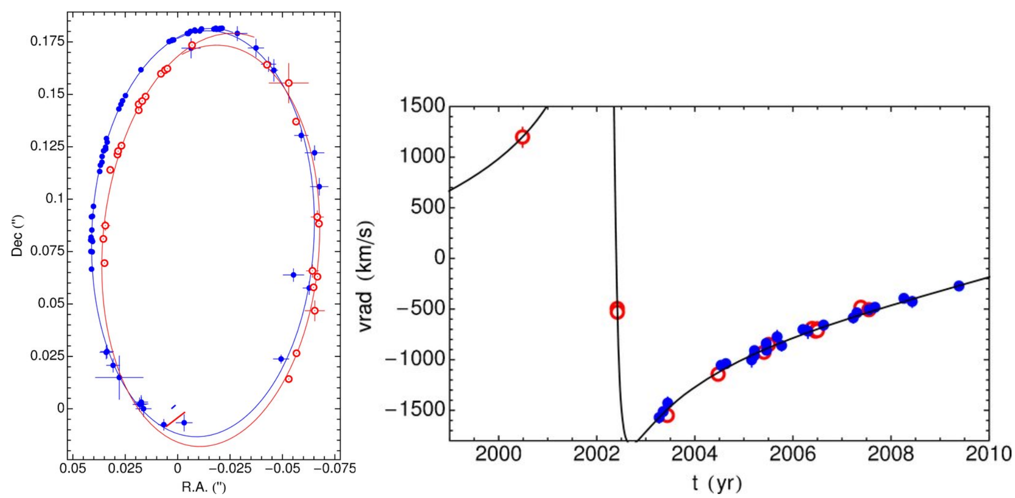

(a) Orbit of S0-2 (b) Radial Velocity of S0-2

Figure 1.4: a) Orbit of star S0-2, showing its apparent position in the plane of the sky in a $\sim$ 16-year period, and b) Radial velocity, with the black line showing the prediction from the orbital fit, from [41]. The red and blue data points are observations from W.M. Keck telescopes and the Very Large Telescope (VLT), respectively. The data from these two different observatories produce the same result of a central SMBH of 4.3×10^6 $M_\odot$.

In the central arcsecond of the Milky Way ($\sim$2 light-months), lies about 20 bright stars clustered close together. These so-called "S-type stars" have Keplerian orbits which we can model very easily and their positions are studied in very high resolution (in the order of a tenth of a milliparsec) by ground-based telescopes such as European Southern Organization's (ESO) Very Large Telescope (VLT) in Chile and the Keck Telescopes on Mauna Kea. Continuous monitoring of the positions and radial velocities of S-type stars in the nuclear star cluster have enabled us to determine their elliptical orbits and measure the period of those orbits.

By Kepler's third law, the period of an orbit, T, is given by:

$$T = \frac{2\pi a^{3/2}}{\sqrt{GM_{BH}}} \approx 1.48 \left(\frac{M_{BH}}{4\times 10^6\ \mathrm{M}_\odot}\right)^{-1/2} \left(\frac{a}{10^{-3}\ \mathrm{pc}}\right)^{3/2} \mathrm{yr}, \tag{1.13}$$

where a is the semi-major axis of the orbit. A decade ago, the star named S0-2 completed one full 15.8 year-orbit around the focal point (Fig. 1.4). S0-2 and another star have come within 5 microparsecs (μpc) of the center, where they were both observed to move at over 10000 kms^{-1} – extraordinary for stars. Over 2 dozen stars near the center have orbits that are fit extremely well by a central potential from a single mass of $4.3 \pm 0.5 \times 10^6$ M$_\odot$ [41, 42, 43].

1.3 Estimating Black hole masses: A secondary method

The methods described above only allow us to calculate SMBH masses for a handful of galaxies. If you go far enough (which isn't very far, cosmologically speaking), you lose the ability to resolve a SMBH's sphere of influence. Estimating M_{BH} is no mean feat – high resolution observations, intelligent modeling of galactic centers and the central potential, and rigorous assessment of the random and systematic errors involved in the process are only some of the challenges. But knowing M_{BH} alone for a few, or even hundreds of, galaxies doesn't give us much meaningful statistical information about SMBHs in general. How does one estimate M_{BH} for galaxies further away than their r_h can be resolved or even for a large set of galaxies?

The answer lies in one of the oldest tenets of observational astrophysics: find phenomenological relations from empirical data. There exist many famous examples of such relationships which are foundational to the field, including the aforementioned Period-Luminosity relation of Cepheid variables, the Mass-Luminosity relation (where the luminosity of a stellar object is proportional to some power of its mass),the Tully-Fisher relation for spiral galaxies (which relates mass or intrinsic luminosity, for example, to angular velocity of width of emission lines), and the main sequence of stars (where stars belonging to this sequence lie on a well-defined temperature-luminosity line). In astronomy, where a lot of research is open to contestation and many fundamental questions are still unanswered, clear, unambiguous patterns in the observations made can be incredibly useful tools for moving forward. Observed relationships can inspire the search for the underlying physics that explains them, even if potential explanations are murky.

In that vein, we were fortunate enough to observe various relationships between SMBHs and properties of their host galaxies. As early as 1995, Kormendy and Richstone found that the 8 galaxies for which secure M_{BH} measurements existed at the time, M_{BH} was about 2-3% of the mass of stars in the host galaxy [44]. Over time, it was established that M_{BH} correlates strongly with L_{sph}, the luminosity of the spheroid of the host galaxy (which correlates with mass). Observations of L_{sph} carried out at various wavelength bands from the optical to the near infrared have confirmed a correlation of the form:

$$\log M_{BH} = a + b \log y, \tag{1.14}$$

where y is L_{sph} at a given waveband. The scatter around the correlation has been observed to decrease as the sample is reduced to only elliptical galaxies. The best correlation of M_{BH}-L_{sph} showed an intrinsic scatter of about 0.3 dex, less than a third of a magnitude [45]. Relationships have also been found between M_{BH} and other properties of the host galaxy, including n, the Sérsic index of light distribution, and light concentration, which is the ratio of the fluxes within two different radii (usually one-third of the half-light radius to the half-light radius. Much like it sounds, the half-light radius, R_e, is the radius within which half the total light of a galaxy is contained[5]).

The M-sigma relation

However, a stronger correlation was found between M_{BH} and σ, the central velocity dispersion of the galaxy – the so-called M-sigma relation. Both Gebhardt et. al. [30] and Ferrarese & Merritt [29] found a significant difference between this and the M_{BH}-L_{sph} relation, which can be seen in Fig. 1.5. When one includes only measurements for which they could spatially resolve data within r_h, the M_{BH}-L_{sph} relation barely shows a difference in the scatter, however M_{BH}-σ becomes a lot tighter. At the time, this was interpreted to mean that the scatter in the M-sigma relation can be accounted for by looking at measurement errors alone. This zero *intrinsic* scatter in the relation implied there is something fundamental about this relationship. The growing number of studies in years following those pioneering works discounted the notion of zero intrinsic scatter in M_{BH}-σ, but it consistently produced strong, low-scatter correlations for many different data sets.

However well M_{BH} correlated with σ, there was raging debate in the years following the discovery about the slope of the correlation, i.e. the value of b in eqn (1.14). The disagreement was between slopes of $\sim$4, as reported by [30], and $\sim$5, as found by [29]. Possible explanations for this difference were: a) different fitting procedures, i.e. algorithms, were used to fit the linear regression of log M_{BH} and $\log \sigma$, b) Some galaxies were included for which r_h were not resolved, as discussed above, and c) systematic differences in the velocity dispersion measurements used by the two groups, including systematic errors in such measurements [46, 47].

But procedural differences aside, the disagreement in the M-sigma slope is important because of the underlying theoretical models that support different values of the slope. While going too far into the details of the physical modeling of SMBHs and AGNs is beyond the scope of this thesis, it's worth illuminating some of the fundamentals of those models. First, we assume that SMBHs are initially "seeded" as black holes with $M_{BH} \sim 10^6$ M$_\odot$, after which they grow by accretion of matter onto them. The notion of seeding is justified because quasars have been discovered at $z \sim 7$, so SMBHs had already been in place just 800 million years after the big bang,

[5] Watch this come into play later.

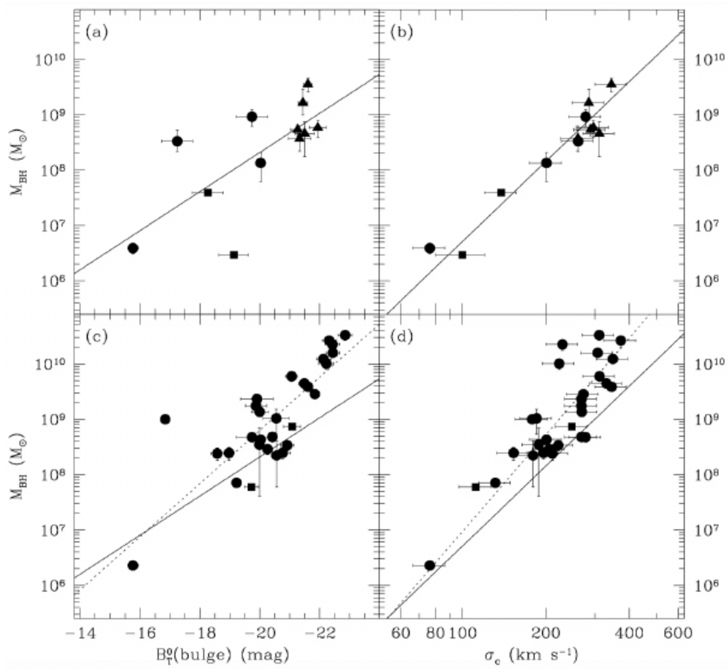

Figure 1.5: M_{BH}-L_{sph} (left panels) and M_{BH}-σ (right panels) relation for a sample fo 13 galaxies from Ferrarese & Merritt [29]. The top panels show the relationship for galaxies where r_h, the SMBH sphere of influence, were resolved, while the bottom shows the entire relationship.

giving very little time for alternative initial scenarios like dense, high-mass nuclear star clusters collapsing in on themselves[6].

If one is to consider relations like the M-sigma as physically fundamental aspects of SMBHs, then there arises the need to preserve the relation throughout cosmic time. A lot happens from the time of the first stars to the present day: especially important are ultra-violent events like galaxy mergers – in some cases these merge the central SMBHs too – which can change the structure of an entire galaxy and feed tremendous amounts of gas to the nucleus. How then, do galaxies and their SMBHs regulate this relationship?

This begets the need for some sort of "negative feedback," which acts as a self-regulating mechanism for SMBH growth. The radiation field from an accreting SMBH causes gas to flow outwards. These outflows can expel the ambient matter from the surroundings of the SMBH once the SMBH reaches a critical mass (or energy), halting its growth. This critical mass is the mass that produces enough energy to exceed the binding energy of the galactic spheroid as material falls into the black hole. The form of the outflow is treated differently by the different models of SMBH formation and growth. If the gas in the outflow doesn't cool, then all of the energy produced by the SMBH can be used to drive the gas outward. This "energy-driven flow" requires that $M_{BH} \propto \sigma^5$ for the mass required to unbind the spheroid so that feedback can

[6]See Rees (1984) for a fascinating discussion of possible creation mechanisms [48].

be initiated. On the other hand, if all of the energy in the flow is kinetic, we have a "momentum-driven flow." Here, radiation pressure from the active SMBH is the driver of the outflow and we require that $M_{BH} \propto \sigma^4$ [37]. Observations at low and high redshifts support the energy-driven outflow hypothesis, which agrees with the empirically observed slope of ~ 5 in M-sigma. Numerical simulations over the past few years have reproduced the tightness of the M-sigma relation as we observe today, with some favoring momentum-driven outflow feedback models and some energy-driven outflow [49, 50].

The M-sigma relation has been used to test our estimates of M_{BH} in nearby galaxies derived from existing observations. For instance, measurements from AGN reverberation mapping were seen to be a few to a hundred times larger than the scaled value from the relation. The errors, which correlated with decreasing instrumental resolution of the measurements, highlighted the uncertainties inherent in claiming a M_{BH} value from direct measurements [46]. In any case, by using a scaling relation in the form of eqn (1.14), it is possible to estimate M_{BH} of a SMBH in any galaxy for which we have an easy-to-measure property, such as L_{sph} or σ.

In section 2.2, I use the most comprehensive list of M_{BH} to date, along with the M-sigma relation observed in those galaxies, to individually estimate M_{BH} for a large sample of local galaxies (at $0.03 \leqslant z \leqslant 0.1$).

1.4 Data and sample selection

Our first step in estimating the BHMF of SMBHs in nearby galaxies is to obtain the central velocity dispersion, i.e. the velocity dispersion within the central 1.5 arcseconds of a galaxy ($1.5''$). This I will call σ. The photometric and spectroscopic observations were obtained from the Sloan Digital Sky Survey (SDSS). The σ values I use are from reduction of spectra from SDSS, performed by the Portsmouth group and accessible as publicly available catalogs[7].

1.4.1 Velocity dispersion of galaxies

Dispersion, in statistics, gives the spread around the mean, of a distribution of a measurement or quantity. Measuring the velocities of gravitationally bound sources of light within a given region gives us a distribution of velocities, since some of these sources move faster than the others. The velocity dispersion, σ, is simply the statistical dispersion about the mean velocity in this distribution. A combined spectrum (superposition of many stars) has emission lines which are Doppler-shifted, i.e. widened, and this width can be used to obtain σ. Since most emission line widths follow a Gaussian distribution, the central area encompassing 68% of the area of a line gives us the standard deviation, also known as the $\pm 1\sigma$ of the distribution.

The velocity dispersion of a galaxy measures the random, line-of-sight motion of stars due to a gravitational potential well. The stellar spheroids we've been concerning ourselves are usually slow rotators (though late-type galaxies are *overall* fast

[7] http://www.sdss.org/dr14/spectro/galaxy_portsmouth/

rotators). This is why the motion of stars is random with respect to a spheroid, since the spheroid's rotation doesn't impact them enough that they're bound to move in a preferred circular direction. As a result, σ reflects the dynamics of the stellar population of a galaxy. This is why it's very curious that a SMBH, which occupies only a very small area at the center of a galaxy's spheroid – with radius the order of milliparsecs (mpc), while a galaxy's size is typically in the kiloparsecs (kpc) – is so closely linked to the the random motion of stars very far away from it, as evidenced by the M-sigma relation. Perhaps this suggests something fundamental about how the formation and growth of SMBHs and their host galaxies are tied together.

Since it directly probes the gravitational potential well, σ is a fundamental observable of a galaxy, tying it to the galaxy's formation and evolution. σ has been correlated with other observables such as M_{BH} as mentioned above, and the luminosity of elliptical galaxies – via the Faber-Jackson relation [51]. And recently, significant attention has been devoted to using σ in understanding properties of the halo of dark matter (DM) surrounding galaxies. Since DM makes up about 70-80% of the total matter in the universe and is one of the key building blocks of galaxies and the universe in large scales, this is a powerful new probe in deciphering our cosmic origins. Studies of velocity dispersion and the velocity dispersion function (see section 2.1) of galaxies are interesting by themselves, but I will use them primarily in mapping out the BHMF and understanding what the observational constraints tell us about SMBH growth and their relationship to their host galaxy.

Velocity dispersion measurements are made from spectroscopy, which eliminates the biases in photometry inherent in determining quantities such as luminosity or stellar mass. Though this also requires high signal-to-noise ratio spectra, the alternative method of obtaining σ is by using the aforementioned Faber-Jackson relation. This states that $L \propto \sigma^4$, so by simply measuring the luminosity of a spheroid, one gets an estimate of velocity dispersion. Though this is less observationally taxing since photometry is simpler in principle than spectroscopy, it produces far more uncertainties than we *need* to deal with. For one, photometric measurements need various corrections, including instrumental biases. Then there's the issue of L depending on the Hubble type of a galaxy – elliptical, spiral, or lenticular – which is not an issue with just measuring σ. Last but not least, the $L - \sigma^4$ relation has significant scatter and is not well-defined for spiral bulges or non-ellipticals in general.

1.4.2 Sloan Digital Sky Survey (SDSS)

The Sloan Digital Sky Survey (SDSS) saw first light in 1998 and entered routine operations from 2000. Since then, it's collected spectra of over a million galaxies and 100000 quasars, and imaged over half a billion objects in the sky. The survey uses a wide-field 2.5 m telescope located at the Apache Point Observatory (APO) in New Mexico, which has an imaging camera with 30 CCD chips and two double spectrographs[8]. Images are taken in five different wavelength bands: u, g, r, i, and z. The survey has so far imaged more than 14000 square degrees of the sky – about a

[8]Imaging mode retired in 2009. Need to run a *goroutine* for this am I right?

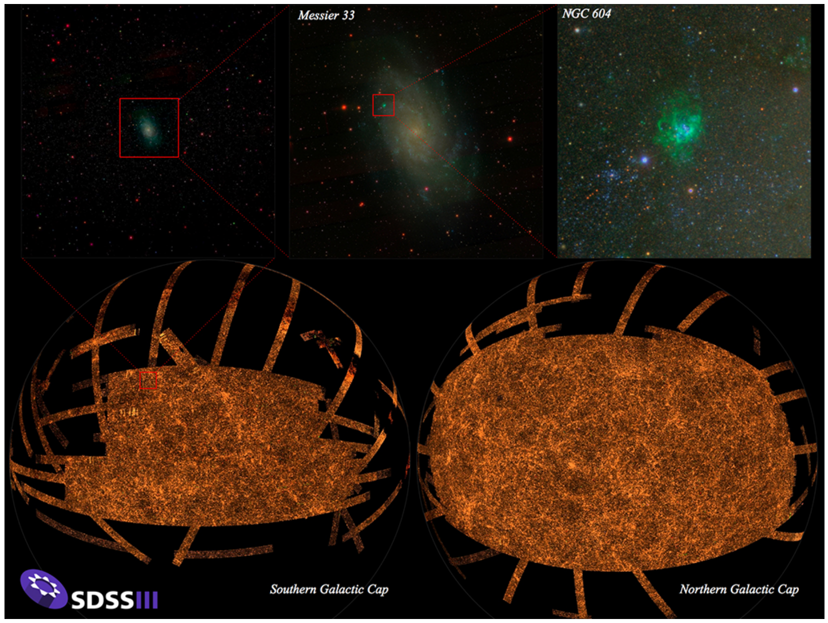

Figure 1.6: Figure showing the information available from SDSS on small and large scales. *Top panels:* SDSS view of the galaxy M33, with different zoom-ins. *Bottom panels:* A map of the whole sky derived from an SDSS image, showing the clusters and walls of galaxies, i.e. the largest single structures in the entire universe. Figure credit: M. Blanton and SDSS

third of it. This makes it the largest, most comprehensive survey and information repository for nearby galaxies. A summary of the survey and its early data release is described by Stoughton et. al. (2002) [52], the technical details given by York et. al. (2000) [53], and the main galaxy sample is detailed by Strauss et. al. (2002) [54].

The imaging data are used to select "spectroscopic targets": objects in the sky above a certain observed brightness, or flux level. For SDSS, this limit corresponds to an apparent magnitude in the r-band – in the Petrosian system [55] – of $r_p < 17.77$ mags. Spectra are only taken of objects brighter than this apparent magnitude. Spectroscopic information exists for a million and a half galaxies as of today, including nearby ones up to a redshift (z) of 0.7 and quasars up to $z = 6$.

Of these, there are galaxies that are active at their centers, and those that are quiescent. I obtained σ measurements of nearly 1 million ($\sim$950000) galaxies from the SDSS main galaxy sample from its 12th data release. In particular, I use the σ measurements from the Value Added Catalogs of the Portsmouth group [56], who make use of SDSS spectra to derive kinematics and emission line properties of these galaxies. They use the Gas and Absorption Line Fitting (GANDALF[9]) [57] code to fit the spectrum of a galaxy to templates of stellar population so that the stellar continuum and absorption lines from the ionized gas can be separated (the models are from Maraston & Strømback [58] and based on the libraries from [59]). By comparing

[9]In keeping with the proud tradition of acronyms that will make you chuckle or shake your head (or do both).

the SDSS spectra and the templates, the best-fit velocity dispersion within 1.5″ of the center was derived for each galaxy, using the Penalized PiXel Fitting (pPXF) code [60]. The templates are capped at $\sigma = 420$ km s^{-1}, so that is the upper limit of reliable measurements for our sample. Furthermore, measurements of $\sigma \lesssim 70$ km s^{-1} have low signal-to-noise (S/N) ratio of data, so they are unreliable too. The σ measurements from the Portsmouth group all have S/N>10 and the median uncertainty is 7 km s^{-1}.

I also obtained photometric data from the catalogs, primarily in order to obtain a statistically complete sample of galaxy σs, which will be described in detail in the next chapter. Of particular interest to my analysis are the apparent r-band magnitudes, r_p, based on which targets are selected for spectroscopy. These observed brightnesses are converted to absolute magnitudes, defined as the apparent magnitude an object would have if it was exactly 10 pc away from us. However, we're taking magnitudes from a fraction of the electromagnetic spectrum, instead of integrating over the whole thing, meaning that light in that band will be redshifted to the rest-frame of the observer (us) by the time it gets to us. The way to deal with this pesky bias is to introduce what is called a "K-correction," which makes it possible to compare measurements through a single band, of different objects at different distances (hence redshifted by different amounts). To get from the observed r_p to the absolute r-band magnitude, M_r, we use:

$$r_p = M_r + \left[5 \log\left(\frac{D_L}{10\text{pc}}\right)\right] + K_r(z), \tag{1.15}$$

where K_r is the K-correction for the r-band – dependent on the comoving distance D_C – and D_L is the luminosity distance (in pc). The K-corrections I used were the $z = 0$ corrections from the NYU value added galaxy catalog [61]. I apply a K-correction to each galaxy and find that the mean K_r is $\sim$0.175 mags. From here on out, I will refer to the K-corrected absolute r-magnitude as M_r.

For my sample, I only use galaxies at $z \leqslant 0.1$, which corresponds to $D_L \sim 460$ Mpc, or $\sim$1.2 billion light years. This allows me to construct a BHMF of the *local* universe, which is a rather arbitrary term to describe the current-day universe as it appears to us, but I define it to mean $z \leqslant 0.1$. This redshift cut brought down the sample size to $\sim$364000 galaxies.

Chapter 2

Analysis: Velocity dispersion and SMBH-host galaxy correlation

2.1 The Velocity Dispersion Function (VDF)

Our [scientific] understanding comes through the development of theoretical models which are capable of explaining the existing observations as well as making testable predictions...Fortunately, a variety of sophisticated mathematical and computational approaches have been developed to help us through this interface, these go under the general heading of statistical inference.

- P. C. Gregory (2005)

Statistical methods have been employed by astronomers for decades to understand global properties of objects we observe in the universe. These methods have been used, along with some reasonable starting assumptions, to make inferences beyond the dataset(s) themselves, about the underlying population under study. The first of the statistically-derived properties studied in this thesis will be the Velocity Dispersion Function. The VDF is a statistical distribution of the central velocity dispersions, σ, for a sample of galaxies. It is defined as the number density of galaxies per unit magnitude (dex) of σ.

For a sample of galaxies – let's call it S – the number of galaxies with velocity dispersion σ in an interval of width $d\sigma$ is given by $N_S(\sigma)d\sigma$. If the volume sampled at velocity dispersion σ is $V_S(\sigma)$, then the VDF of sample S is given by:

$$\Phi_S(\sigma)d\sigma = \frac{N_S(\sigma)\ d\sigma}{V_S(\sigma)}. \tag{2.1}$$

Now, we make an assumption, which is backed by observations. We assume the universe is homogenous on large scales – scales $\gtrsim$ few hundreds of Mpc – meaning that a property derived for a volume on these scales should hold *globally* for all of space. This is pretty apparent if one compares one patch of the sky a few hundred Mpc across with another patch of the same length – they observe virtually the same distribution of matter[1]. Thus, if we randomly choose a sample S, in the limit of large sample volume, we approach a *universal* limit for galaxy VDFs:

$$\Phi(\sigma) = \lim_{V_S(\sigma)\to\infty} \Phi_S(\sigma). \tag{2.2}$$

This assumption helps us obtain a global VDF for galaxies by constructing a VDF for a select sample of galaxies contained in a large enough volume, thereby circumventing the problem of only being able to find a VDF for a finite sample of galaxies (*phew!*). The same idea is applied toward estimating the mass distribution of SMBHs in the next chapter, i.e. in constructing the BHMF.

2.1.1 Selection Effects: Completeness of the sample

If we want to statistically analyze properties of a galaxy population like the VDF, we require a sample that covers the entire distribution of the properties under study: absolute magnitude, M_r, and velocity dispersion, σ. We want to make sure that our sample is **complete**; that it's not biased toward any property. Completeness analysis helps us ensure that our sample isn't preferentially selecting, say just the brightest galaxies or the highest σ galaxies. As an analogy, consider a statistical study of the population of a town that randomly samples a number of people living in the town. There is a possibility that this random selection could have a large number of middle-aged people and males, which would bias the sample in terms of age and gender. Thus, it may not be representative of the true population of the town. In much the same way, I want to ensure that my final sample is representative of the true population of galaxies, covering the full range of σ. To construct a statistically complete sample, I follow the approach outlined by Sohn et. al. (2017) [62].

I've already restricted my sample size to $z \leqslant 0.1$, which makes it a *volume-limited* sample. However, as mentioned in section 1.4.2, SDSS spectroscopy is only complete for objects above $r_p = 17.77$ mags, making it a *magnitude-limited* sample. The magnitude-limited sample is complete in *apparent* magnitude, not *absolute* magnitude, M_r, which by eq. (1.15) depends on redshift z. So, the survey is only complete up to a magnitude limit, $M_{r,\text{lim}}$, for any volume limited by z_{max}, the maximum z of that volume.

This is illustrated in Fig. 2.1a, where the magnitude, M_r, is plotted against the redshift, z, for a sample that is limited to a volume contained in $z \leqslant 0.09$. The vertical dashed red line gives the maximum redshift, $z_{max} = 0.09$ of this volume-limited sample. The SDSS spectroscopic survey limit, given by the black line, intersects with z_{max} at $M_r = -20.36$, which is given by the horizontal dashed red line. So within the volume contained in $z \leqslant 0.09$, this sample is complete for galaxies with $M_r \leqslant$[2]-20.36 (these are the blue points in Fig. 2.1a). The sample of galaxies with $M_r \geqslant -20.36$ is therefore incomplete in absolute magnitude and thus rejected – these are the grey

[1] By the way, this is one of the fundamental cosmological principles that observational astronomy relies upon.

[2] M_r goes the opposite way from normal quantities, so the more negative it is, the brighter an object is.

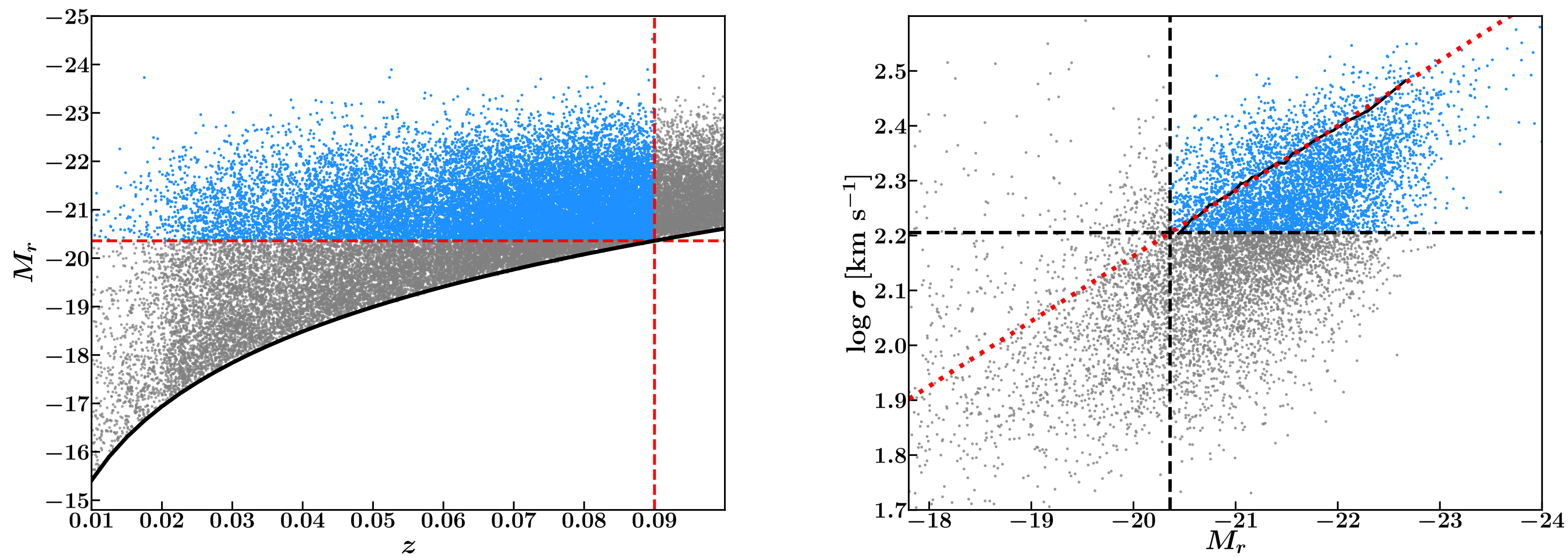

(a) (b)

Figure 2.1: Demonstrating the incompleteness of a volume-limited sample at $z \leqslant 0.09$. Blue points comprise the complete sample, and grey points are the incomplete data points or galaxies not part of this volume. Only 10% of the data is shown for clarity. a) Absolute r-band magnitude, M_r v.s. redshift, z, for our magnitude-limited sample. The vertical dashed red line indicates the maximum redshift for this volume-limited sample. The black solid curve shows the SDSS completeness limit as a function of redshift. The dashed red horizontal line is the magnitude limit, $M_{r,\mathrm{lim}}$, at which the $z \leqslant 0.09$ sample is complete. b) M_r v.s. $\log \sigma$ for the $z \leqslant 0.09$ magnitude-limited sample. The vertical black dashed line shows the magnitude limit, $M_{r,\mathrm{lim}}$. The diagonal black solid curve running through the blue points represent the 95% completeness limit of the $\log \sigma$ distribution, calculated in bins with the 10000 brightest objects. The intersection of the best-fit of this curve – the red dotted line – with $M_{r,\mathrm{lim}}$ gives us the σ-completeness limit for this sample, shown by the horizontal dashed black line.

points below the horizontal line in Fig. 2.1a. So if we were to derive a VDF based on the sample constituting just the blue galaxies, it would be complete to $M_r = -20.36$.

But there's more to it. Fig. 2.1b plots the logarithmic velocity dispersion, $\log\sigma$, against M_r, with the vertical dashed line indicating $M_{r,\mathrm{lim}}$ for a redshift of 0.09. The first thing to notice here, is the large scatter in the σ distribution at any given magnitude. For instance, at $M_r = -20.36$, $\log\sigma$ can range from $\sim$1.7 to $\sim$2.5, so σ varies from $\sim$50 km s^{-1} to $\sim$315 km s^{-1} for this one fixed magnitude! Converting $M_{r,\mathrm{lim}}$ to a limit at which σ is complete is therefore not a trivial exercise, and my sample is only complete in M_r, not in σ. Everything to the right of $M_{r,\mathrm{lim}}$ in Fig. 2.1b is included in the magnitude-limited sample, but there are many galaxies with very low σ compared to others in this sample. This is concerning, because galaxies with relatively low σ make it into the sample by being bright enough while others at comparable σs are rejected because they don't make the brightness cut. This biases my sample toward brighter galaxies.

So how do we make sure we have a sample that is not only complete in the distribution of M_r, but also σ? The diagonal black curve amidst the blue points in Fig. 2.1b reflects the 95$^{\mathrm{th}}$ percentile of the σ distribution up to the magnitude limit. 95% of the sources with $M_r \leqslant M_{r,\mathrm{lim}}$ have σ below this limit. By fitting a best-fit line to the curve, the red dotted slope, we can find the intersection of this limit with $M_{r,\mathrm{lim}}$. The horizontal level corresponding to this intersection (the horizontal black dashed line) gives us the all-important σ-completeness limit, i.e. the minimum σ for which this sample is $\sim$ 95% complete. For each volume-limited sample (with the $z \leqslant 0.09$ sample shown), let's call this limit $\sigma_{lim,\mathrm{VL}}$. Very few galaxies fainter than $M_{r,\mathrm{lim}}$ should have $\sigma \geqslant \sigma_{lim,\mathrm{VL}}$. The criterion for a **$\boldsymbol{\sigma}$-complete** sample then, is $\sigma > \sigma_{lim}$, i.e. only galaxies with dispersions above the σ-completeness at their individual redshifts should be included in the σ-complete sample. The bottom line from this example is that completeness in σ depends on redshift, just as completeness in M_r does.

To construct a σ-complete sample, I will parametrize the σ-completeness limit of each original volume-limited sample as function of redshift, i.e. derive $\sigma_{\mathrm{lim}}(z)$. This I will do empirically, by obtaining $\sigma_{lim,\mathrm{VL}}$ for each volume-limited subsample and repeating the same procedure as above with 40 different such subsamples, each a subset of my full sample at $z \leqslant 0.1$. The subsamples will each have a volume with maximum redshift increased by $\triangle z = 0.0025$, starting from $z = 0$, and ending at $z = 0.1$. The procedure for deriving σ_{lim} is outlined below:

1. For a single volume-limited subsample, find the magnitude completeness limit, $M_{r,\mathrm{lim}}$, at z_{max}, the maximum redshift of this volume.

2. For this subsample, derive the 95$^{\mathrm{th}}$ percentile of the σ distribution up to $M_{r,\mathrm{lim}}$. I did this by selecting the 10000 smallest[3] M_r and finding the 95$^{\mathrm{th}}$ percentile score of σ in that set: σ_{95}. This process I repeated for the next 10000 brightest objects and so on (keeping σ_{95} for each bin), until $M_{r,\mathrm{lim}}$ was reached.

[3]Nothing special about 10000; it's just easy to work with and a small enough number relative to the total sample size of $\sim$364000.

3. Find a linear best-fit to the distribution of σ_{95}s, which is simply the 95$^{\text{th}}$ percentile distribution of σ for galaxies with $M_r \leqslant M_{r,\text{lim}}$, and obtain its intersection with $M_{r,\text{lim}}$. The intersection is $\sigma_{\text{lim}}(z_{max})$, the σ-complete level for this subsample's z_{max}.

4. Repeat steps 1-3 for all the volume-limited subsamples, so that σ_{lim} is found for z_{max} ranging from 0.0025 to 0.1.

5. Parametrize σ_{lim} as function of z from the results of step 4.

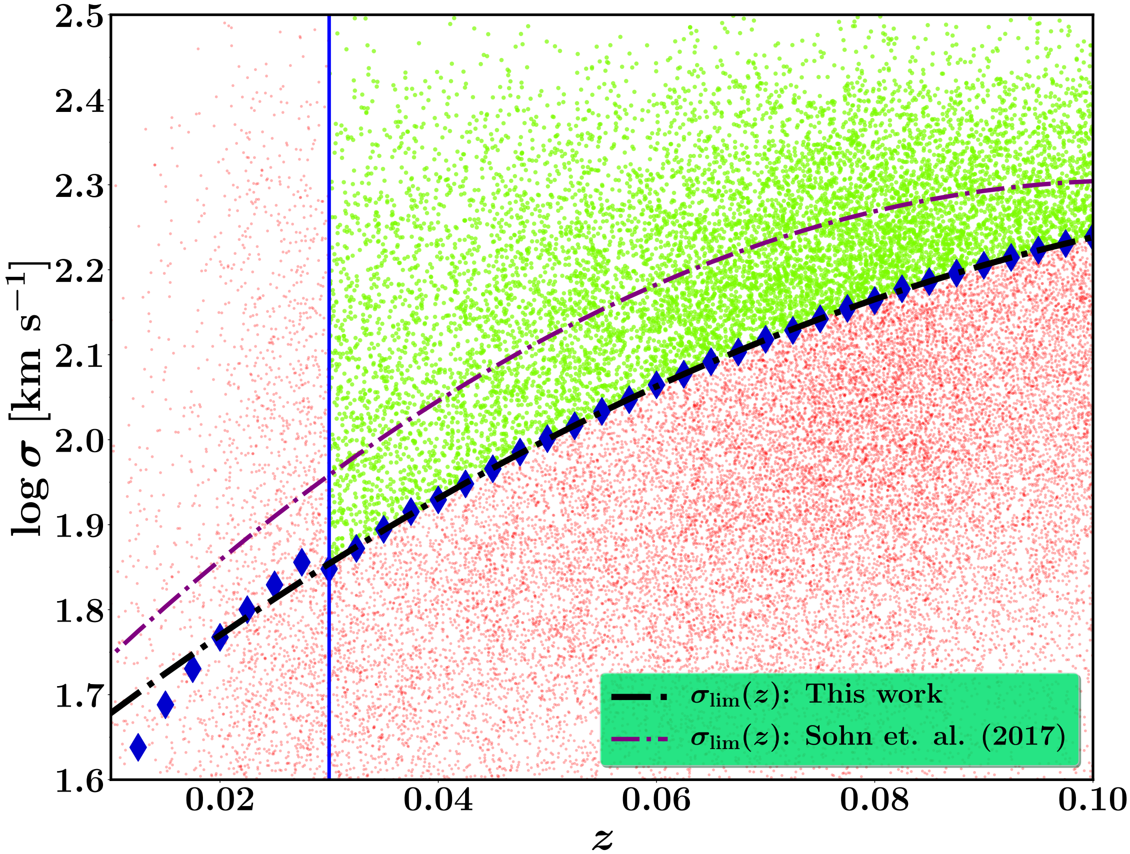

Figure 2.2: $\log \sigma$ v.s z for 40 volume-limited subsamples, each with z_{max} increasing by $\Delta z = 0.0025$. The blue diamonds indicate the σ-limit for a given redshift. The black dot-dashed line shows the 2$^{\text{nd}}$ order polynomial fit (eq. (2.3)) to $0.03 \leqslant z \leqslant 0.1$, while the purple dot-dashed line shows a similar polynomial fit by Sohn et. al. [62] for quiescent galaxies in the SDSS in the same redshift range. The light green points are galaxies included in our final σ-complete sample, while red points are excluded. The blue line is drawn to indicate my lower redshift limit.

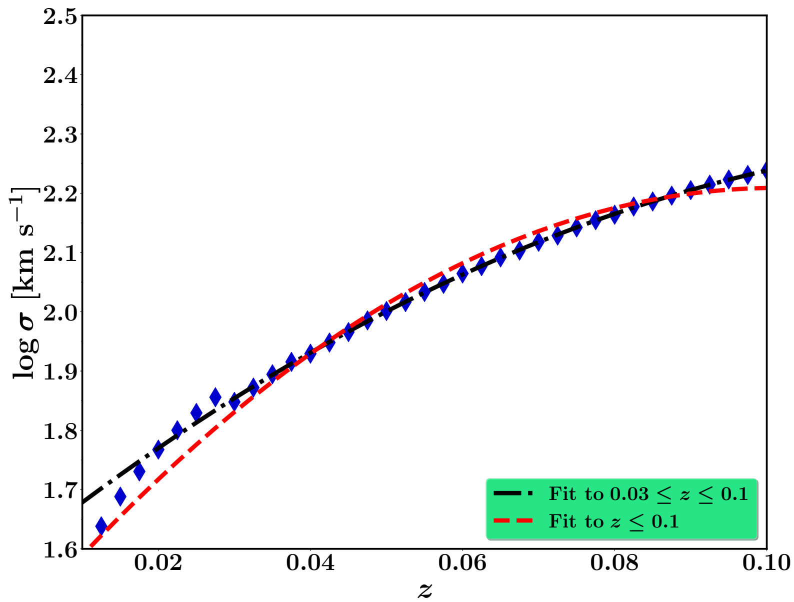

Figure 2.3: Two different 2^{nd} order polynomial fits to σ_{lim}: the dashed red curve shows the fit to all points, i.e. $z \leqslant 0.1$, and the dot-dashed black curve shows the fit to the range $0.03 \leqslant z \leqslant 0.1$. The latter is adopted for $\sigma_{\text{lim}}(z)$ (eq. (2.3)).

For step 5, I plot each of the 40 σ_{lim} values for the corresponding z_{max} in $\log \sigma - z$ space, as shown in Fig. 2.2. σ_{lim} increases as z_{max} increases, due to an increase in luminosity. This is to be expected as we require a brighter magnitude limit for completeness at a higher volume. The points in the plot are fit to a 2^{nd} order polynomial. Inspecting the plot, we observe that there's a break in the nice downward curving of $\sigma_{\text{lim}}(z)$at $z \leqslant 0.03$. This can be explained by the low number of galaxies in the volume of those subsamples.

Therefore, I fit a 2^{nd} order polynomial to all subsamples, i.e $z \leqslant 0.1$, and to those subsamples limited to $0.03 \leqslant z \leqslant 0.1$. Fig. 2.3 shows that the dashed red line polynomial doesn't do a great job at describing the $z \leqslant 0.1$ range, while the dashed black line describes the $0.03 \leqslant z \leqslant 0.1$ range very well. Hereafter, I adopt the polynomial fit to $0.03 \leqslant z \leqslant 0.1$, parameterizing σ_{lim} as:

$$\sigma_{\text{lim}}(z) = 1.57 + 10.47z - 37.7z^2 \tag{2.3}$$

In Fig. 2.2, I compare the results of my σ-completeness analysis with those of Sohn et. al. (2017), who use SDSS galaxies in the same volume. The primary difference between our analyses is that they exclude all actively star-forming galaxies in this volume. These are galaxies with a higher D_n4000 index, defined by the ratio of flux between the 4000-4100 Å and 3850-3950 Å wavebands. This quantity is an indicator of the age of the stellar population of a galaxy and helps to separate actively star-forming (higher D_n4000) and quiescent (lower D_n4000) galaxies (See Ref. [63]).

Though my process of obtaining $\sigma_{\rm lim}(z)$ is very similar to theirs, I make no such cuts based on star formation activity, since I ultimately want to describe SMBHs in as many nearby galaxies as possible.

Sohn et. al. also parametrizes their σ-completeness limit with a 2$^{\rm nd}$ order polynomial curve, which, as shown by the purple dot-dashed curve in Fig. 2.2, lies above my own (their fit was also constrained to $0.03 \leqslant z \leqslant 0.1$ as the $z \leqslant 0.03$ behavior deviated from the fit like ours). It makes sense that their completeness limit lies above ours when we inspect the properties of our σ-complete samples (mine is shown in Fig. 2.4). The distribution of σ in their σ-complete sample peaked around $\sigma \sim 200$ km s^{-1}, while mine peaked around $\sigma \sim 160$ km s^{-1}. So, larger values of σ would need be needed to achieve completeness in the Sohn et. al. sample.

The σ-complete sample

Using eq. (2.3), I estimate $\sigma_{\rm lim}$ for redshift in my sample. The interpretation of this value is that it's the minimum σ at which my sample is complete for the volume covered by this redshift. The final criterion in my sample selection therefore, is that I'll only include galaxies which have $\sigma > \sigma_{\rm lim}(z)$, with z being the redshift of the particular galaxy in question. My final sample, which I refer to as the σ-complete sample hereafter, includes **96842 galaxies** in the redshift range $0.03 \leqslant z \leqslant 0.1$. This is a much larger sample size than used in most studies estimating the VDF in local galaxies or even in deriving the BHMF. Sohn et. al.'s sample, which is one of the largest in deriving the local VDF, had 40,660 quiescent galaxies – about a factor of 2 smaller than mine. The studies that I compare my BHMF to in chapter 3 also use significantly smaller (sometimes by factors > 10) samples in their derivations.

Fig. 2.4 displays some properties of the sample compared to my original magnitude-limited sample. For the σ-complete sample, the peak of the σ distribution shifts significantly to the right of the peak in the magnitude-limited sample: the mean σ changes from ~ 79 km s^{-1} to ~ 160 km s^{-1}. Since the original sample has many galaxies with unreliable ($\sigma \lesssim 70$ km s^{-1}) measurements, an analysis of that sample would produce flawed results with large systematic and random uncertainties. The distribution of uncertainties in σ measurements, $\Delta\sigma$, tells a similar story. The significantly reduced spread in $\Delta\sigma$ ensures further that I minimize the proportion of uncertain measurements in my sample, with most $\Delta\sigma$ values under 15 km s^{-1}. The mean $\Delta\sigma$ is reduced from ~ 15 km s^{-1} to ~ 6 km s^{-1} as I adopt the σ-complete sample. There's also a greater proportion of brighter galaxies in my final sample compared to the original. But most importantly, now I have confidence in my sample not being biased towards absolute magnitude, or velocity dispersion, allowing for a neutral statistical treatment of the data. In other words, we can now assume the sample reflects a true distribution of a galaxy population, much like having a sample representative of different properties of a *human* population.

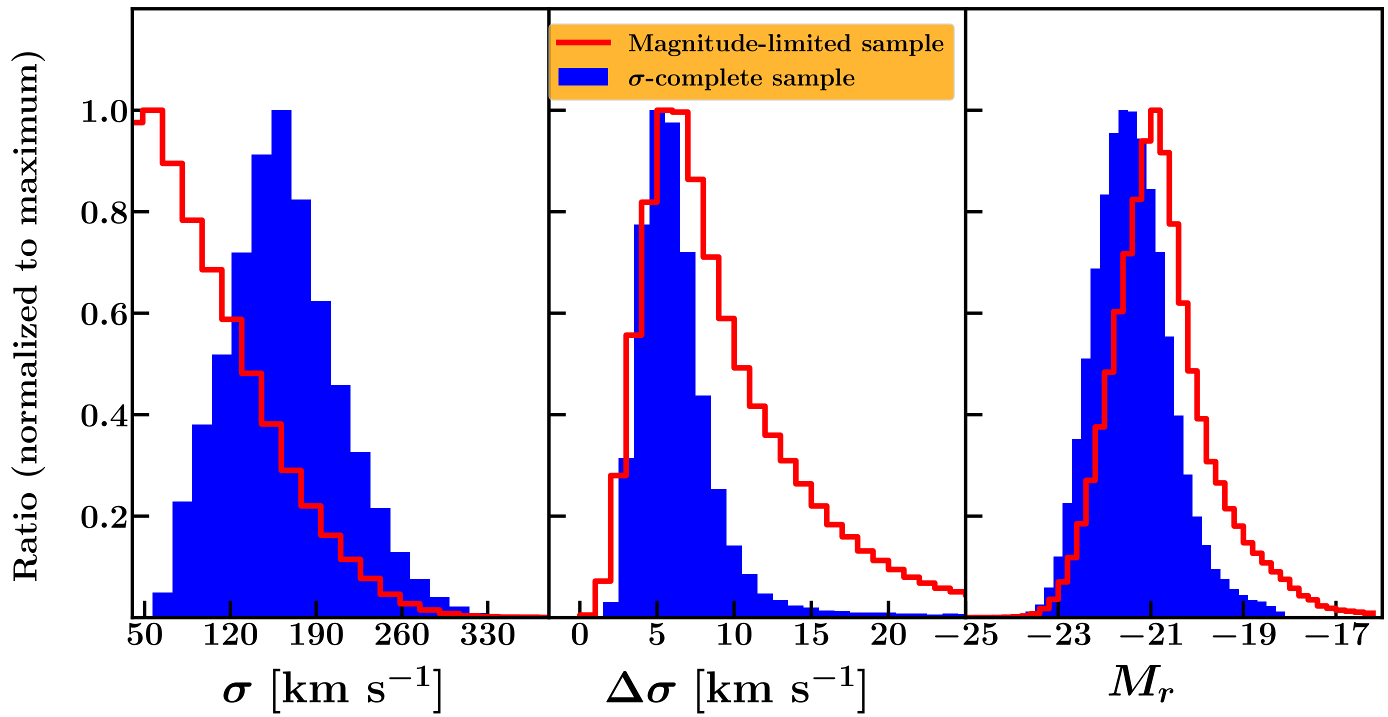

Figure 2.4: Comparison of properties of the σ-complete sample, shown in blue, with magnitude-limited sample, shown in red outline. The vertical axis shows the ratio of the number of objects in the interval with the maximum height to the number in the interval specified. *Left*: Distribution of velocity dispersions, σ, in bins of 20 km s^{-1}, *Center*: Distribution of the uncertainty in velocity dispersions, $\Delta\sigma$ in bins of 1 km s^{-1}. *Right*: Distribution of absolute magnitudes, M_r in bins of 0.2 mags.

2.1.2 Constructing the VDF

The Velocity Dispersion Function (VDF) gives a statistical distribution of the velocity dispersion of a galaxy. The VDF has been an extensively studied quantity in extragalactic astronomy, since it helps connect predicted models of galaxy formation and evolution with observations. While the luminosity function, LF, of galaxies is sometimes converted to a VDF via the Faber-Jackson relation, this only really applies for elliptical galaxies and other issues, as already outlined, include the need for a specific waveband to compare between theory and observations. The VDF can also help characterize the observable differences between star-forming and quiescent galaxies.

There are several methods for constructing a statistical distribution function like the VDF, including the **$1/V_{max}$ method**, the parametric maximum likelihood STY method, and the non-parametric stepwise maximum likelihood (SWML) method. These three methods are outlined quite instructively in Weigel et. al. (2016) [64], who use it to construct a distribution function for the stellar mass of galaxies (stellar mass function). I choose the $1/V_{max}$ method, because of its simplicity and also because we do not have to assume a functional form of the VDF to begin with[4]. The one major disadvantage with this method is that it can be biased if there are inhomogeneities on large scales, in the quantity studied. This will not be a problem for us, because the volume scales we're working with is at least in the order of gigaparsecs, much larger than the scales on which inhomogeneities may exist.

The $1/V_{max}$ method corrects for an effect that observational astronomers have been familiar with for almost a century, called the **Malmquist bias**. As already seen, surveys like the SDSS spectroscopic survey only select objects brighter than a limiting apparent magnitude. Since brightness is the only screening factor, faint objects can only be seen if they are close enough to us, while very bright objects can be seen from very far away. This gives a false impression about the true distribution and number of objects in the volume surveyed, as it *appears* to us that there are many more luminous objects than faint ones within a certain distance from us. The problem with this selection bias is that brighter objects contribute significantly more to distribution functions like the VDF, or say, the average luminosity of the volume surveyed, than they would had we been able to detect fainter objects in our sample.

The $1/V_{max}$ method takes into account the *relative* contribution to the VDF of each galaxy with dispersion σ, by *volume-weighting* the velocity dispersions. We first need to divide velocity dispersions in 41 bins of $\Delta \log \sigma = 0.02$, ranging from $\log \sigma = 1.84$ km s^{-1} to $\log \sigma = 2.64$ km s^{-1}. Then, the number density of galaxies in a specific σ bin j is given by the following sum:

$$\Phi_j(\sigma)\Delta \log \sigma = \sum_{i}^{N_{bin}} \frac{1}{V_{max,i}}, \tag{2.4}$$

where N_{bin} is the number of galaxies in the bin and $V_{max,i}$ is the maximum volume at which a galaxy i at redshift z_i with velocity dispersion σ_i could be detected in. Ah, the usefulness of this method becomes clearer as we see that galaxies with higher

[4] The method was first used by Schmidt (1968) [65].

σ (which can be seen further out) have a larger volume over which they could be detected. Their contribution to the VDF are thus proportionately weighted down by this larger volume. Had it not been for this important weighting, this method would simply involve counting the number of objects in each σ bin (which would make it a boring and very inaccurate thing to do).

With all our terminology and assumptions (a flat universe that obeys Λ-CDM cosmology) from section 1.1.2 in place, we define $V_{max,i}$ as:

$$V_{max,i} = \frac{4\pi}{3}\frac{\Omega^{\rm survey}}{\Omega^{\rm sky}}\left[D_C(z_{max,i})^3 - D_C(z_{min,i})^3\right]. \tag{2.5}$$

We're taking the volume of a sphere with radius given by the comoving distance at the maximum redshift that galaxy i could be found at, $D_C(z_{max,i})$, subtracted by the volume with radius given by the comoving distance at the *minimum* redshift the galaxy could be found at, $D_C(z_{min,i})$. So this is what we call a *comoving volume element* of a galaxy, i.e. the 3-D slice in which it can be detected. $z_{min,i} = 0.03$ for all galaxies, since that is the lower redshift limit of our sample. We include a scale factor, $(\Omega^{\rm survey}/\Omega^{\rm sky})$, since SDSS wasn't surveying the entire sky. $\Omega^{\rm sky}$ is the solid angle of the sky and is equal to 41253 deg^2. Similarly, $\Omega^{\rm survey} = 9200$ deg^2 is the solid angle covered by the SDSS spectroscopic survey. For $z_{max,i}$, I take the maximum redshift galaxy i could have, based on σ_i and the completeness limit from above (Fig. 2.2 and eq. (2.3)).

The VDF, $\Phi(\sigma)$, was finally calculated from Eq. (2.4), for the range $1.84 \leqslant \log\sigma \leqslant 2.64$. Note that the unit of $\Phi(\sigma)$ is Mpc^{-3} dex^{-1}, which gives a volume density per unit magnitude, as we require. The errors on the VDF were estimated by a Monte Carlo method. I ran 10000 simulations of the VDF calculation, each time randomly modifying my σ values with the associated uncertainty, $\Delta\sigma$, assuming a gaussian error distribution. So a particular σ value would be perturbed normally taking $\Delta\sigma$ as the standard deviation in the σ distribution. The resulting VDF, and associated uncertainties, is shown in Fig. 2.5, and tabulated in Table 2.1.

Fig. 2.5 shows both the VDF obtained for our final sample, as well as for a sample at $0.03 \leqslant z \leqslant 0.09$ which is not complete in σ. The VDF for the latter is simply the number of galaxies in each σ bin divided by the volume of the entire sample. Though the overall shape of the VDF is similar for both samples in the $2.0 \lesssim \log\sigma \lesssim 2.5$ range, the volume-limited VDF starts to drop at $\log\sigma < 2.05$ while the σ-complete VDF remains flat – steepens slightly even – at $\log\sigma < 2.05$. This once again demonstrates the shortcomings of a statistically incomplete sample: the volume-limited sample is only complete for $\log\sigma > 2.2$ (from eq. (2.3)), so σ is incompletely sampled as we start to go to lower values.

The large error bars on the VDF points in Fig. 2.5 are mostly due to low number statistics. The largest uncertainties came from bins with fewer than 50 objects. These were the bins with $\gtrsim 30\%$ uncertainty in $\Phi(\sigma)$ (see Table 2.1). Consequently, the VDF is reliable for $1.86 \leqslant \log\sigma \leqslant 2.5$.

$\log\sigma$ [km s^{-1}]	$\Phi(\sigma)$ [$\times 10^{-4}$ Mpc^{-3} dex^{-1}]	N_{bin}
1.84	$63.59^{+143.08}_{-137.78}$	12
1.86	$156.79^{+23.39}_{-23.39}$	181
1.88	$155.26^{+11.61}_{-11.18}$	361
1.90	$150.48^{+7.23}_{-7.23}$	562
1.92	$122.19^{+5.10}_{-4.91}$	647
1.94	$124.95^{+3.76}_{-3.62}$	897
1.96	$111.88^{+2.88}_{-2.88}$	1049
1.98	$111.15^{+2.31}_{-2.31}$	1300
2.00	$108.20^{+1.85}_{-1.85}$	1583
2.02	$99.22^{+1.54}_{-1.43}$	1807
2.04	$93.16^{+1.27}_{-1.32}$	2049
2.06	$86.45^{+1.01}_{-1.05}$	2313
2.08	$88.06^{+0.87}_{-0.84}$	2821
2.10	$87.82^{+0.73}_{-0.73}$	3376
2.12	$85.14^{+0.59}_{-0.62}$	3865
2.14	$84.27^{+0.52}_{-0.50}$	4575
2.16	$83.62^{+0.43}_{-0.42}$	5392
2.18	$78.81^{+0.38}_{-0.38}$	6082
2.20	$71.63^{+0.29}_{-0.30}$	6662
2.22	$64.42^{+0.26}_{-0.24}$	7184
2.24	$64.50^{+0.24}_{-0.25}$	7193
2.26	$58.06^{+0.25}_{-0.24}$	6477
2.28	$51.06^{+0.25}_{-0.24}$	5694
2.30	$45.91^{+0.26}_{-0.24}$	5121
2.32	$40.89^{+0.25}_{-0.24}$	4561
2.34	$33.80^{+0.26}_{-0.24}$	3769
2.36	$28.37^{+0.26}_{-0.25}$	3164
2.38	$23.10^{+0.26}_{-0.24}$	2576
2.40	$17.66^{+0.25}_{-0.24}$	1967
2.42	$11.53^{+0.25}_{-0.24}$	1285
2.44	$8.44^{+0.26}_{-0.24}$	940
2.46	$5.29^{+0.25}_{-0.24}$	587
2.48	$3.03^{+0.25}_{-0.24}$	336
2.50	$1.76^{+0.24}_{-0.25}$	194
2.52	$0.77^{+0.25}_{-0.26}$	84
2.54	$0.46^{+0.26}_{-0.25}$	49
2.56	$0.25^{+0.25}_{-0.25}$	28
2.58	$0.15^{+0.27}_{-0.27}$	15
2.60	$0.12^{+0.27}_{-0.27}$	12
2.62	$0.09^{+0.25}_{-0.25}$	10
2.64	$0.10^{+0.25}_{-0.24}$	11

Table 2.1: Data points for the VDF. The second row lists the VDF, $\Phi(\sigma)$, and associated upper and lower limit uncertainties, for a bin of width $\Delta\log\sigma = 0.02$. The third row lists number of objects in each bin, N_{bin}.

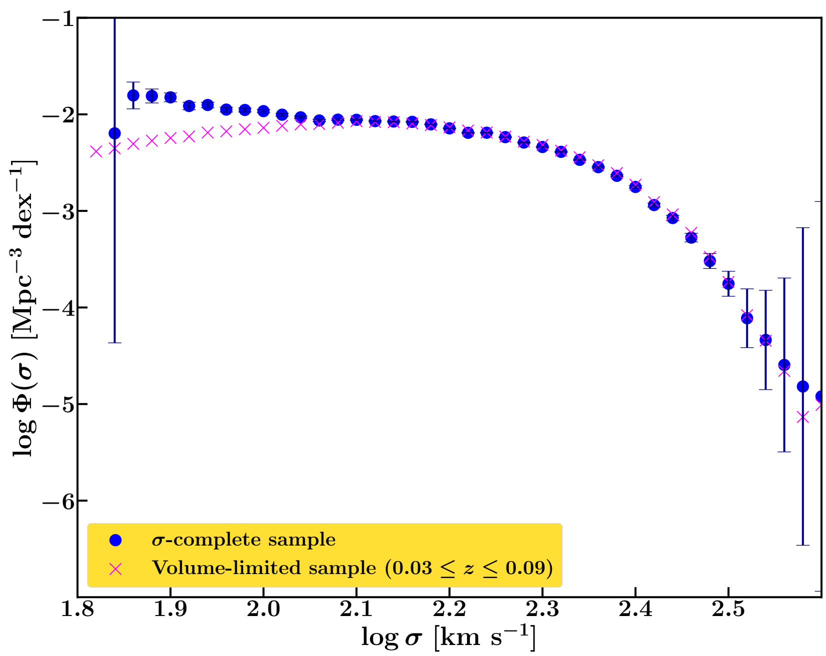

Figure 2.5: VDF for our σ-complete sample – shown by blue circles – and for a volume-limited sample at $0.03 \leqslant z \leqslant 0.09$ – shown by pink crosses. The vertical axis shows magnitudes of VDF $\Phi(\sigma)$. The volume-limited VDF declines for $\log \sigma < 2.05$.

The Schechter function and Press-Schechter theory

The luminosity, stellar mass, velocity dispersion and other distribution functions of galaxies are often described by a **Schechter function**, first proposed by Paul Schechter in 1976 [66]. In an attempt to approximate the observed luminosity function, $\Phi(L)$, of galaxies, Schechter proposed the following analytical expression:

$$\Phi(L)dL = \Phi_\star \left(\frac{L}{L_\star}\right)^\alpha \exp\left[\frac{-L}{L_\star}\right] \frac{dL}{L_\star}, \tag{2.6}$$

where $\Phi_\star$, α, and $L_\star$ are all parameters determined by the data the expression is fit to. This is essentially a gamma function, i.e. a power law combined with an exponential function. $\Phi(L)$ is a power law at low luminosities and switches to an exponential choke; it is truncated at higher luminosities. This change in the slope of $\Phi(L)$ (in $\log \Phi - \log L$ plane) occurs at a characteristic luminosity, $L_\star$, the corresponding luminosity function being $\Phi_\star$ (in units of $\mathrm{Mpc}^{-3}\ \mathrm{dex}^{-1}$ like $\Phi(L)$). The dimensionless α gives the slope of the power-law portion. The observational impetus for the widespread use of this expression to fit observed luminosity distributions is that very few galaxies with very high intrinsic brightnesses are seen, and while the number density of galaxies per unit magnitude is seen to decrease at a constant rate with increasing brightness, there is ample evidence for a rapid cutoff at high enough luminosities.

The expression was developed from the **Press-Schechter theory** (1974) of self-similar gravitational condensation, which proposed a formalism to explain the various scales at which matter is clumped in the universe – ranging from stars (very small) to galaxy clusters (very large) [67]. The earliest stages of the lifetime of our universe are marked with density perturbations, or fluctuations, in both small and large scales, and with its expansion, these perturbations grew linearly in space. After a period of time, when these perturbations reach a certain threshold, the material within them collapses to form structures of a comparable scale ("self-similar"). This has an enormously significant implication in our Λ-CDM view of the universe: the formation of structure in the universe follows a *hierarchical* pattern. In the distant universe, density perturbations formed low-mass clumps which over time merge with other clumps of similar size to form larger clumps on lager scales. These collapsed systems are called "dark matter halos" and are responsible for matter coalescing together in the form of stars, star clusters, galaxies and galaxy clusters. N-body simulations trace these halos through cosmic time and determine their properties which in turn inform us what properties are expected of galaxies as they evolve. The reader might find instructive an extended formalism for this model, presented in Bond et. al. (1991) [68].

Press-Schechter theory considers the different scales of density perturbations and predicts the number of objects within a mass range $[M, M+dM]$. For instance, it can be used to obtain the mass distribution of galaxies with masses between 10^8 $M_\odot$ and 10^{10} $M_\odot$ at any given time. The simple prediction of this theory is that masses are distributed in a power law fashion for low masses, which is followed by an exponential cutoff of the distribution at masses above some characteristic mass. This formalism was extended to describe galaxy luminosities, and the data fit the power law + exponential falloff structure of the luminosity function very well, except at the very bright end, where it under-predicted the number density of galaxies observed. Similarly, recent N-body simulations show agreements with the model except underestimating the number of very massive galaxies [69].

The point of this digression is that I want to approximate my VDF with a function similar in form to the Schechter function. By looking at Fig. 2.5, we can already see that the observed VDF behaves like a power law with a logarithmic slope at the faint σ end and decreases rapidly after a certain point. This might tempt us to simply change variables from the $L - \sigma^4$ relation and simply rewrite eq. (2.6) in terms of σ; for example the exponential part would become $\exp[-(\sigma/\sigma_\star)^4]$ and we'd expect to see a sharper cutoff at the high σ end. But $L - \sigma^4$ is poorly defined for non-elliptical galaxies and as already noted in 2.1.1, there can be significant scatter in σ at a fixed L. Even if we were to take the mean σ at a fixed L, it wouldn't scale linearly in L. So if $\Phi(L)$ is well fit by a Schechter function, we should not use the same functional form to fit $\Phi(\sigma)$.

Rather, I use a *Schechter-like* function, with the same power-law behavior, followed by an exponential cutoff at a characteristic σ, to parametrize the VDF. Following the functional form of the BHMF from Graham et. al. (2007) [70] and Aller & Richstone (2002) [71], I introduce two different Schechter-like functions. The first one has 3 free parameters, α, $\Phi_\star$, and $\sigma_\star$:

$$\Phi(\sigma)\ d\sigma = \Phi_\star \left(\frac{\sigma}{\sigma_\star}\right)^{\alpha+1} \exp\left[\frac{-\sigma}{\sigma_\star}\right]\ d\sigma. \tag{2.7}$$

The slope of the power law has been adjusted to $\alpha+1$, where $\alpha = -1$ corresponds to a flat distribution at $\sigma < \sigma_\star$. The characteristic truncation value of σ is $\sigma_\star$, where $\Phi(\sigma_\star) = \Phi_\star$. The second Schechter-like function I use has an additional β parameter like the original function:

$$\Phi(\sigma)\ d\sigma = \Phi_\star \left(\frac{\sigma}{\sigma_\star}\right)^{\alpha+1} \exp\left[1 - \left(\frac{-\sigma}{\sigma_\star}\right)^{\beta}\right]\ d\sigma. \tag{2.8}$$

Number of (free) parameters	$\boldsymbol{\alpha}$	$\boldsymbol{\beta}$	**log $\boldsymbol{\Phi_\star}$ [Mpc^{-3} dex^{-1}]**	**log $\boldsymbol{\sigma_\star}$ [km s^{-1}]**
3	0.95 ± 0.09	–	-1.42 ± 0.14	1.5 ± 0.48
4	-1.90 ± 0.17	7.82 ± 0.45	-2.80 ± 0.31	2.45 ± 0.18

Table 2.2: Best-fit parameters for eq. (2.7) – top row – and (2.8) – bottom row.

Table 2.2 lists the best-fit parameters to equations (2.7) and (2.8). The uncertainties on the parameters were derived by using the same Monte-Carlo simulations by which uncertainties on the VDF were found (again, assuming a gaussian error distribution). From Fig. 2.7, it is clear that the 4-parameter function, i.e. eq. (2.8), is a better functional fit to the observed VDF. The fit to the 3-parameter function is highly uncertain, as seen by the large shaded region. Plus, the exponential cut-off is at a very low σ ($\sigma \sim 31$ kms), so it's not describing our observed distribution well. The 4-parameter function, however, gives a more reliable fit for $1.86 \leqslant \log\sigma \leqslant 2.5$ – the high uncertainties for $\log\sigma > 2.5$ probably result in higher than actual number densities at that range. I also note that this function isn't a perfect description of the data at all ranges, since it slightly overestimates the VDF at $2.32 \lesssim \log\sigma \lesssim 2.46$.

Comparison of my observed VDF with past works yields reasonable agreement. Shown in Fig. 2.6 are the VDFs derived from SDSS velocity dispersions by Sheth et. al. (2003) [72], Bernardi et. al. (2010) [73], and Sohn et. al. (2017). Sheth et. al. only examined early-type galaxies, so it's natural that their VDF lies below ours for the most part. However, the Sheth et. al. VDF also declines rapidly for $\log\sigma \lesssim 2.2$, because their sample only used about 9000 galaxies from the available SDSS data at the time, and because it was not complete in σ. In contrast, both Bernardi et. al. and Sohn et. al. considered early and late-type galaxies. The former, however, used a magnitude-limited sample instead of one that was complete in σ.

While the Sohn et. al. sample was complete in σ, it only contained quiescent galaxies, as mentioned above, so it was a subset of my sample. The large number of galaxies with $\log\sigma \lesssim 2$ helped characterize my low σ end, thereby making our VDF *rise* slightly at the low σ end, rather than fall or flatten. This is most likely

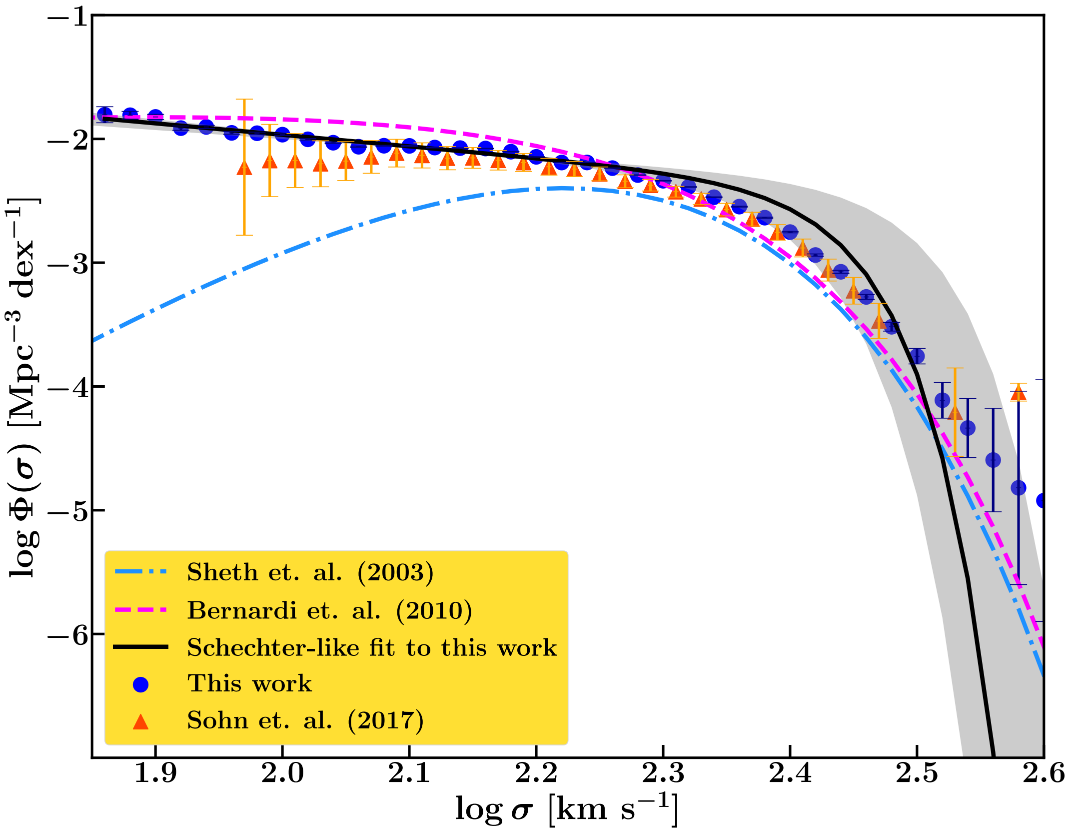

Figure 2.6: Comparison of the VDF from this work (observed VDF in blue, 4-parameter Schechter-like function fit in black curve) with that of Sohn et. al. (2017) (orange triangles), Bernardi et. al. (2010) (magenta dashed line), and Sheth et. al. (2003) (light blue dot-dashed line). The grey shaded region indicates $\pm 1\sigma$ uncertainty in the fit to our observed VDF.

due to star-forming galaxies in my sample, whose VDF has been noted to be much steeper than quiescent galaxies at the low and medium σ range for all redshifts [74]. My analysis also reaffirms the accepted notion and the findings of these works that galaxies with $\sigma \gtrsim 350$ km s^{-1} are extremely rare, since just over a hundred such galaxies were found. I will use the parametrized form of our VDF (eq. (2.8)) to estimate the BHMF, assuming a log-normal distribution around the M_{BH}-σ relation, in the next chapter.

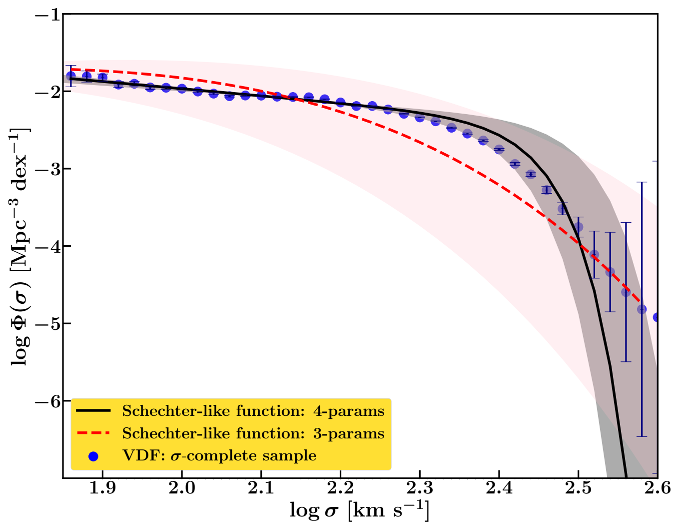

Figure 2.7: Schechter-like fits to the observed VDF (blue points): Red dashed line is eq. (2.7) and black line is eq. (2.8), with parameters listed in Table 2.2. The pink and grey shaded regions indicate the $\pm 1\sigma$ uncertainty of the 3 and 4 parameter function fits, respectively.

2.2 Correlations: Using M_{BH}-σ to estimate masses

As discussed in the last chapter, tight correlations between measured black hole masses and their host galaxies' σ can help us estimate M_{BH} for a much larger sample of galaxies for which we don't have M_{BH} data. With the assumption that all the galaxies in my final sample from SDSS host a SMBH at their center, I can estimate the mass of the central black hole for each galaxy from the M-sigma relation. The most recent estimate of M_{BH}-σ has increased the sample size of SMBHs for which we have M_{BH} by almost two times the previous largest compilation. This is outlined in Van Den Bosch (2016), who compiled 230 M_{BH} values from the literature [32].

All of these measurements are in galaxies that are very close to us and include early-type, late-type, and even dwarf galaxies. 206 measurements use dynamical tracers: stellar kinematics, gas kinematics, and masers, in galaxies near enough that their sphere of influence (section 1.2) can be resolved. The remaining 24 are from reverberation mapping from temporally resolved galaxies: M_{BH} is obtained using time delays in the broad line region of these nearby AGNs. Log-linear regressions between M_{BH} and σ were fitted via the *mlinmixerr* and *linmixerr* algorithms [75]. The resulting correlation between logM_{BH} and $\log\sigma$ was found to be:

$$\log\left(\frac{M_{BH}}{M_\odot}\right) = (8.32 \pm 0.04) + (5.35 \pm 0.23)\log\left(\frac{\sigma}{200\ \mathrm{km\ s^{-1}}}\right). \tag{2.9}$$

The black hole mass, M_{BH}, is in units of $M_\odot$ and the host galaxy's velocity dispersion, σ, is in km s^{-1}. The result of this fit is shown in Fig. 2.8, which uses different symbols to indicate the different M_{BH} measurement methods. Upper limits shown in the figure are not used in the fit. This relation, especially its slope > 5 is similar to most recent works, especially that of McConell & Ma (2013) [31], whose sample was the basis of this sample. The scatter around log M_{BH}, ϵ, is 0.49 ± 0.03, which is almost half an order of magnitude, as opposed to $\epsilon \sim 0.3 - 0.4$ in most other studies of M_{BH}-σ. Van Den Bosch attributes this larger-than-usual scatter in M_{BH}-σ primarily to the large sample size including many more low-mass ($\sim 10^6$ $M_\odot$) SMBHs, but also to artificial exclusion of outliers in previous studies and to the fitting routine he used which is known to produce a larger scatter with respect to other routines.

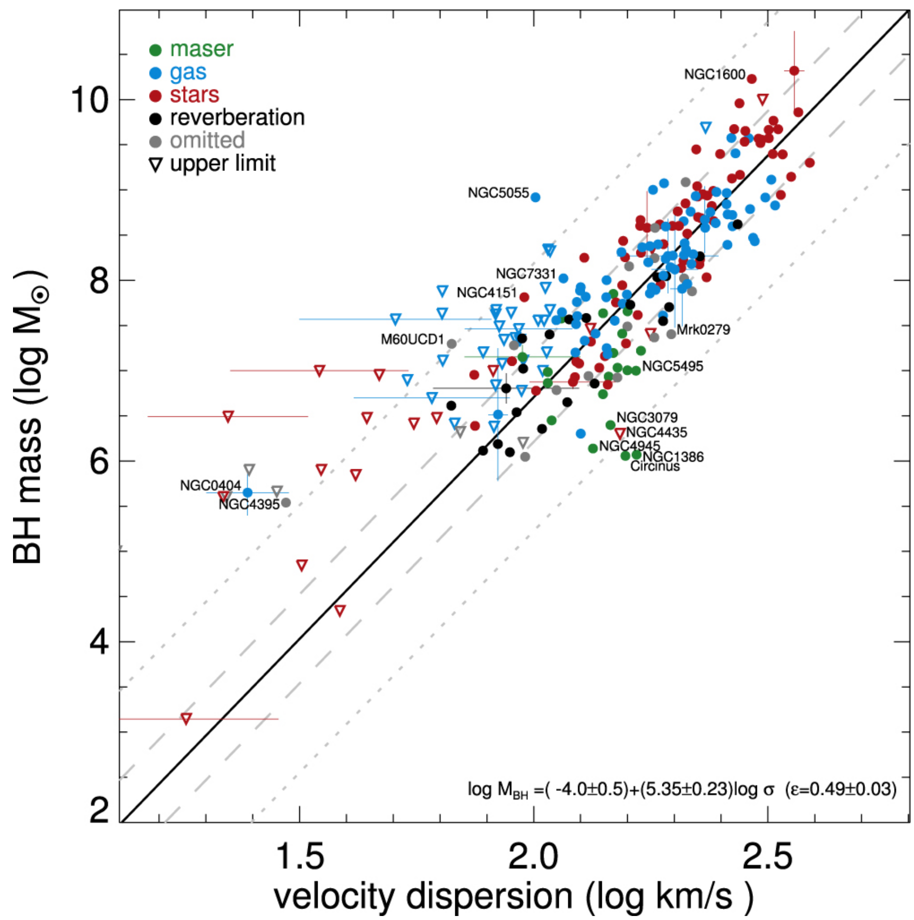

Figure 2.8: The black hole mass-velocity dispersion (M_{BH}-σ) relation from Van den Bosch (2016). This solid line shows the M_{BH}-σ relation from eq. (2.9), from 230 galaxies. Upper limits of M_{BH} are shown as open triangles – these are not included in the fit. Different colors denote different types of M_{BH} measurements. Error bars are only shown for the objects with the largest uncertainties. The grey dashed and dotted lines denote 1 and 3 times the intrinsic scatter ($\epsilon = 0.49 \pm 0.03$), respectively.

The largest issue with taking this correlation at face value is the heterogeneity of the sample: not only do M_{BH} measurement methods vary, so do the definitions of σ used in different samples. Different σ measurements in this sample use different instruments and methods. However, the fact of these inhomogeneities is not enough to offset the **black hole fundamental plane (BHFP)** we observe. According to the Virial Theorem, all gravitational systems sit on a 3-D plane of given by:

$$GM_{1/2} = R_{1/2}\sigma_{1/2}^2, \tag{2.10}$$

where $M_{1/2}$ is half the mass of these systems, $R_{1/2}$ is half their size, and $\sigma_{1/2}$ half of the second moment of the velocity tensor of those systems. None of these quantities are measurable directly, so we adopt in their place the luminosity, L, the half-light radius, R_e, and σ, respectively. As it's been shown over and over again here, various empirical relationships have emerged out of studying galaxies for quite a long time. The Faber-Jackson relation relates L to σ, the Tully-Fisher relation relates L to angular velocity, V_C, the Kormendy relation (1977) relates L and R_e. These relations are interpreted to be projections of the 3-D plane, which we call a *fundamental plane*.

SMBHs and their host galaxies, being gravitational systems, may also have a fundamental plane relating the observables, L, R_e, and σ. In particular, we expect SMBHs and the *spheroids* wherein they lie to obey a fundamental plane. This is because, inside the half-light radius (which is a subset of the spheroid's size), the gravitating mass consists almost entirely of stars, dark matter and the central BH, meaning that properties like the velocity dispersion of stars should be strongly linked with the spheroid's mass and size. Indeed, this is what Van den Bosch observes for his sample: L, R_e, and σ all lie on a fundamental plane given by the form $\sigma \propto L_k^\alpha R_e^\beta$ (eq. (1) in Van den Bosch (2016); L_k is the K-band luminosity and α and β empirically determined coefficients). The scatter in the relation is a mere 0.07 ± 0.01, which led Van den Bosch to conclude that the if heterogeneity of σ in his sample gave rise to significant errors, they would not lie on such a tight fundamental plane.

He extends this argument to unify this galactic fundamental plane (GFP) to black hole masses. A correlation was observed between M_{BH} (these are the measured masses, independent of the M_{BH}-σ relation) and L and R_e of the form $M_{BH} \propto L_k^\alpha R_e^\beta$ with a scatter a little over half a dex. By combing this with the GFP, Van den Bosch finds $M_{BH} \propto \sigma^{5.3}$, which is consistent with eq. (2.9). Thus, a BHFP is observed for this sample, again implying possibly some physical mechanism(s) resulting in the coevolution of SMBHs and their host galaxies. The GFP and BHFP are shown in Figs. 2.9a and 2.9b, respectively.

As of this writing, this work is the first in which the Van den Bosch M_{BH}-σ relation is applied to a construction of the local BHMF. The large sample size and establishment of a GFP and BHFP of the whole sample will help produce a statistically significant description of the accretion history and distribution of masses in SMBHs. I use eq.(2.9) on all 96842 galaxies in my sample to estimate the mass of their central SMBHs. The resulting M_{BH} is shown in a histogram in Fig. 2.9. The median value of M_{BH} in this sample is $\log\left(\frac{M_{BH}}{M_\odot}\right) = 7.93$. The lower bound is seen to be a million solar masses, or $\log\left(\frac{M_{BH}}{M_\odot}\right) = 6$, while very few galaxies are predicted to host SMBHs with $\log M_{BH} \gtrsim 9.5$ $M_\odot$, meaning it will be difficult to characterize this very high mass end of the observed BHMF. In the next chapter, I will use these M_{BH} values in concert with a $1/V_{max}$ method like with the VDF to construct the BHMF. I

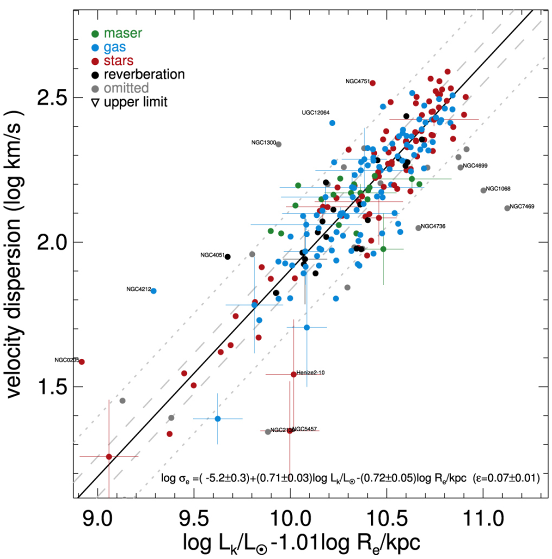

(a) The galactic fundamental plane (GFP), of velocity dispersion, σ, K-band luminosity, L, and half-light radius, R_e, of host galaxies of the SMBHs studied in Van den Bosch (2016). The scatter around $\log \sigma$ is 0.07 ± 0.01.

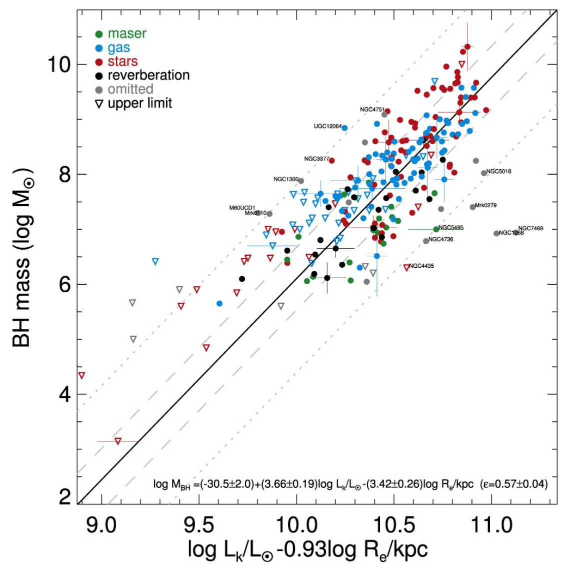

(b) The black hole fundamental plane (BHFP) of SMBH mass, M_{BH}, and host galaxy's $K-$*band* luminosity, L, half-light radius, R_e, from Van den Bosch (2016). The scatter around log M_{BH} is 0.57 ± 0.04.

will also convolve the VDF obtained in the previous section with the M_{BH}-σ relation to obtain another measure of the BHMF.

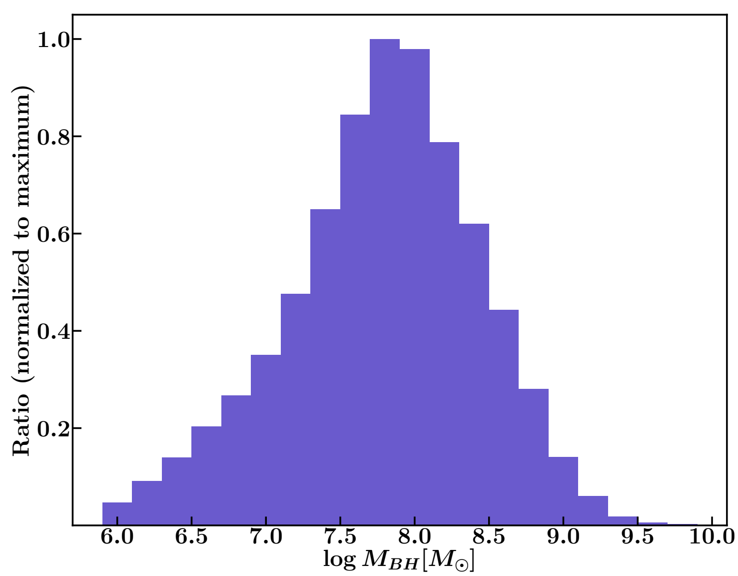

Figure 2.9: Histogram of M_{BH} values for the final sample, obtained by converting σ to M_{BH} using eq. (2.9).

Chapter 3

Mass function from observations

3.1 The Black Hole Mass Function (BHMF)

Now that I have described the velocity dispersion, σ, of galaxies in my sample and a correlation linking σ to the mass of a galaxy's central black hole, M_{BH}, the stage is set for us to derive the BHMF. The Black Hole Mass Function (BHMF) is the number density of supermassive black holes of a given mass per unit logarithmic mass, given by:

$$\Phi(M_{BH})\, d\log M_{BH} = \frac{N(M_{BH})\, d\log M_{BH}}{V(M_{BH})}, \tag{3.1}$$

where $N(M_{BH})$ is the number of SMBHs with mass M_{BH} and $V(M_{BH})$ is the volume sampled at mass M_{BH}. There are two methods primarily used to derive the BHMF. The first relies on a $1/V_{max}$ approach as we used in deriving the VDF above, i.e. we count the number of SMBHs in equal mass bins, after correcting for the Malmquist bias. I call this the **direct method**. The second method, which I call the **VDF method**, uses the parametrized form of the VDF and convolves it with the M_{BH}-σ relation – assuming a log-normal distribution of M_{BH} – to generate a BHMF. Note that both of these uses the M_{BH}-σ relation from Van den Bosch (2016).

3.1.1 The direct ($1/V_{max}$) method

Much like we did with the VDF in 2.1.2, the $1/V_{max}$ method estimates the relative contribution of each SMBH with mass M_{BH} to the BHMF, by weighing the individual masses. The procedure I follow is similar to that of Graham et. al. (2007) [70] and Vika et. al. (2009) [76]. Using eq. (2.9), I first convert σ of all the galaxies in my sample to a central black hole mass, M_{BH} (assuming of course, that each of these galaxies host a SMBH). Then I divide up M_{BH} into 20 equal bins of size $d\log M_{BH} = 0.2$, starting from $\log\left(\frac{M_{BH}}{M_\odot}\right) = 6$, and ending at $\log\left(\frac{M_{BH}}{M_\odot}\right) = 10$. So we're probing the mass range of 1 million to 10 billion $M_\odot$. As Fig. 2.9 showed already, very few SMBHs are predicted to have $\log M_{BH} \gtrsim 9.5\ M_\odot$, and none have $\log M_{BH} < 6\ M_\odot$.

Similar to eqn. (2.4), then, the BHMF is computed by:

$$\Phi_j(M_{BH})\Delta \log M_{BH} = \sum_{i}^{N_{bin}} \frac{1}{V_{max,i}}, \tag{3.2}$$

where now $V_{max,i}$ is the maximum volume at which a SMBH i at redshift z_i with mass M_{BH} could be detected in. Again, I sum over all N_{bin} galaxies in the j bin.

Of course, there are a number of sources of uncertainty associated with this process. In fact, three primary sources of uncertainty need to be accounted for:

i) The uncertainty in the coefficients in eq. (2.9), i.e. the gradient and y-intercept of the M_{BH}-σ relation.

ii) The uncertainty in the measurement of σ, $\Delta\sigma$.

iii) The scatter in the M_{BH}-σ relation: $\epsilon = 0.49 \pm 0.03$.

I quantify the impact of these on the derived BHMF by using a Monte Carlo method to model the uncertainties. The uncertainties are perturbed individually and collectively and their impact on the resulting BHMF is estimated. In other words, I repeat the following steps 10000 times in deriving uncertainties:

1. Randomly modify the coefficients of eq. (2.9) by the corresponding uncertainties in both, assuming a gaussian error distribution for both.

2. Randomly modify σ by the corresponding uncertainty, $\Delta\sigma$, again assuming a gaussian error distribution in σ. This, in conjunction with the modified coefficients from step 1, is used to calculate M_{BH} from (a modified version of) eq. (2.9).

3. Perturb M_{BH} from step 2 by the scatter in eq. (2.9), ϵ. This assumes – surprise, surprise – a gaussian error distribution in log M_{BH}.

The resulting BHMF and associated uncertanties are shown in Fig. 3.1 and listed in Table 3.1. Like the VDF, the BHMF was described well by a 4-parameter Schechter-like function. The best-fit Schechter function parametrizing the BHMF is given by:

$$\Phi(M_{BH})\; d\log M_{BH} = \Phi_\star \left(\frac{M_{BH}}{M_\star}\right)^{\alpha+1} \exp\left[1 - \left(\frac{M_{BH}}{M_\star}\right)^{\beta}\right] \; d\log M_{BH}. \tag{3.3}$$

Here, $M_\star$ is the characteristic truncation mass – the point at which the function transitions from a power law to an exponential fall-off – and $\Phi_\star = \Phi(M_\star)$. Again, α and β are dimensionless parameters. The best-fit parameters of this function to my data were: $\alpha = -1.15 \pm 0.08$, $\beta = 0.90 \pm 0.17$, $M_\star = (6.41 \pm 0.18) \times 10^8$ $M_\odot$, and $\Phi_\star = (3.25 \pm 0.09) \times 10^{-4}$ Mpc^{-3} dex^{-1}. Using the errors as the $\pm 1\sigma$ uncertainties for each parameter and assuming a gaussian error distribution in each, I repeated

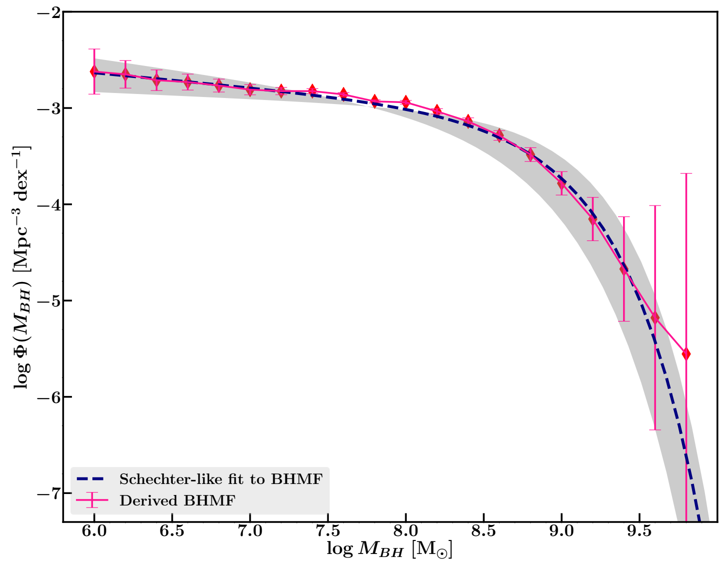

Figure 3.1: The BHMF derived from the $1/V_{max}$ method. The observed BHMF points are the pink diamonds, while the best-fit Schechter-like function parametrizing the data (eq. (3.3)) is the dashed dark blue line. The grey shaded region indicates the $\pm 1\sigma$ uncertainty of the fit.

the Schechter fit 10000 times. The Schechter fit and the resulting 68% confidence interval of the fit are shown as the dark blue dashed line and the grey shaded region, respectively. The Schechter function reasonably describes the data in the range $6 \leqslant \log\left(\frac{M_{BH}}{M_\odot}\right) \leqslant 9.6$.

The observed M_{BH} distribution and its Schechter-like characterization implies that the local universe is much more numerously populated with low to medium mass SMBHs – those in the range $6 \leqslant \log\left(\frac{M_{BH}}{M_\odot}\right) \leqslant 8$ – than high mass ($\log\left(\frac{M_{BH}}{M_\odot}\right) \gtrsim 9$) SMBHs. With increasing M_{BH}, we observe a decreasing number density, but up to $M_{BH}= (6.41 \pm 0.18) \times 10^8$ M$_\odot$, this decline is slow, whereas $\Phi(M_{BH})$ falls rapidly after that. It is difficult to accurately characterize the high mass end because of the low number of objects with $\log\left(\frac{M_{BH}}{M_\odot}\right) \gtrsim 9.5$.

3.1.2 The VDF method

This method is used more widely in deriving a BHMF, whether via the M_{BH}-σ relation, or by another scaling relation between black hole mass and a galaxy property. The idea here is to convert the VDF, $\Phi(\sigma)$, to a BHMF, $\Phi(M_{BH})$, using the M_{BH}-σ relation as a bridge between M_{BH} and σ. First, we assume a log-normal distribution for a given M_{BH}. This is justified by looking at Fig. 2.9 and noting that the distribution of predicted M_{BH}s can be described by a gaussian, or normal,

log M_{BH} [$M_\odot$]	**$\Phi(M_{BH})$** [$\times10^{-4}$ Mpc^{-3} dex^{-1}]	**N_{bin}**
6.0	$23.90^{+23.83}_{-10.91}$	609
6.2	$22.38^{+10.83}_{-3.45}$	1194
6.4	$19.44^{+7.06}_{-2.25}$	1823
6.6	$18.61^{+5.15}_{-1.59}$	2651
6.8	$17.11^{+4.77}_{-2.13}$	3492
7.0	$15.51^{+3.88}_{-1.96}$	4571
7.2	$15.00^{+1.95}_{-0.63}$	6219
7.4	$14.99^{+0.39}_{-1.28}$	8490
7.6	$13.84^{+2.24}_{-2.84}$	11027
7.8	$11.71^{+2.96}_{-3.40}$	13063
8.0	$11.46^{+2.75}_{-3.27}$	12789
8.2	$9.23^{+1.10}_{-1.71}$	10292
8.4	$7.26^{+0.19}_{-0.82}$	8098
8.6	$5.19^{+0.56}_{-0.05}$	5784
8.8	$3.28^{+1.08}_{-0.54}$	3660
9.0	$1.65^{+1.44}_{-0.98}$	1840
9.2	$0.70^{+1.34}_{-0.98}$	780
9.4	$0.21^{+1.05}_{-0.78}$	235
9.6	$0.07^{+0.65}_{-0.47}$	73
9.8	$0.03^{+0.39}_{-0.27}$	28

Table 3.1: The BHMF, derived directly from the $1/V_{max}$ method. The uncertainties are obtained from Monte Carlo simulations, as described in the text. The third column lists the number of objects in each bin.

distribution in logarithmic masses, log M_{BH}. The probability of finding M_{BH} in the range $[\log M_{BH}, \log M_{BH}+d\log M_{BH}]$ for a given $\log\sigma$ is $P(\log M_{BH}|\log\sigma)\, d\log M_{BH}$. This is given by:

$$P(\log M_{BH}|\log\sigma)\ d\log M_{BH} = \frac{1}{\sqrt{2\pi\epsilon_{M_{BH}}^2}} \exp\left[-\frac{1}{2}\left(\frac{\log M_{BH} - [a + b\log\sigma]}{\epsilon_{M_{BH}}}\right)^2\right] d\log M_{BH} \quad (3.4)$$

where a and b are the coefficients in the M_{BH}-σ relation, and $\epsilon_{M_{BH}}$ its vertical scatter. Thus, the number of galaxies with SMBH mass M_{BH} in the range $[\log M_{BH}, \log M_{BH} + d\log M_{BH}]$ is found by convolving P with the VDF, $\Phi(\sigma)$:

$$\Phi(M_{BH})\ d\log M_{BH} = \frac{1}{\sqrt{2\pi\epsilon^2_{M_{BH}}}} \int_0^\infty \Phi(\sigma) \exp\left[-\frac{1}{2}\left(\frac{\log M_{BH} - [a + b\log\sigma]}{\epsilon_{M_{BH}}}\right)^2\right] d\log\sigma\ d\log M_{BH} \quad (3.5)$$

I use the 4-parameter Schechter function parametrization of the VDF (eq. (2.8)) as $\Phi(\sigma)$. The VDF-derived BHMF is shown in comparison to the directly derived VDF in Fig. 3.2a. The errors were propagated from the Schechter fit to the observed VDF.

The shapes of both mass functions are very similar, with both showing slow decrease in SMBH number density at low and medium masses, followed by rapid fall-off at higher masses. The differences between the two results can be attributed to how the Schechter function in 2.1.2 fit the observed VDF. The change in behavior from power law to exponential function happens at a higher M_{BH} for the VDF BHMF, but it also has a slightly higher slope of the exponential decline. It estimates a higher number of black holes in the mass range $8 \lesssim \log\left(\frac{M_{BH}}{M_\odot}\right) \lesssim 9.5$, corresponding to the region in which the Schechter-like fit to the VDF overestimates the observed VDF. Statistically speaking, there are no major differences between the two methods, since they both weigh out the contribution of every object to the BHMF in the same volume-dependent way. In fact, it's probably a misnomer calling one of them the $1/V_{max}$ method when really they're both derived from the $1/V_{max}$ technique.

The BHMF can also be expressed as a mass density of SMBHs of a given mass per unit magnitude, which has units of $M_\odot$ Mpc^{-3} dex^{-1}. The comparison of the two mass density BHMFs are shown in Fig. 3.2b. The shapes of the two functions are similar again, showing that mass density increases from the low mass regime to the high mass, followed by a steep decline at the highest masses ($\log\left(\frac{M_{BH}}{M_\odot}\right) > 9.2$). The $1/V_{max}$-derived BHMF peaks at a lower mass and descends less sharply than the VDF-derived BHMF. The latter also predicts $\sim$twice the mass density in the range $9 \lesssim \log\left(\frac{M_{BH}}{M_\odot}\right) \lesssim 9.3$; the larger peak of the blue curve is most likely a consequence of the Schechter function not fitting the observed VDF well in all ranges. These differences are significant enough that they may contribute to producing biased or inaccurate results in further analysis. Therefore, hereafter I mainly consider the BHMF derived directly from the $1/V_{max}$ method.

3.2 SMBH mass density

It is now time to estimate the local SMBH mass density, ρ_{BH}, the total mass of SMBHs per unit volume in the local universe. This is obtained by integrating the product of the BHMF and M_{BH} over the entire mass range probed by the parametrized BHMF, $\Phi(M_{BH})$:

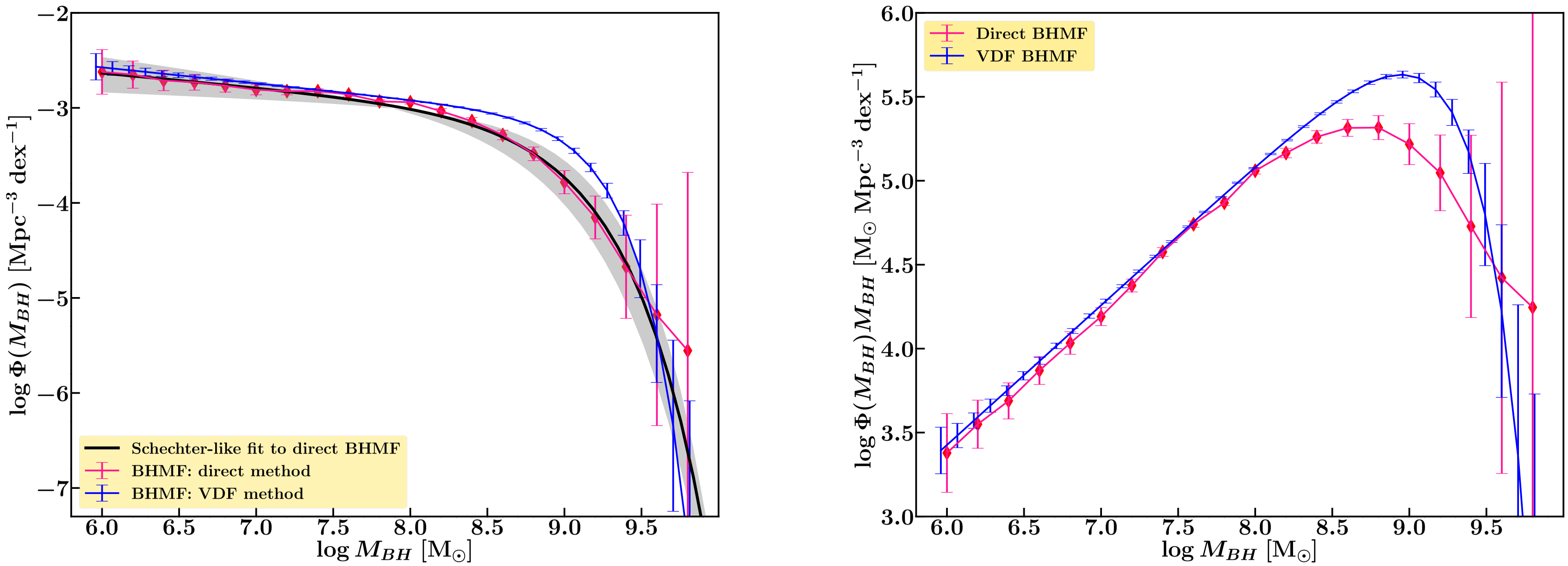

(a) (b)

Figure 3.2: The BHMF compared for the direct ($1/V_{max}$) method – shown in pink – and the VDF method – shown in blue. a) The BHMF as a number density (units of Mpc^{-3} dex^{-1}). The black curve is the Schechter function fit to the $1/V_{max}$ BHMF, and again the grey shaded region is the fit's $\pm 1\sigma$ uncertainty. b) The BHMF as a mass density per unit magnitude (units of $M_\odot$ Mpc^{-3} dex^{-1}).

$$
\begin{aligned}
\rho_{BH} &= \int_{\log(M_{BH}/M_\odot)=6}^{\log(M_{BH}/M_\odot)=9.6} \Phi(M_{BH}) M_{BH} \; d\log M_{BH} \\
&= \frac{\Phi_\star e M_\star}{\beta \ln 10} \left[\gamma\left(\frac{\alpha+2}{\beta}, \left(\frac{10^{9.6} M_\odot}{M_\star}\right)^{\beta} \right) - \gamma\left(\frac{\alpha+2}{\beta}, \left(\frac{10^{6} M_\odot}{M_\star}\right)^{\beta} \right) \right]
\end{aligned}
\tag{3.6}
$$

where $\gamma(a,x) = \int_0^x t^{a-1} e^{-t} \, dt$ is the lower incomplete gamma function of a and x. The derivation is worked out in full in Appendix A.

I perform 10000 Monte Carlo realizations of this calculation, by varying the best-fit parameters of eq. (3.3) by their $\pm 1\sigma$ uncertainties assuming gaussian distributions. The resulting histogram of ρ_{BH} values are shown in Fig. 3.3. I take the median of this distribution to be the best value of the local mass density ρ_{BH}, and I take the $+1\sigma$ uncertainty as the difference between the 84$^{\text{th}}$ percentile and mean value, and the -1σ uncertainty as the difference between the mean and the 16$^{\text{th}}$ percentile value. I find that $\rho_{BH} = \left(2.71^{+0.55}_{-0.43}\right) \times 10^5$ M$_\odot$ Mpc^{-3} for SMBHs of masses between 10^6 and $10^{9.6}$ M$_\odot$. This is in agreement with previous determinations, as we'll see soon.

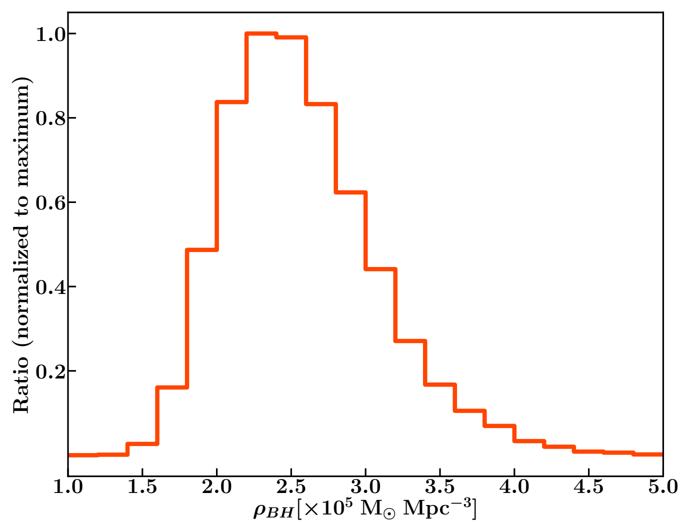

Figure 3.3: Values of the local mass density of SMBHs for 10000 different solutions to eq. (3.6), each time varying the best-fit parameters of eq. (3.3) assuming their errors are normally distributed. The bins are each of width 0.2×10^4 M$_\odot$ Mpc^{-3}.

3.3 Soltan's Argument revisited: The local and integrated mass density

Andrzej Soltan, like quite a few astronomers of his time, believed that quasars were powered by mass accretion on to SMBHs. His simple method of using observed quasar counts to characterize the mass accretion history of SMBHs up to the present day has withstood the test of time [77]. The average radiative efficiency, ϵ, of a SMBH tells us what fraction of the mass accreted onto it is converted to luminous energy[1]:

$$\epsilon = \frac{L_{bol}}{\dot{M}_{acc}c^2}. \tag{3.7}$$

$\dot{M}_{acc}$ is the rate at which mass accretes on to a black hole, so $\dot{M}_{acc}c^2$ is what you'd get if all the mass accreted on to it was converted to energy. L_{bol} is the (total) bolometric luminosity produced by the black hole (this is in units of power, so ϵ works out to be dimensionless). However, not all of the accreting mass will be eaten up by the black hole. The actual rate at which mass accretes on to a SMBH, or the SMBH growth rate, is given by:

$$\dot{M}_{BH} = (1-\epsilon)\dot{M}_{acc}c^2, \tag{3.8}$$

the factor of $(1-\epsilon)$ accounting for the mass radiated away during the accretion process. Soltan integrated the observed quasar count, the number density of quasars of luminosity L at redshift z, i.e. $\Phi(L,z)$, over all L and z. This gives us the *integrated mass density* accreted by SMBHs:

$$\rho_{BH,int} = \frac{1-\epsilon}{\epsilon c^2}\int_0^{z_{max}}\int_{L_{min}}^{L_{max}} L'_{bol}\Phi(L',z)\frac{dt}{dz}\, dL'\, dz, \tag{3.9}$$

So, if we know ϵ – or more practically, assume a fixed value of ϵ – the energy radiated from the observed AGN population gives us the the integrated mass density of SMBHs in those systems. If this value happens to be similar to the local SMBH mass density which we obtain from observations of *nearby* galaxies, then we can safely claim that the primary mode of SMBH growth is mass accretion during AGN phases. If we set these two cumulative mass densities to be equal: $\rho_{BH,int} = \rho_{BH}$, then it sets a constraint on ϵ, an average radiative efficiency of SMBHs throughout cosmic time.

In 1982, our instruments were far more limited than they are now, so we couldn't observe many of the dimmer quasars we can today. Thus, Soltan's estimate of the accreted mass density of quasars was only a lower limit. By assuming $\epsilon = 0.1$, he concluded that at least $\gtrsim 8\times10^4$ M$_\odot$ of quasar mass was accumulated in every Mpc^{-3} of the universe. Over the past two decades, this estimate has been improved significantly, with $\rho_{BH,int}$ always found to be of the order of 10^5 M$_\odot$ Mpc^{-3}. For example, Shankar et. al. (2009) found that the local mass density derived from various scaling relations such as M_{BH}-n and M_{BH}-L_{sph} yield an average radiative efficiency, $\epsilon\sim0.065-0.07$ in order to match local mass density to the integrated one [79]. They also showed that $\epsilon \gtrsim 0.15$ would require local mass densities to be about two times lower than they are observed to be.

This match of the local and integrated mass densities suggests that accretion of *baryonic* matter accounts for virtually all of the growth of SMBHs across cosmic time. This warrants the assumption that accretion of dark matter isn't a significant aspect

[1]The maximum radiative efficiency is only around 30%, or $\epsilon\sim0.3$. See Thorne (1974) [78].

of SMBH growth, as accepted by many authors, including Shankar et. al. (2004) [80] and Graham et. al. (2007). This assumption would also be consistent with a number of physical mechanisms that link stellar, so baryonic, properties of a galaxy to its central black hole, signaling that galaxies and their SMBHs coevolve.

By this working assumption, I can estimate the fraction of baryonic matter of the universe inside SMBHs. The fraction of the entire mass-energy budget of the universe that are baryons is given by $\Omega_{baryon} = (0.0222 \pm 0.007)$: this is the ratio of the density of baryons to the critical density of the universe, $\frac{\rho_{baryon}}{\rho_{critical}}$ [81]. Given the critical density of the universe, $\rho_{critical} = 1.36\times$ $M_\odot$ Mpc^{-3} (Graham et. al. 2007), we can find the fraction of the universe's mass-energy budget that is just SMBHs, Ω_{BH}:

$$\Omega_{BH} = \frac{\rho_{BH}}{\rho_{critical}}. \tag{3.10}$$

The fraction of baryons in the universe that is locked up inside SMBHs is then simply $\frac{\Omega_{BH}}{\Omega_{baryon}}$. I find that $(0.009 \pm 0.002)\%$ of baryonic matter is inside a SMBH, so about 1 part in 10000. For comparison, Graham et. al. found $(0.0024 \pm 0.01)\%$ and Vika et. al. found $(0.0027 \pm 0.0007)\%$.

3.4 Past works and constraints on SMBH growth and evolution

> *Despite the flexibility of our [theoretical] framework, no one model provides a good fit to all the data we consider.*
>
> \- F. Shankar (2013)

Several authors and groups have derived the local SMBH mass function using a variety of techniques. While the M_{BH}-σ relation has been a popular choice for scaling relation, many have also opted for M_{BH}-L_{sph}, M_{BH}-$M_{spheroid}$, and other observed correlations to relate M_{BH} to the host galaxy. The general approach is the same as outlined in this thesis, but far more have chosen to convolve a scaling relationship with the observed distribution of a galaxy property than to directly measure the BHMF by volume-weighting. A comparison of my (direct) BHMF with some others in the literature for which the data was available for plotting is shown in Fig. 3.4.

Notably, all the observed BHMFs show a similar distribution of black hole masses, especially in the shape of the curve. The Graham et. al. BHMF was derived from a log-quadratic relation between M_{BH} and n, the Sérsic index of 1769 galaxies in the Millennium Galaxy Catalogue (MGC) at $0.013 < z < 0.18$. Vika et. al. used the M_{BH}-L_{sph} relation from the same survey, with a sample of 1743 galaxies in the same volume. Both these studies are severely constrained by low-number statistics and systematic uncertainties in the BHMF derivation procedure. In particular, Graham

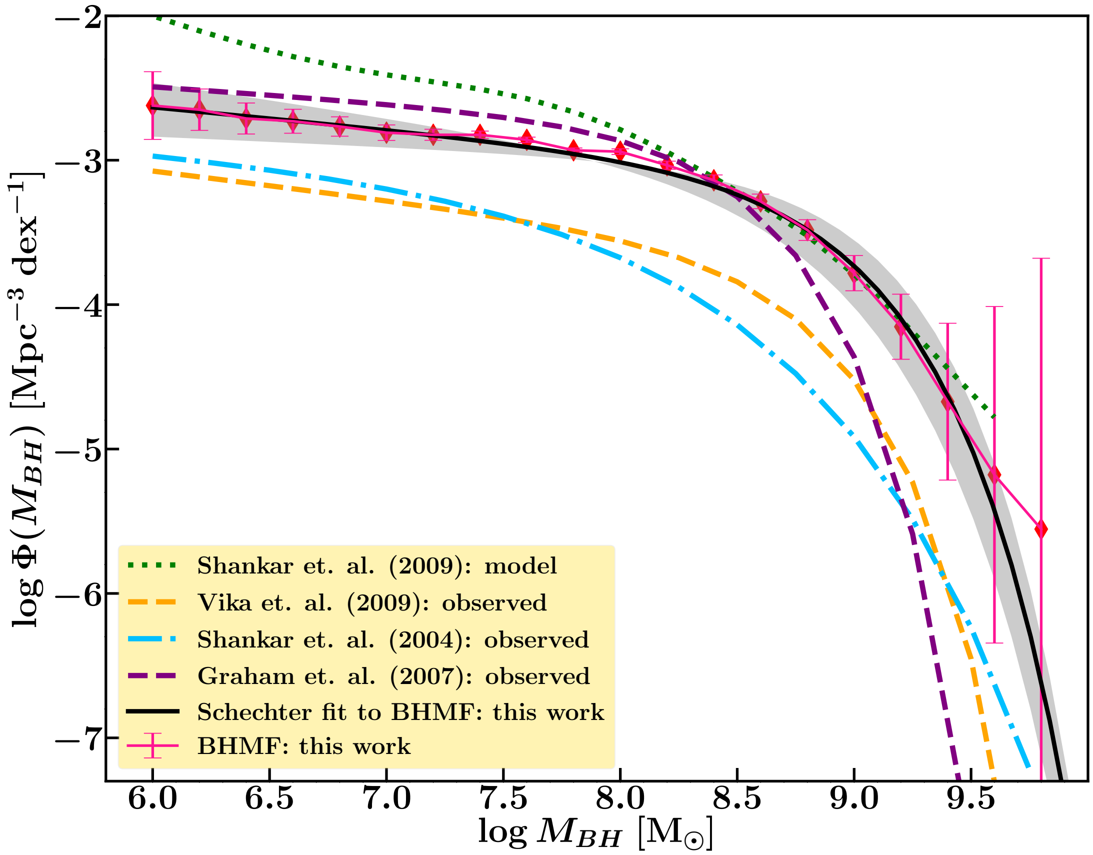

Figure 3.4: Comparisons between BHMF from this work and others. The green dotted line shows the BHMF produced by a model that assumes a mean radiative efficiency, $\epsilon = 0.065$. The blue dot-dashed, orange dashed, and purple dashed curves are all observed BHMFs obtained by a similar procedure to mine. Note that the Shankar et. al. (2004) BHMF was derived only for early type galaxies.

et. al. found quite significant scatter in their M_{BH}-n correlation, and Vika et. al. made some underlying assumptions about the difference between light contained in an elliptical spheroid and a spiral bulge. The latter adopted a constant ratio of light contained in the spheroid to the total light, B/T, which has been observed to introduce significant systematic uncertainties in the BHMF (see also Li et. al. (2011) [82]).

On the other hand, the Shankar et. al. (2004) determination shown in Fig. 3.4 only considers early-type galaxies. The BHMF shown also used a luminosity function, but only from SDSS early-type galaxies. Though they showed that early-type galaxies contribute about 3 times as much to the local mass density, ρ_{BH}, as late-types, the plot also illustrates that a significant fraction of the number density is missed if late-type galaxies are not considered in a derivation of the local BHMF.

The green dotted line in Fig. 3.4 shows the results of a theoretical model proposed by Shankar et. al. (2009). They predicted that the mass function, $\Phi(M_{BH})$, evolves self-consistently, with a mean accretion rate, $\dot{M}_{BH}$, and an average radiative efficiency, ϵ, as above. The plot shows the resulting BHMF from the model with $\epsilon = 0.065$. While the shape faithfully reproduces our observed BHMF, the model over-predicts the number of SMBHs with masses $6 < \log\left(\frac{M_{BH}}{M_\odot}\right) < 8$.

Perhaps the most significant difference between mine and other observed BHMFs is the high mass range, where my BHMF predicts more black holes of over a billion $M_\odot$ ($\log\left(\frac{M_{BH}}{M_\odot}\right) > 9$). While it is possible that this represents an actual distribution of high-mass black holes in the current universe, it is more likely that this difference is caused by my sample selection. I refer the reader back to 2.1.1, especially Fig. 2.1b, where I show the $\log\sigma - M_r$ distribution for a volume-limited sample. Though I remarked that very few galaxies fainter than $M_{r,\mathrm{lim}}$ should have σ above σ_{lim}, a not-negligible portion of my σ-complete sample might comprise of such galaxies, which weren't excluded because of the empirically determined σ-completeness limit. These objects would slip through the cracks of my volume-weighting scheme, since being fainter, they could be overweighed by volume and that could lead to overestimating their contribution to the BHMF.

Low-luminosity and high-σ objects are quite rare too, because a high σ begets the need for a lot of mass (remember σ probes the gravitational potential well of the entire galaxy). High masses are only achievable with high luminosities. A possible physical interpretation for these objects is that they're galaxies undergoing a merger process, so that multiple SMBHs could be involved in the system. A merging galaxy is incompatible with our entire methodology so far, not only because I've assumed a single central SMBH at the center of each galaxy, but also because mergers as a mode of growth was neglected from the beginning. The results below also support a scenario where SMBHs grow almost entirely via accretion.

I compare my estimated value of ρ_{BH} with those from the literature – the compilation is shown in Table 3.2. My estimate of $\rho_{BH} = \left(2.71^{+0.55}_{-0.43}\right) \times 10^5\ M_\odot\ \mathrm{Mpc}^{-3}$ agrees well with all, albeit is slightly higher (except the Salucci et. al. determination, which was one of the first estimates of ρ_{BH} by using the BHMF). It also agrees with Shankar et. al's (2009) range of $\rho_{BH} \sim (1.5-2.7)\times 10^5\ M_\odot\ \mathrm{Mpc}^{-3}$. My results agree especially well with Fukugita & Peebles (2004), who use the M_{BH}-L_{sph} and M_{BH}-σ relations to calculate the contribution of SMBHs to the cosmic energy inventory to find $\rho_{BH} = \left(2.50^{+1.86}_{-0.93}\right) \times 10^5\ M_\odot\ \mathrm{Mpc}^{-3}$ [86].

Lastly, I compare my local mass density with the integrated mass density in the literature to test our theory of SMBH growth via AGN accretion and find what constraints my data sets on the average radiative efficiency of SMBHs. Hopkins et. al. (2007) uses the bolometric quasar luminosity function (QLF) at $z = 0-6$ by combining observations of over 50000 objects in the optical, mid-infrared and X-ray [87]. Their comprehensive study yields an integrated mass density at $z = 0$,

Author(s)	**Reference**	$\boldsymbol{\rho_{BH}}$ $[\times\mathbf{10^5}\ \mathrm{M}_\odot\ \mathrm{Mpc}^{-3}]$	**Scaling relation**	**Galaxy types**
Graham et. al. (2007)	[70]	1.6807 ± 0.6517	M_{BH}-n	All
Vika et. al. (2009)	[76]	1.63268 ± 0.5488	M_{BH}-L	All
Marconi et. al. (2004)	[83]	$2.254^{+1.33}_{-0.98}$	M_{BH}-L + M_{BH}-σ	All
Shankar et. al. (2004)	[80]	2.058 ± 0.77	M_{BH}-L + M_{BH}-σ	All
Yu & Tremaine (2002)	[84]	1.421 ± 0.28	M_{BH}-σ	Early
Aller & Richstone (2002)	[71]	1.176 ± 0.56	M_{BH}-L	All
Salucci et. al. (1999)	[85]	4.02	M_{BH}-L + M_{BH}-$M_{spheroid}$	All
Fukugita & Peebles (2004)	[86]	$2.50^{+1.86}_{-0.93}$	M_{BH}-L + M_{BH}-σ	All

Table 3.2: Local SMBH mass densities obtained via the BHMF from the literature. For each value, the scaling relation used in the mass function construction is shown. All but Yu & Tremaine (2002) estimated the BHMF for all galaxy types. The value obtained in this work is $\rho_{BH} = \left(2.71^{+0.66}_{-0.44}\right) \times 10^5\ \mathrm{M}_\odot\ \mathrm{Mpc}^{-3}$.

of $\rho_{BH,int} = \left(2.36^{+0.61}_{-0.49}\right)\left(\dfrac{0.1}{\epsilon}\right) \times 10^5$ M$_\odot$ Mpc^{-3}. Demanding this match my local ρ_{BH}, the average radiative efficiency required is $\epsilon = 0.0868$. Marconi et. al. (2004) determine $\rho_{BH,int} = 2.2\left(\dfrac{1-\epsilon}{9\epsilon}\right) \times 10^5$ M$_\odot$ Mpc^{-3}, using the AGN LF from Ueda et. al. (2003) [88]. The radiative efficiency to match my ρ_{BH} is $\epsilon = 0.0827$ in this case. Similarly, a comparison with the accreted mass density in Shankar et. al. (2004) yields $\epsilon \sim 0.0778$.

As already mentioned, the Shankar et. al. (2009) model with $\epsilon = 0.065$ over-predicts the BHMF compared to our observed distribution, requiring a slightly higher ϵ to match the local and accreted mass densities (since higher ϵ translates to less mass accreted). An updated model from Shankar et. al. (2013) resulted in $\epsilon \sim 0.07$ matching the observed local BHMF for a number of studies [89]. My results require slightly higher values of radiative efficiency (meaning gas is radiated away more efficiently), but agrees with the notion of an average radiative efficiency of $\epsilon \sim 0.1$ that most authors set or find. Overall, my results support the currently-accepted picture that SMBHs grow primarily via mass accretion during active phases and that the universe is far more heavily populated by SMBHs of small to medium size ($\sim 10^6 - 10^8$ M$_\odot$) than very large ones ($\gtrsim 10^9$ M$_\odot$). Furthermore, SMBHs build up their masses from small to large black holes, with the mass distribution dropping with increasing mass.

Various semi-empirical, semi-analytical (sometimes more of one than the other) models are being developed to explain the phenomena of SMBH growth, mass accretion, and their coevolution with host galaxies. As our instrumental limitations are overcome, our observational capabilities improve significantly, allowing us to probe far deeper into the universe and into the mystery shrouding SMBHs. With that, the constraints in evolutionary processes governing SMBHs are set more tightly. Consequently, our theoretical modeling in recent years has been able to better account for observations in the local and distant universe.

We assumed quite a few things on our way, not the least of which is a single average rate at which all massive black holes radiate energy, regardless of mass. While quite a few authors have assumed that scaling relations like the M_{BH}-σ don't evolve with time, more complex models are attempting to incorporate their possible time-evolution. As I mentioned, we didn't even consider galactic mergers, which would complicate our picture of a self-consistent evolution in the BHMF significantly (though we have a somewhat reasonable backing that mergers shouldn't play too big a role in growing SMBHs to their present size[2]). Many of the issues surrounding SMBH demography and models of SMBH growth and AGN feedback are summarized in Kelly & Merloni (2012) [90] and Shankar (2013) [91].

[2]See Shankar (2013) for an overview of more complex models that incorporate mergers into SMBH growth.

Conclusion

Supermassive black holes are fascinating objects with complex physical mechanisms governing their growth and even more mysterious processes linking them to the galaxies in which they live. Despite studying galaxies and SMBHs in quite some detail for the last year, I found that there is much more information to be extracted from these two fundamental constructs of our world than we've even learned to grasp.

In this thesis, I investigated black hole demographics from a statistical point-of-view, by characterizing the SMBH mass distribution. The first step in deriving the BHMF was to tackle selection biases – of which I now know there are many in astronomy – by selecting a sample mostly ($\sim 95\%$) complete in σ. This does quite a good job in eliminating many of the biases that might have been present in our sample from the Sloan Digital Sky Survey. I measured the VDF for ~ 96000 galaxies from $z = 0.03$ to $z = 0.1$ using a volume-weighting method that weighed out the notorious Malmquist Bias.

The VDF for my sample showed a gradual decrease in the number density of galaxies with increasing σ, before a characteristic $\sigma_\star$, where the number density plummets rapidly. The selection of a statistically complete sample and the inclusion of all galaxy morphological and star-forming types observed helped me characterize the low σ ($\log \sigma \lesssim 2$ km s^{-1}) end of the distribution well, although significant uncertainties exist for larger σ ($\log \sigma \gtrsim 2.5$ km s^{-1}). A parametrized form of the distribution in $\Phi(\sigma)$, with a power law and exponential fall-off, could be fit to the observed distribution, much like it's been seen with other galaxy distributions, such as $\Phi(L)$. However, the fit is unable to describe the observed VDF at all ranges. Then I used observations of SMBHs very near us, and obtained the M_{BH}-σ relation from the largest available sample to us. The strong correlation between M_{BH} and these galaxies' velocity dispersions, along with the existence of a galactic and black hole fundamental plane, indicates some physical mechanism tying the growth of SMBHs to that of galaxies.

Finally, the BHMF was generated, both by directly applying the $1/V_{max}$ method of counting galaxies and by combining the VDF parameterization with the M_{BH}-σ relation from Van den Bosch (2016). Though both methods produced similar shapes and overall results to the BHMF, the direct method gives more secure outcomes, since the uncertainty in the VDF fit is carried over to the BHMF, possibly over-predicting the true number of black holes with medium to high masses ($8 \lesssim \log(M_{BH}/M_\odot) \lesssim 9.5$). The Schechter function did a better job in describing the BHMF in all ranges than the VDF, however low-number statistics contributed to uncertain fit to the data at very high masses ($\log(M_{BH}/M_\odot) \gtrsim 9.5$). I observed a larger number density of SMBHs, relative to many other works, at masses $\log(M_{BH}/M_{\odot}) \gtrsim 9$, which I speculate to be an effect of faint, yet high σ galaxies, possibly undergoing mergers, which could introduce an additional bias in my sample.

I computed the mass density accreted by SMBHs of masses $6 \leqslant \log(M_{BH}/M_{\odot}) \leqslant 9.6$ to the present day and found $\rho_{BH} = \left(2.71^{+0.55}_{-0.43}\right) \times 10^5$ $M_{\odot}$ Mpc^{-3}, which agrees with most previous estimates. I also estimated the fraction of the baryonic mass-energy budget of the universe consumed by SMBHs, and found a slightly larger fraction than previously estimated. Furthermore, my results validated the picture where mass accretion during the active phases of a SMBH is the most important mode of SMBH growth, by matching the integrated mass density from observations of distant AGNs with the locally observed mass density. The matches required that SMBHs radiate away, on average, in the range of $\sim 7.5 - 9\%$ of the mass that they accrete (generally agreeing with the widely speculated value of 10%).

The buildup of SMBH mass over cosmic time may, however, have far more complicated moving parts than I've been able to model with the machinery in this thesis. The field of SMBH research is exciting and extremely relevant. There are many different directions this line of study can take, not the least of which is fully describing the distribution of M_{BH} for a higher range of masses, as our instrumental capabilities increase, and we have better information to better understand especially the very high mass end of the distribution. Statistical approaches can be extremely useful in inferring the properties and distribution of objects in our universe and help us formulate a clearer picture of how the world we know today evolved, where we came from, and where we're fated to go next in our adventure through space and time.

I set the lower M_{BH} limit to 10^6 $M_{\odot}$. Is there an upper limit to how big a black hole can get? [92] While the mathematical formulation of my results support a model where matter grew hierarchically, there is much that can be done via empirical work, or cosmological simulations, to explain if SMBH evolution also follows a similar pattern, i.e. do the smallest black holes form first, followed by the larger ones? Estimating the BHMF at higher redshifts is also very helpful in understanding their coevolution with galaxies, especially if the redshift-dependence of the scaling relations can be assessed well...do the same M_{BH}-σ-like correlations exist earlier in time? Black hole mergers, once not very well understood, can be studied in great detail now due to the titanic advances of LIGO's gravitational wave detection technology. Gravity waves are probably the hottest topic in astronomy right now, and it's ushered in an unprecedented era of globally collaborative multi-messenger astronomy. After much anticipation, the James Webb Space Telescope (JWST) is scheduled to go up next year, ushering in a second wave of *HST*-like space-based observations into the hearts of galaxies near and far.

Astronomy has always felt like a very pure journey into my own self-discovery. All you need is a curiosity of what's out there and how we ended up in this tiny blue rock circling an average-sized star in a tiny island universe among so many others. Truly, there is something poetic and sensational about massive, violent objects like SMBHs being intrinsically tied to our own cosmic story. As Einstein once said, "God does not play dice with the universe." Maybe He plays poker face, and it's up to us to decipher what it means.

Appendix A

The SMBH mass density integral

Eq. (3.6), which lets us compute ρ_{BH}, the SMBH mass density, is given in full as:

$$\rho_{BH} = \int_{\log(M_{BH}/M_{\odot})=6}^{\log(M_{BH}/M_{\odot})=9.6} \Phi_{\star} \left(\frac{M_{BH}}{M_{\star}}\right)^{\alpha+1} \exp\left[1 - \left(\frac{M_{BH}}{M_{\star}}\right)^{\beta}\right] M_{BH}\; d\log M_{BH}. \tag{A.1}$$

To deal with this, we'll first turn the $d\log M_{BH}$ into a dM_{BH}, by noting that $\dfrac{d\log M_{BH}}{dM_{BH}} = \dfrac{1}{M_{BH}\ln 10}$. The M_{BH}s cancel out and the integral turns into:

$$\rho_{BH} = \frac{1}{\ln 10}\int_{10^6}^{10^{9.6}} \Phi_{\star} \left(\frac{M_{BH}}{M_{\star}}\right)^{\alpha+1} \exp\left[1 - \left(\frac{M_{BH}}{M_{\star}}\right)^{\beta}\right]\; dM_{BH}. \tag{A.2}$$

Now, let $\overline{M} = \dfrac{M_{BH}}{M_{\star}}$, so that $d\overline{M} = \dfrac{dM_{BH}}{M_{\star}}$. Then the limits also change from 10^6 and $10^{9.6}$ to $\dfrac{10^6}{M_{\star}}$ and $\dfrac{10^{9.6}}{M_{\star}}$ and we get:

$$\rho_{BH} = \frac{\Phi_{\star} e M_{\star}}{\ln 10}\int_{10^6/M_{\star}}^{10^{9.6}/M_{\star}} \overline{M}^{\alpha+1} \exp\left(-\overline{M}^{\beta}\right)\; d\overline{M}, \tag{A.3}$$

where I factored out $\Phi_{\star}$, $M_{\star}$ and $\exp(1)$. Now, we let $t = \overline{M}^{\beta}$ and $dt = \beta\overline{M}^{\beta-1}\; d\overline{M}$. This changes our limits to: $t_{up} = \left(\dfrac{10^{9.6}}{M_{\star}}\right)^{\beta}$ and $t_{down} = \left(\dfrac{10^{6}}{M_{\star}}\right)^{\beta}$. Our integral can now be expressed with respect to t:

$$\rho_{BH} = \frac{\Phi_{\star} e M_{\star}}{\beta\ln 10}\int_{t_{down}}^{t_{up}} \frac{(t^{1/\beta})^{\alpha+1}}{(t^{1/\beta})^{\beta-1}} e^{-t}\; dt. \tag{A.4}$$

The point of this change of variables is that we can get ρ_{BH} in the following form:

$$\rho_{BH} = \frac{\Phi_\star e M_\star}{\beta \ln 10} \int_{t_{down}}^{t_{up}} t^{\left(\frac{\alpha+2}{\beta}\right)-1} e^{-t}\ dt. \tag{A.5}$$

This integral has the form of the lower *incomplete gamma function*[1]:

$$\gamma(a,x) = \int_0^x t^{a-1} e^{-t}\ dt. \tag{A.6}$$

The last thing we have to do to arrive at our answer in eq. (3.6) is turn the lower limit of our integral into 0, so we divide it up into two integrals:

$$\begin{aligned}\rho_{BH} &= \frac{\Phi_\star e M_\star}{\beta \ln 10} \int_{t_{down}}^{t_{up}} t^{\left(\frac{\alpha+2}{\beta}\right)-1} e^{-t}\ dt. \\ &= \frac{\Phi_\star e M_\star}{\beta \ln 10} \left(\int_0^{t_{up}} t^{\left(\frac{\alpha+2}{\beta}\right)-1} e^{-t}\ dt - \int_0^{t_{down}} t^{\left(\frac{\alpha+2}{\beta}\right)-1} e^{-t}\ dt \right)\end{aligned} \tag{A.7}$$

So that finally:

$$\rho_{BH} = \frac{\Phi_\star e M_\star}{\beta \ln 10} \left[\gamma\left(\frac{\alpha+2}{\beta}, \left(\frac{10^{9.6} M_\odot}{M_\star}\right)^\beta \right) - \gamma\left(\frac{\alpha+2}{\beta}, \left(\frac{10^{6} M_\odot}{M_\star}\right)^\beta \right) \right]. \tag{A.8}$$

[1]See, for example, Press et. al. (1992) [93] for more uses of this

References

[1] J. D. North. *Cosmos : An illustrated history of Astronomy and Cosmology.* Chicago : University of Chicago Press, 2008. An earlier version published as 'The Fontana history of astronomy and cosmology'.

[2] H. Kragh. *Conceptions of Cosmos: From Myths to the Accelerating Universe A History of Cosmology.* Oxford University Press, 2007.

[3] S. W. Hawking. *A Brief History of Time.* Bantam Books, 1998.

[4] I. Kant. *Allgemeine Naturgeschichte und Theorie des Himmels, oder, Versuch von der Verfassung und dem mechanischen Ursprunge des ganzen Weltgebaudes nach Newtonischen Grundsatzen abgehandelt.* Konigsberg ; Leipzig : Johann Friederich Petersen, 1755.

[5] H. Shapley. The scale of the universe. In *Bulletins of the National Research Council*, volume 2, pages 171–193, 1921.

[6] H. D. Curtis. The scale of the universe. In *Bulletins of the National Research Council*, volume 2, pages 194–217, 1921.

[7] C.J Conselice, A. Wilkinson, K. Duncan, and A. Mortlock. The evolution of galaxy number density at $z < 8$ and its implications. *Astrophys. J.*, 830(2):83, 2016.

[8] W. W. Bryant. *A history of astronomy.* London : Methuen & co, 1907.

[9] J. Michell. *Philosophical Transactions of the Royal Society of London Series I*, 74:35–57, 1784.

[10] P. S. Laplace. *Exposition du systéme du monde.* Paris : De l'Imprimerie du Cercle-Social, 1796. Master microform held by: Readex.

[11] K. S. Thorne. *Black Holes and Time Warps: Einstein's Outrageous Legacy.* Commonwealth Fund Book Program. W.W. Norton, 1994.

[12] S. Chandrasekhar. The density of white dwarf stars. *The London, Edinburgh, and Dublin Phil. Magazine and Journal of Science*, 11(70):592–596, 1931.

[13] S. Chandrasekhar. Stellar configurations with degenerate cores. *Mon. Not. R. Astron. Soc.*, 95:226–260, January 1935.

[14] F. Özel and P. Freire. Masses, radii, and the equation of state of neutron stars. *Ann. Rev. Astron. Astrophys.*, 54(1):401–440, 2016.

[15] J. R. Oppenheimer and H. Snyder. On Continued Gravitational Contraction. *Physical Review*, 56:455–459, September 1939.

[16] C. K. Seyfert. Nuclear Emission in Spiral Nebulae. *Astrophys. J.*, 97:28, January 1943.

[17] F. Hoyle and W. A. Fowler. On the nature of strong radio sources. *Mon. Not. R. Astron. Soc.*, 125:169, 1963.

[18] I. Robinson, A. Schild, and E. L. Schucking, editors. *Quasi-stellar sources and gravitational collapse*, 1965.

[19] A. Hewish et al. Observation of a Rapidly Pulsating Radio Source. *Nature*, 217:709–713, February 1968.

[20] M. Oda et al. X-Ray Pulsations from Cygnus X-1 Observed from UHURU. *Astrophys. J.*, 166:L1, May 1971.

[21] C. T. Bolton. Identification of Cygnus X-1 with HDE 226868. *Nature*, 235:271–273, February 1972.

[22] V. C. Rubin and W. K. Ford, Jr. Rotation of the Andromeda Nebula from a Spectroscopic Survey of Emission Regions. *Astrophys. J.*, 159:379, February 1970.

[23] W. L. W. Sargent et al. Dynamical evidence for a central mass concentration in the galaxy M87. *Astrophys. J.*, 221:731–744, May 1978.

[24] T. R. Lauer et al. Planetary camera observations of the double nucleus of M31. *Astrophys. J.*, 106:1436–1447, October 1993.

[25] J. L. Tonry. Evidence for a central mass concentration in M32. *Astrophys. J. L.*, 283:27–30, August 1984.

[26] F. Macchetto et al. The Supermassive Black Hole of M87 and the Kinematics of Its Associated Gaseous Disk. *Astrophys. Journal*, 489:579–600, November 1997.

[27] J. H. Lacy et al. Observations of the motion and distribution of the ionized gas in the central parsec of the Galaxy. II. *Astrophys. J.*, 241:132–146, October 1980.

[28] R. Schödel et al. A star in a 15.2-year orbit around the supermassive black hole at the centre of the Milky Way. *Nature*, 419:694–696, October 2002.

[29] L. Ferrarese and D. Merritt. A Fundamental Relation between Supermassive Black Holes and Their Host Galaxies. *Astrophys. J. L.*, 539:L9–L12, August 2000.

[30] K. Gebhardt et al. A Relationship between Nuclear Black Hole Mass and Galaxy Velocity Dispersion. *Astrophys. J. L.*, 539:L13–L16, August 2000.

[31] N. J. McConnell and C. P. Ma. Revisiting the Scaling Relations of Black Hole Masses and Host Galaxy Properties. *Astrophys. J.*, 764:184, February 2013.

[32] R. C. E. Van den Bosch. Unification of the fundamental plane and Super Massive Black Hole Masses. *Astrophys. J.*, 831:134, November 2016.

[33] G. de Vaucouleurs. On the distribution of mass and luminosity in elliptical galaxies. *Mon. Not. R. Astron. Soc.*, 113:134, 1953.

[34] J. L. Sérsic. Influence of the atmospheric and instrumental dispersion on the brightness distribution in a galaxy. *Boletin de la Asociacion Argentina de Astronomia La Plata Argentina*, 6:41, 1963.

[35] A. G. Riess et al. A 2.4% Determination of the Local Value of the Hubble Constant. *Astrophys. J.*, 826:56, July 2016.

[36] D. W. Hogg. Distance measures in cosmology. *ArXiv Astrophysics e-prints*, May 1999.

[37] D. Merritt. *Dynamics and Evolution of Galactic Nuclei.* Princeton: Princeton University Press, 2013, July 2013.

[38] L. Ferrarese and H. Ford. Supermassive Black Holes in Galactic Nuclei: Past, Present and Future Research. *Space Sci. Revs.*, 116:523–624, February 2005.

[39] D. A. Neufeld, P. R. Maloney, and S. Conger. Water maser emission from X-ray-heated circumnuclear gas in active galaxies. *Astrophys. J.*, 436:L.127–130, December 1994.

[40] M. C. Bentz. AGN Reverberation Mapping. *ArXiv e-prints*, May 2015.

[41] S. Gillessen et al. The Orbit of the Star S2 Around SGR A* from Very Large Telescope and Keck Data. *Astrophys. J.L.*, 707:L114–L117, December 2009.

[42] S. Gillessen et al. Monitoring Stellar Orbits Around the Massive Black Hole in the Galactic Center. *Astrophys. J.*, 692:1075–1109, February 2009.

[43] A. M. Ghez et al. Measuring Distance and Properties of the Milky Way's Central Supermassive Black Hole with Stellar Orbits. *Astrophys. J.*, 689:1044–1062, December 2008.

[44] J. Kormendy and D. Richstone. Inward Bound—The Search For Supermassive Black Holes In Galactic Nuclei. *Ann. Rev. Astron. Astrophys.*, 33:581, 1995.

[45] A. W. Graham. The black hole mass - spheroid luminosity relation. *Mon. Not. R. Astron. Soc.*, 379:711–722, August 2007.

[46] D. Merritt and L. Ferrarese. The M$_\bullet$-σ Relation for Supermassive Black Holes. *Astrophys. J.*, 547:140–145, January 2001.

[47] S. Tremaine et al. The Slope of the Black Hole Mass versus Velocity Dispersion Correlation. *Astrophys. J.*, 574:740–753, August 2002.

[48] M. J. Rees. Black Hole Models for Active Galactic Nuclei. *Ann. Rev. Astron. Astrophys.*, 22:471–506, 1984.

[49] A. R. King. Black hole outflows. *Mon. Not. R. Astron. Soc.*, 402:1516–1522, March 2010.

[50] J-W. Lee, J. Lee, and H-C. Kim. The M-sigma Relation of Super Massive Black Holes from the Scalar Field Dark Matter. *ArXiv e-prints*, December 2015.

[51] S. M. Faber and R. E. Jackson. Velocity dispersions and mass-to-light ratios for elliptical galaxies. *Astrophys. J.*, 204:668–683, March 1976.

[52] C. Stoughton et al. Sloan Digital Sky Survey: Early Data Release. *Astron. J.*, 123:485–548, January 2002.

[53] D. G. York et al. The Sloan Digital Sky Survey: Technical Summary. *Astron. J.*, 120:1579–1587, September 2000.

[54] M. A. Strauss et al. Spectroscopic Target Selection in the Sloan Digital Sky Survey: The Main Galaxy Sample. *Astron. J.*, 124:1810–1824, September 2002.

[55] V. Petrosian. Surface brightness and evolution of galaxies. *Astrophys. J.*, 209:L1–L5, October 1976.

[56] D. Thomas et al. Stellar velocity dispersions and emission line properties of SDSS-III/BOSS galaxies. *Mon. Not. R. Astron. Soc.*, 431:1383–1397, May 2013.

[57] M. Sarzi et al. The SAURON project - V. Integral-field emission-line kinematics of 48 elliptical and lenticular galaxies. *Mon. Not. R. Astron. Soc.*, 366:1151–1200, March 2006.

[58] C. Maraston and G. Strömbäck. Stellar population models at high spectral resolution. *Mon. Not. R. Astron. Soc.*, 418:2785–2811, December 2011.

[59] P. Sánchez-Blázquez et al. Medium-resolution Isaac Newton Telescope library of empirical spectra. *Mon. Not. R. Astron. Soc.*, 371:703–718, September 2006.

[60] M. Cappellari and E. Emsellem. Parametric Recovery of Line-of-Sight Velocity Distributions from Absorption-Line Spectra of Galaxies via Penalized Likelihood. *Pub. Astron. Soc. Pacific*, 116:138–147, February 2004.

[61] M. R. Blanton et al. New York University Value-Added Galaxy Catalog: A Galaxy Catalog Based on New Public Surveys. *Astron. J.*, 129:2562–2578, June 2005.

[62] J. Sohn, H. J. Zahid, and M. J. Geller. The Velocity Dispersion Function for Quiescent Galaxies in the Local Universe. *Astrophys. J.*, 845:73, August 2017.

[63] G. Kauffmann et al. Stellar masses and star formation histories for 10^5 galaxies from the Sloan Digital Sky Survey. *Mon. Not. R. Astron. Soc.*, 341:33–53, May 2003.

[64] A. K. Weigel, K. Schawinski, and C. Bruderer. Stellar mass functions: methods, systematics and results for the local Universe. *Mon. Not. R. Astron. Soc.*, 459:2150–2187, June 2016.

[65] M. Schmidt. Space Distribution and Luminosity Functions of Quasi-Stellar Radio Sources. *Astrophys. J.*, 151:393, February 1968.

[66] P. Schechter. An analytic expression for the luminosity function for galaxies. *Astrophys. J.*, 203:297–306, January 1976.

[67] W. H. Press and P. Schechter. Formation of Galaxies and Clusters of Galaxies by Self-Similar Gravitational Condensation. *Astrophys. J.*, 187:425–438, February 1974.

[68] J. R. Bond, S. Cole, G. Efstathiou, and N. Kaiser. Excursion Set Mass Functions for Hierarchical Gaussian Fluctuations. *Astrophys. J.*, 379:440, October 1991.

[69] S. Cole, J. Helly, C. S. Frenk, and H. Parkinson. The statistical properties of Λ-cold dark matter halo formation. *Mon. Not. R. Astron. Soc.*, 383:546–556, January 2008.

[70] A. W. Graham et al. The Millennium Galaxy Catalogue: the local supermassive black hole mass function in early- and late-type galaxies. *Mon. Not. R. Astron. Soc.*, 378:198–210, June 2007.

[71] M. C. Aller and D. Richstone. The Cosmic Density of Massive Black Holes from Galaxy Velocity Dispersions. *Astron. J.*, 124:3035–3041, December 2002.

[72] R. K. Sheth et al. The Velocity Dispersion Function of Early-Type Galaxies. *Astrophys. J.*, 594:225–231, September 2003.

[73] M. Bernardi et al. Galaxy luminosities, stellar masses, sizes, velocity dispersions as a function of morphological type. *Mon. Not. R. Astron. Soc.*, 404:2087–2122, June 2010.

[74] R. Bezanson, P. van Dokkum, and M. Franx. Evolution of Quiescent and Star-forming Galaxies since $z \sim 1.5$ as a Function of their Velocity Dispersions. *Astrophys. J.*, 760:62, November 2012.

[75] B. C. Kelly. Some Aspects of Measurement Error in Linear Regression of Astronomical Data. *Astrophys. J.*, 665:1489–1506, August 2007.

[76] M. Vika et al. The Millennium Galaxy Catalogue: the $M_{bh} - L_{spheroid}$ derived supermassive black hole mass function. *Mon. Not. R. Astron. Soc.*, 400:1451–1460, December 2009.

[77] A. Soltan. Masses of quasars. *Mon. Not. R. Astron. Soc.*, 200:115–122, July 1982.

[78] K. S. Thorne. Disk-Accretion onto a Black Hole. II. Evolution of the Hole. *Astrophys. J.*, 191:507–520, July 1974.

[79] F. Shankar, D. H. Weinberg, and J. Miralda-Escudé. Self-Consistent Models of the AGN and Black Hole Populations: Duty Cycles, Accretion Rates, and the Mean Radiative Efficiency. *Astrophys. J.*, 690:20–41, January 2009.

[80] F. Shankar et al. Supermassive black hole demography: the match between the local and accreted mass functions. *Mon. Not. R. Astron. Soc.*, 354:1020–1030, November 2004.

[81] M. Tegmark et al. Cosmological constraints from the SDSS luminous red galaxies. *Phys. Rev. D.*, 74, December 2006.

[82] Y-R Li, L. C. Ho, and J-M Wang. Cosmological Evolution of Supermassive Black Holes. I. Mass Function at $0 < z \lesssim 2$. *Astrophys. J.*, 742, November 2011.

[83] A. Marconi et al. Local supermassive black holes, relics of active galactic nuclei and the X-ray background. *Mon. Not. R. Astron. Soc.*, 351:169–185, June 2004.

[84] Q. Yu and S. Tremaine. Observational constraints on growth of massive black holes. *Mon. Not. R. Astron. Soc.*, 335:965–976, October 2002.

[85] P. Salucci, E. Szuszkiewicz, P. Monaco, and L. Danese. Mass function of dormant black holes and the evolution of active galactic nuclei. *Mon. Not. R. Astron. Soc.*, 307:637–644, August 1999.

[86] M. Fukugita and P. J. E. Peebles. The Cosmic Energy Inventory. *Astrophys. J.*, 616:643–668, December 2004.

[87] P. F. Hopkins et al. An Observational Determination of the Bolometric Quasar Luminosity Function. *Astrophys. J.*, 654:731–753, January 2007.

[88] Y. Ueda et al. Cosmological Evolution of the Hard X-Ray Active Galactic Nucleus Luminosity Function and the Origin of the Hard X-Ray Background. *Astrophys. J.*, 598:886–908, December 2003.

[89] F. Shankar, D. H. Weinberg, and J. Miralda-Escudé. Accretion-driven evolution of black holes: Eddington ratios, duty cycles and active galaxy fractions. *Mon. Not. R. Astron. Soc.*, 428:421–446, January 2013.

[90] B. C. Kelly and A. Merloni. Mass Functions of Supermassive Black Holes across Cosmic Time. *Advances in Astronomy*, 2012:970858, 2012.

[91] F. Shankar. Black hole demography: from scaling relations to models. *Classical and Quantum Gravity*, 30(24):244001, December 2013.

[92] X-B Wu et al. An ultraluminous quasar with a twelve-billion-solar-mass black hole at redshift 6.30. *Nature*, 518(512), 2015.

[93] W. H. Press et al. *Numerical recipes in FORTRAN: The art of scientific computing 2nd edition*. Cambridge University Press, 1992.